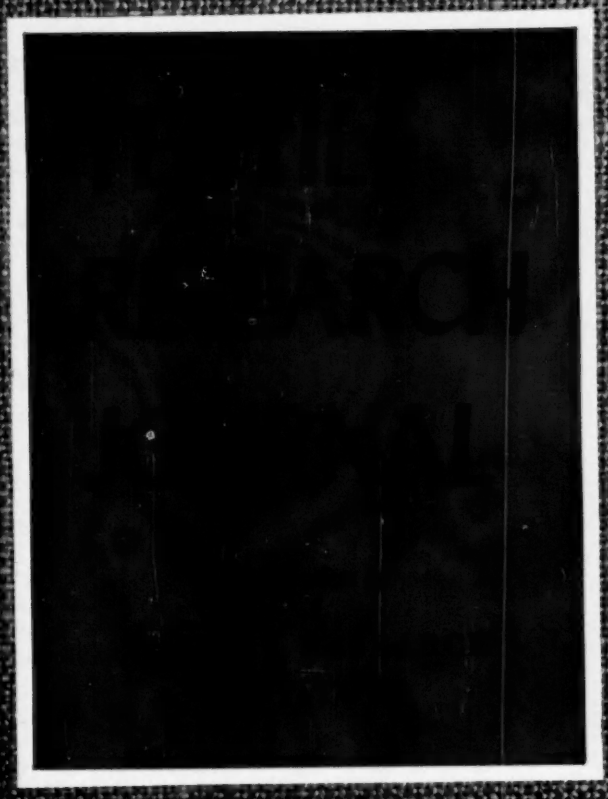

One of a series

FORMALDEHYDE, METHACRYLAMIDE AND OXTAIL SOUP made their appearance in the Applications Lab each noon. The first two were used in filling free space in Lincoln fibers, the last in filling space elsewhere. Steaks were out of the question — Petty Cash was pinched, and no one had heard of upgrading thrifty meat cuts with Tona® enzyme-balanced meat tenderizers.

By which devious path we come to our advertising message: Did you know that Wallerstein has as good a name in meats as in textiles? Wallerstein enzymes are used to tenderize meats in packing houses, restaurants and homes — Wallerstein antioxidants to guard the flavor and color of franks, hams and luncheon meats.

This has more than noon-hour significance for you! Constant searching for enzymes to be used in many fields — meat, beer, pharmaceuticals, to name a few besides textiles — fills our shelves with scores of commercial, development and experimental enzymes of all descriptions. Purity ranges from AR grade on down. The probability is good that some of these enzymes could be put to use by enterprising textile researchers. Perhaps you? If you were to tell us about your requirements, we might be able to pick you out a few interesting numbers. And, remember, please, we make Rapidase® and Serizyme®, too!

WALLERSTEIN COMPANY
Division of Baxter Laboratories, Inc.
Staten Island 3, N.Y.

If you haven't investigated Cellase™, a new high potency cellulase, write Dept. R-8 for a free sample.

TEXTILE RESEARCH JOURNAL

Volume 31 — *August 1961* — Number 8

Editor:
Richard K. Toner

Production Editor:
Dorothy Dana Hollmann

Advisory Board

Herbert J. Ball
Earl E. Berkley
John Boulton
C. H. Fisher
Walter J. Hamburger
Milton Harris
R. M. Hoffman
Harold P. Lundgren
Herman Mark
Edward R. Schwarz
George Switlyk
Helmut Zahn

TEXTILE RESEARCH JOURNAL, published monthly at Prince and Lemon Streets, Lancaster, Pa., is devoted to the interest of research in textile and allied industries. It is published by Textile Research Institute.

Manuscripts and communications should be sent to the Publications Department, P.O. Box 625, Princeton, N. J.

Second-class postage paid at Lancaster, Pa.

Subscription rates: $25.00 per year; additional for postage, 50 cents to Canada, $1.00 to all other countries. Single copies, $2.50 each.

Contents copyright © 1961 by Textile Research Institute. Advertising rates supplied on request.

IN THIS ISSUE

Studies in the Light Absorption of Dyes. Part IV: The Relation of Transmission and Reflection of Light by Diffusing Materials, to Concentration of Color. *C. H. Giles, S. M. K. Rahman, and D. Smith* 679

The Influence of Changes in Moisture Content on the Wrinkle Recovery of Fabrics.

Part I. *A. M. Farnworth and Joel Lindberg* 687

Part II. *Joel Lindberg* 695

Lightfastness Studies of Basic Dyes on Acid-Modified "Dacron" Polyester Fiber. *S. B. Macrov and H. Kobsa* ... 697

Wool Fabric Stabilization by Interfacial Polymerization. Part I: Polyamides. *R. E. Whitfield, L. A. Miller, and W. L. Wasley* 704

Adsorption of Direct Cotton Dyes by Chemically Modified Celluloses. *E. H. Daruwalla, P. J. Kangle, and G. M. Nabar* 712

Stress–Strain Relationships in Yarns Subjected to Rapid Impact Loading. Part VII: Stress–Strain Curves and Breaking-Energy Data for Textile Yarns. *Jack C. Smith, Paul J. Shouse, Josephine M. Blandford, and Kathryn M. Towne* 721

The Theory of Shrinkproofing of Wool.

Part II: Chemical Modification of the Fiber Surface and its Effect on Felting Shrinkage, Friction, and Microscopic Appearance. *J. H. Bradbury* 735

Part III: A Method for Determination of the Force on a Fiber During Felting. *J. H. Bradbury and H. Groll* ... 743

Twist and Tension as Factors in Yarn Characteristics. *K. Sreenivasan and K. S. Shankaranarayana* 746

LETTERS TO THE EDITOR

A Quick Method for Determining the Elongation, the Breaking and Tearing Strengths of Plain Woven Fabrics. *Gain L. Louis and Louis A. Fiori* 754

IN COMING ISSUES .....inside back cover

REPRINT REQUESTS SHOULD BE DIRECTED TO THE AUTHORS

SEE ARTICLES FOR ADDRESSES

—PORTABLE—
TENSION DEVICE

FOR MEASURING TENSION APPLIED IN SPINNING, WINDING AND WARPING

The Custom Tension Recordograph has now been reduced in size and cost. This portable unit is now transistorized to reduce the size. The Sensing Head fits into the cover with the lead in cables. The range is 0 to 800 grams. Others upon request.

CUSTOM SCIENTIFIC INSTRUMENTS, INC.

541 Devon Street • Kearny, N. J.

AUGUST 1961
VOL. 31 NO. 8

TEXTILE RESEARCH JOURNAL

Studies in the Light Absorption of Dyes.[1]

Part IV: The Relation of Transmission and Reflection of Light by Diffusing Materials to Concentration of Color

C. H. Giles, S. M. K. Rahman, and D. Smith

Colour Chemistry Research Laboratory, Department of Chemical Technology, The Royal College of Science and Technology, Glasgow, C.1.

Abstract

A linear relation between the logarithm of the color concentration of a diffusely reflecting colored surface and its reflectance density is derived as a simple extension of Beer's law and confirmed experimentally using a variety of dyed fabrics.

The experimental results indicate that Beer's law is not usually obeyed by the dye present in dyed materials, probably on account of the presence of adsorbed dye aggregates. It is in fact only obeyed by true solutions or by suspensions of particles of constant size distribution.

The application of Beer's law to transmission and reflection systems is discussed, and it is shown that a more general relation is obtained by substituting for c, the color concentration factor in the Beer's law formula, the empirical factor $\left(\frac{c}{1+ac^x}\right)$, where a and x are constants (probably functions of the refractive index difference between the dye and surrounding medium), and x is a simple fraction.

In a test with dyed viscose rayon fabrics it is shown that about 20% of the reflected light is specularly reflected from the surfaces of lightly dyed fibers.

Introduction

The relationship between intensity of incident and reflected light for diffusing surfaces has been the subject of many investigations, from 1890 onwards [7, 17].

Apparently the first investigators to examine the relationship between reflected light intensity from a colored surface and the concentration of color were Cunliffe and Lambert, in 1929 [8]. They found empirically a linear relation between the reflection density of certain dyed fabrics and the log of their dye concentration, but only up to a concentration of *ca.* 1–1.5%, beyond which the curves bent towards the concentration axis. This observation was made as a small part of an exhaustive investigation of the light fading of dyes on wool; it was limited to two dyes (C. I. 15620 and 16150) on wool only. It appears that no further examination of this relation was made until it was rediscovered by Baxter et al. [4] in this laboratory.

[1] Parts I and II, see references [6] and [5], Part III, *J. Chem. Soc.*, 1209 (March 1961).

They found a linear relation between reflection density and the log of concentration of some direct dyes on viscose rayon, over the whole range of concentrations measured.[2] Meanwhile, however, several other authors [e.g. 3, 12, 13, 15, 16] had examined the subject, theoretically and by experiment, and had produced a number of functions, often complex, of reflectance which vary linearly with color concentration in a diffusely reflecting surface. The simple relation that Cunliffe and Lambert's work first suggested might hold seemed, however, to offer some advantages over the others, e.g., it enables the effect of changes in the physical state of dyes in fibers to be compared directly with corresponding effects in solutions or transparent films (see below); it uses a function of reflectance read directly on the measuring apparatus (the spectrophotometer scale is calibrated in units of reflection density), and it can be plotted directly. We have therefore investigated it more exhaustively. The present paper shows that it is consistent with simple theoretical considerations and also useful in experimental investigations of the physical state of dyes in fibers.

General Discussion

Theoretical treatments of varying degrees of complexity have been proposed by earlier investigators. The simplest is that used by Pineo (in connection with the design of a recording spectrophotometer), who considered the application of the ordinary Beer's law relation to the reflection system. We do the same, but derive a new final relation. Some previous authors have considered the process by which light passes into and out of the diffusely reflecting surface as consisting of two separate effects, *viz.*, scatter and absorption. This treatment is unnecessarily complex, and we (following Pineo) do not use it.

Consider the quite general case of light illuminating any mass of material composed of transparent colored particles or fibers. The emergent light can be considered to consist of a very large number of individual rays, each of which has traversed a different path, having suffered many deviations by scattering, reflection, and refraction. A step-wedge is a model of this type of system.

[2] Cunliffe and Lambert used a visual spectrophotometer. The departures from linearity they observed may have been caused by the difficulty of visually assessing low intensity reflected light. Baxter et al. used a photoelectric instrument.

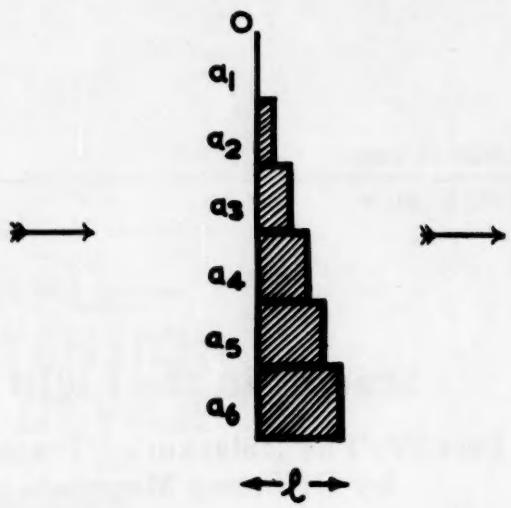

Fig. 1. Schematic diagram of equivalent paths of a light beam transmitted or reflected by a mass of colored particles.

Most of the rays will have passed through colored particles; these will have been selectively absorbed. Some may have been only specularly reflected from outer surfaces and so will not have suffered absorption. In the model there are a very large number of very small steps; nearly all the steps are colored, but a few are uncolored, representing the specularly reflected light (Figure 1). The absorption of light suffered by each individual colored ray will vary with the concentration of the coloring matter in the particles in accordance with Beer's law, but the emergent light as a whole does not do so (cf. Figure 2b). This may be illustrated by a simple numerical example. Consider two emergent colored rays, 1% and 10% of the original light intensity, i.e., giving optical densities of 2 and 1 respectively. The mean transmission is 5.5%, corresponding to an optical density of 1.26. If the concentration of coloring matter is doubled, optical density values double (to become 4 and 2), but the percentage transmissions do not alter proportionately; in fact these become 0.01% and 1%. An instrument would measure mean transmission, which is now 0.505%, corresponding to an optical density of 2.30. The optical density of the emergent light is therefore increasingly less than proportional to the concentration of coloring matter (cf. Figure 2).

The argument is the same whether the absorption of light is measured by transmission or by

reflection. Beer's law is obeyed in both cases when the material is in the form of simple transparent films (Figure 3). The only difference in theory between the two methods of measurement is that the optical density by reflectance is double that by transmission, because the length of the light path is doubled. In practice it is not exactly double. With clear, non-scattering films the position of the photocell relative to the direction of illumination in reflectance, and difficulties in holding the films flat, cause the light path by reflectance to be rather more than double that by transmission; with slightly scattering films it is rather less than double, because some of the scattered light must return to the photocell without having traversed the whole thickness of film (Figure 3).

Quantitative Treatment

In the definition of Beer's law, the path length should strictly be defined as the thickness of the total number of molecules that any given direct light ray passes through, and this will obviously vary with concentration, c, of the coloring matter. Therefore we may say that cl is the true path length, if l is defined as the path length for unit concentration.

On the basis of the suggested model there is virtually an infinite number of path lengths available for any ray. In the step-wedge diagram (Figure 1) the thickness of each step, cl_i, corresponds to the length of path of the light through a material containing a monodisperse coloring matter with molar extinction coefficient ϵ, and in a concentration c; and the width, a, of each step corresponds to the probability that the ray will take the respective path; l_i is the path length at unit concentration.

It is assumed that Beer's law, i.e.,

$$\frac{I_{Ti}}{I_{0i}} = 10^{-\epsilon c l_i} \tag{1}$$

can be applied to the light passing through any step or path, where I_{0i}, I_{Ti} are the intensities of light entering and leaving the path i. The intensity of light, I_0, entering all paths is assumed to be the same. If the flux of light entering any step is $I_0 a_i$, then the flux when it leaves is

$$I_{Ti} a_i = a_i I_0 10^{-\epsilon c l_i} \tag{2}$$

If there are n steps or paths, the total flux of light entering all paths is

$$I_0 = \sum_{i=1}^{n} a_i I_0 \tag{3}$$

and the total flux of light leaving all paths is

$$I_T = \sum_{i=1}^{n} a_i I_0 10^{-\epsilon c l_i} \tag{4}$$

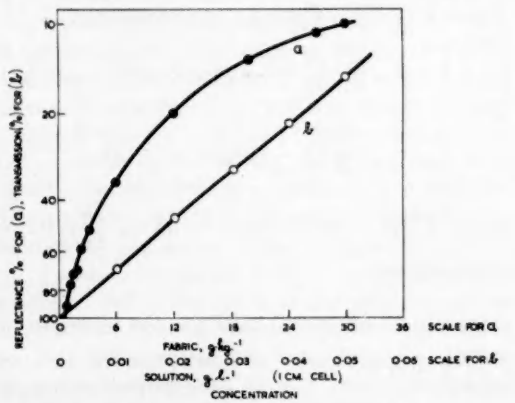

Fig. 2. Reflectance (λ5400 Å) and transmission–concentration curves for a direct dye (C. I. 35780) (a) on viscose rayon fabric (residual dyebaths measured at λ5300 Å) and (b) in aqueous solution. Beer's law is obeyed in solution. (The wide difference in length of light path in the two cases accounts for the differences in concentration range.)

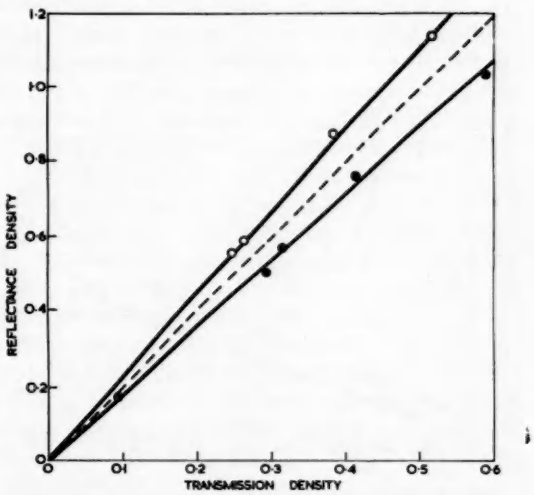

Fig. 3. Relation between optical density of colored films (scattering and non-scattering) measured by transmission and by reflectance. ○ Clear films of (sec.) cellulose acetate dyed with C. I. Disperse Violet 4. (All measurements at λ6200 Å.) ● Slightly translucent films of gelatin, containing a dissolved acid wool dye (Polar Yellow R) and a little titanium dioxide. (All measurements at λ4350 Å.)

Thus

$$\frac{I_T}{I_0} = \frac{\sum_{i=1}^{n} (a_i 10^{-\epsilon c l_i})}{\sum_{i=1}^{n} a_i} \qquad (5)$$

Pineo [15] considered the probability that the frequency of paths is an exponential function of their length, but found that the actual relation he obtained in practice appeared to indicate that longer paths are more effective than assumed. Better agreement with practice was obtained by a more elaborate treatment using the first-order Bessel function. He thus obtained the relation

$$\log qL = \log \frac{(1 - R)^2}{2R}$$

where q is the "absorbing power" of the color, L is a constant, proportional to the size of the microscopical structural inhomogeneities in the reflecting surface, and R is the reflectance. This equation gave an almost linear variation with color concentration.

We now assume that since there is virtually an infinite number of paths available, there is an equal probability of a ray taking any given path, i.e., all values of a_i are equal say to a. If n tends to infinity, so that $na = w$ (the total "width" of all paths), then a can be replaced by dy, where y is the distance from 0 (Figure 1) of any path of length l. It is further assumed that $l = \alpha y$ where α is a constant (i.e., that there is a constant gradation of path lengths).

Hence from Equation 5 we have

$$\frac{I_T}{I_0} = \frac{\int_0^w 10^{-\epsilon c \alpha y} dy}{\int_0^w dy} \qquad (6)$$

$$= \frac{\int_0^L 10^{-\epsilon c l} (dl/\alpha)}{w} \qquad (7)$$

where $L = \alpha w$ = the longest path length at unit concentration, thus

$$\frac{I_T}{I_0} = \frac{1}{\alpha w} \left[- \frac{1}{\epsilon c \log_e 10} 10^{-\epsilon c l} \right]_0^L \qquad (8)$$

$$= \frac{1}{L} \left[- \frac{1}{\epsilon c \log_e 10} 10^{-\epsilon c L} + \frac{1}{\epsilon c \log_e 10} \right] \qquad (9)$$

$$= \frac{1}{\epsilon c L \log_e 10} [1 - 10^{-\epsilon c L}] \qquad (10)$$

Now, the value of ϵ for organic coloring matters is very high, of the order of 10^4, and L is of the order of 10^{-1} (because experimentally it is found, with closely woven fabrics, that no further change in reflection density occurs beyond a fabric thickness of *ca.* 1 mm.) so that Equation 11, for substances colored with organic coloring matters, and for all except very low values of c approximates to

$$\log \frac{I_T}{I_0} = - \log c + A \qquad (11)$$

or

$$\log \frac{I_0}{I_T} = \log c + A'$$

where A and A' are constants and $\log \frac{I_0}{I_T}$ is the reflection density.

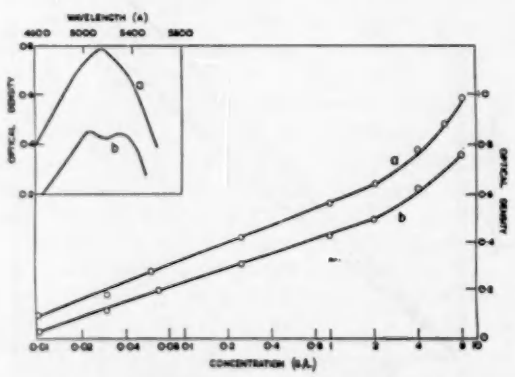

Fig. 4. Optical density–log concentration relation for aqueous dye solutions measured using whole visible wave band (Hilger Spekker absorptimeter, no filter; 1-cm. cells), showing similarity to relation for diffusely reflecting surfaces.
(a) C. I. Acid Red 18 (16255), recrystallized sample.
(b) C. I. Acid Red 1 (18050), commercial sample.
Insert shows respective absorption spectra: a, 0.049 g./l.; b, 0.28 g./l. (1-cm. cells).

Comparison with Broad-Band Spectrophotometry

The optical density–concentration relation for solutions of a dye having symmetrical absorption bands, measured in white light, should resemble the relation for the reflection density–concentration in diffusely reflecting surfaces. The reason is that under these circumstances the measured optical density can be considered the result of an integra-

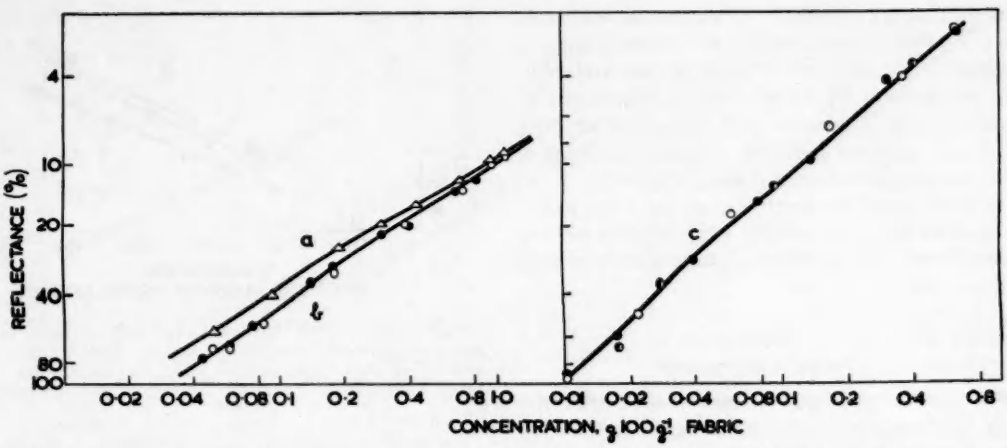

Fig. 5. Reflectance–concentration curves for dyed fabrics, (a) direct cotton red dye (C. I. 35780) on viscose rayon fabric, treated with optical dissolving agent (ethyl salicylate) (λ_{rf}, 5400 Å, residual dyebaths measured at 5300 Å); (b) the same on untreated fabric; (c) acid wool orange dye (C. I. 16230) on wool flannel fabric, λ_{rf}, 4950 Å. Different symbols on curves b, c represent replicate experiments.

λ_{rf} = Wavelength of minimum reflection of fabric,
λ_{ex} = Wavelength of maximum absorption of extracted dye solution (see following figures).

tion of transmissions through an infinite number of light paths of continuously varying length, i.e., the absorption band behaves as a step-wedge with infinitely small steps. Results given in Figure 4 do in fact show that up to a density *ca.* 0.5 this relation holds for white light measurements. Thereafter the curves steepen, i.e., the density rises increasingly with concentration. This can be attributed to the variation of spectral sensitivity of the barrier-layer photocells in the absorptiometer. The sensitivity is at a maximum near the middle of the spectrum, and falls towards each end; at 4500 Å and at 6200 Å it has fallen to about half the maximum and at 4000 Å and 7000 Å to about 30% and 10% respectively [11]. To obtain the high densities (>0.5) shown in Figure 4, without filter, highly concentrated dye solutions are required. These almost completely absorb the mid-spectrum light (the optical density is too high for measurement with the optimum filter), and the instrument response will then increasingly depend on the marginal wave bands at each end of the spectrum, so that the sensitivity falls steadily, and the apparent optical density rises more rapidly than it would with a photocell of uniform sensitivity across the whole spectrum. Further, these concentrated solutions show light-scattering effects, which will also contribute to the anomalous increase of apparent optical density.

Experimental

Some methods and equipment used were described in a previous paper [5]. Additional details are as follows.

Materials and Methods

Normal commercial dyes and bleached and cleaned fabrics were used. The viscose rayon fabrics of different degrees of crystallinity were respectively of the same construction and filament diameter. Normal methods of dyeing were used, at 95°–100° C., for 90 min. Phenol when used was added to the dyebath (2 moles per mole of dye).

The reflectance measurements with films (Figure 3) were made using white paper as backing and as the blank control. To facilitate stripping from the glass plate, the gelatin films were cast on Cellophane regenerated cellulose sheet, stretched on glass plate. The gelatin solutions used contained varying amounts of dissolved dye, but the same, small, quantity of titanium dioxide, just sufficient to give a slightly translucent appearance to the dried films.

Analyses, etc.

Optical and reflection densities were measured on Unicam spectrophotometers SP500 and SP600. Reflectances were measured (against undyed fabric)

using four layers of fabric. It was found that addition of further layers produced no further change in readings. The dye contents of fabrics and films were determined by colorimetric analysis, either of extracts of fabrics in pure pyridine, or 50% (vol./vol.) aqueous pyridine (Figure 7c, d), or of dyebaths before and after dyeing (Figure 2a, 5a–c) all at 5300 Å, or, for wool (Figure 7e) of solutions of the dyed fabrics in boiling 10% aqueous sodium hydroxide solution (similar solution of undyed wool used as control).

Practical Tests of the Relationship and its Wider Implications. General Confirmation

The further tests now made confirm that the linear relation between the log of dye concentration and reflection density holds for a variety of dyes and fibers over the whole measureable range. In theory the line should tend to curve towards the concentration axis at very low and very high dye concentrations, but in practice this curvature is only apparent at very low concentrations measured at wavelengths somewhat removed from λ_{max} (see below).

Effect of Physical State of Coloring Matter. Apparent Failure of Beer's Law

Equation 12 requires that the graph of reflection density at λ_{max} of a colored surface against the log of concentration of color should have a slope of unity. But in all the cases of dyed fabrics so far examined (cf. Figures 2, 5, 6, 7, 9) the slope measured at λ_{max} is less than unity (unit slope = 45° on the scales used in the present figures). It seems almost certain that this is due to the aggregated state of the dye. It has already been demonstrated [5, 6, 18] that soluble dyes adsorbed in solid substrates are probably always partly aggregated. The degree of aggregation must, by mass action law, increase with concentration. For each species of aggregate there is a different value of ϵ, and the larger species increase with concentration at the expense of the smaller. Also the amount of scattered light from the dye aggregate particles will differ for each species. These conditions lead to an apparent failure of Beer's law. This law cannot therefore be strictly applied to describe the attenuation of each individual ray, as in Equation 1 above. It has however hitherto been assumed that the coloring matter in e.g. dyed fibers is monodisperse and that it does obey Beer's law.

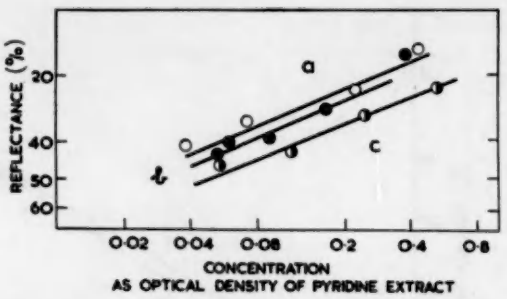

Fig. 6. Direct cotton red dye (C. I. 29100) on viscose rayon fabrics of different crystallinity, λ_{ef}, λ_{ex}, 5400 Å; λ_{ef} is the same for all three types of dyed fabric, (a) normal fiber, (b) strong (Tenasco) fiber, (c) low-swelling (highly crystalline) fiber.

The observed or "apparent" molar extinction coefficient (see below) falls with increase in dye aggregation [5], and thus with increase in dye concentration. We assume therefore that cl in Equations 1–11 should be replaced by an empirical term $\frac{cl}{1+ac^x}$, where a and x are positive constants, and $x<1$. These constants are probably functions of the difference in refractive index between the coloring matter and the surrounding medium. Equation 10 therefore becomes

$$\frac{I_T}{I_0} = \frac{1}{\left(\frac{\epsilon Lc}{1+ac^x}\right)\log_e 10}\left[1 - 10^{-\epsilon L\left(\frac{c}{1+ac^x}\right)}\right] \quad (12)$$

and thus

$$\log \frac{I_T}{I_0} = -\log\left(\frac{c}{1+ac^x}\right) - \log\left[\epsilon L \log_e 10\right] + \log\left[1 - 10^{-\epsilon L\left(\frac{c}{1+ac^x}\right)}\right] \quad (13)$$

For values of ac^x such that $1 + ac^x \simeq ac^x$ (i.e., for large values of c),

$$\log \frac{I_T}{I_0} \simeq -\log\left(\frac{1}{a}\right)c^{1-x} - \log\left[\epsilon L \log_e 10\right] \quad (14)$$

$$\simeq -(1-x)\log c + \text{constant} \quad (15)$$

The effect of the introduction of the $\frac{\epsilon cl}{1+ac^x}$ term, in place of the simple extinction coefficient, into the normal Beer's law relation, may now be considered. In uniformly dyed films the optical density vs. concentration curve lies *below* the line

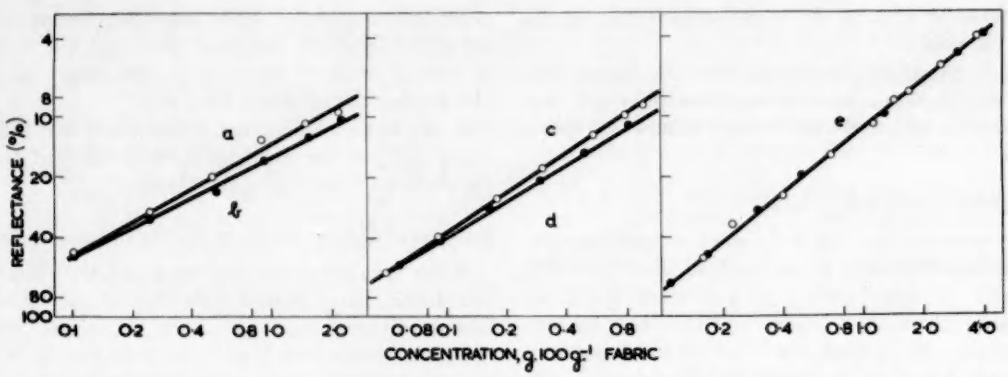

Fig. 7. Reflectance–concentration curves for fabric dyed with and without disaggregating agent (phenol); (a, b) direct cotton yellow (C. I. 13920) on viscose rayon, λ_{rf}, 4200 Å, λ_{ex}, 4100 Å; (c, d) direct cotton blue (C. I. 24410) on viscose rayon, λ_{rf}, 6250 Å, λ_{ex}, 6600 Å; (e) acid wool dye (Polar Yellow R) on wool flannel fabric, λ_{rf}, λ_{ex}, 4300 Å; (○), Phenol in dyebath; (●), no phenol present. There is no change in λ_{rf} in presence of phenol in any of these cases.

to be expected for a truly monodisperse dye[3] [5]. The curve is almost linear over the lower concentration ranges,[4] but with an increase in concentration it becomes convex to the concentration axis (cf. Figure 6 in [5]). Figure 8 illustrates this effect for some hypothetical cases. (Usually this non-linearity, which is well known in the case of solutions, is referred to as a "failure of Beer's law" at higher concentrations. Actually, it probably represents a failure of the law at *all* concentrations, i.e., the curve is actually non-linear from the start.) A linear density vs. concentration curve thus is not necessarily a proof that the dye is molecularly dispersed or that it is aggregated to the same extent at all concentrations. Probably only ideal solutions, or suspensions of constant particle size distribution [5] give truly linear relations.

If the above hypothesis is correct, then a reduction in the degree of aggregation of coloring matter should raise the slope of the log R vs. log c curve, and an increase in aggregation should lower it. This was checked by examining the reflectance of cellulose fabrics dyed with two direct cotton dyes, with and without the presence of phenol, which has been shown by optical tests [5] to cause disaggregation of this type of dye in cellulose films. The presence of phenol increases the slope of the log R vs. log c curve (Figure 7a–d).

In confirmation that this effect is correctly attributed here, a parallel test was made on wool fabric dyed with a dye (Polar Yellow R) which has previously been shown by light-scattering tests [1] and by optical-density measurements [5] *not* to be disaggregated by phenol. Consistent with this, the present results (Figure 7e) show that phenol

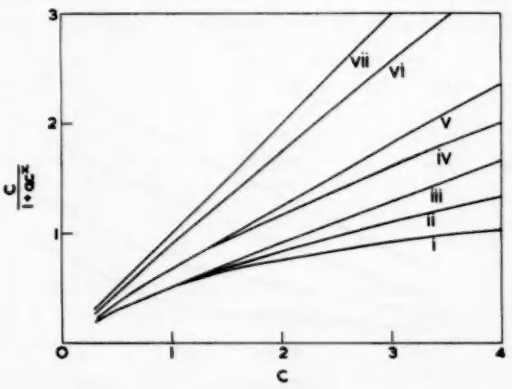

Fig. 8. Plot of the function $\frac{c}{1+ac^x}$ (proportional to optical density) against c for various values of a and x. Values of a and x respectively (i) 1.0, 0.75; (ii) 1.0, 0.5; (iii) 1.0, 0.25; (iv) 0.5, 0.5; (v) 0.5, 0.75; (vi) 1.0, 0.5; (vii) $a = 0$.

[3] Duyckaerts [9] has shown, by theory and experiment, that the extinction of a mass of transparent particles rises with decrease in their size, and the limiting value, corresponding to the true extinction of the solid substance, is reached with a particle size that gets smaller as the intensity of the absorption band becomes greater. Andreasen et al. [2] find that *monodisperse* suspensions of some opaque solids show maximum extinction at grain sizes comparable with the wavelength of the light; the presence of particles of widely varying particle size flattens the maximum in the grain size–extinction curve.

[4] Up to about 0.5 M dye concentration in solid transparent substrates [5]; this is well within the concentration range of dye in normal dyed fibers.

produces no change in the reflectance data of the dye on wool.

It is therefore concluded that the lower than theoretical slopes of all the curves obtained may reasonably be attributed to the "failure" of Beer's law.

Conformity with Beer's Law

It appears that the only solid colored systems likely to obey Beer's law and so give reflection density vs. log c curves of unit slope would be those prepared by a process not involving adsorption, e.g., by mixing insoluble pigment particles in such a way as to ensure constant particle size distribution at all concentrations. In practice this condition is likely to be difficult to achieve because of changes in size distribution caused by capillary effects in the drying process.

Amount of Surface Reflection from Fabrics

An attempt was made to estimate the amount of specularly reflected light, by measuring the reflectance of a series of dyed viscose rayon fabrics before and after wetting with ethyl salicylate, which is an appropriate "optical dissolving agent," i.e., a liquid with almost the same refractive index as the fiber.

This would be expected almost to eliminate surface reflection and scatter. In fact, it actually reduced the reflectance of the most lightly dyed fabric by about 20% (Figure 5). The reduction falls with rise in dye concentration, until at the heaviest shade it is only about 5%. Perhaps the change is due to the increase in aggregate size and consequent reduction in difference between the refractive index of the dyed fiber and the liquid in contact with it, or to some "blinding" of the fiber surface by coverage with dye.

It can be concluded that in this particular fabric about 20% of the incident light is reflected from the surface of the outermost fibers.

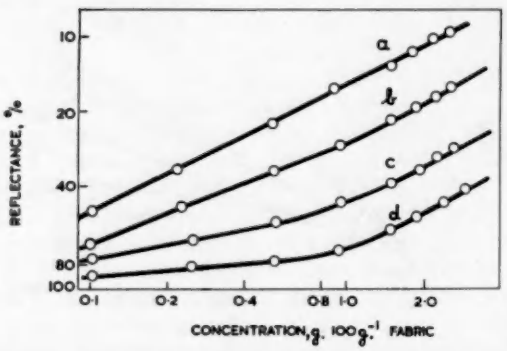

Fig. 9. Reflectance–concentration curves for viscose rayon fabrics dyed with a direct cotton yellow dye (C. I. 13920). Reflectance measured at: (a) 4900 Å (λ_{max}), (b) 4500 Å, (c) 4100 Å, (d) 3900 Å.

Reflectance Measurements at Various Wavelengths

When measurements are made at wavelengths increasingly far removed from that of the absorption maximum, the value of the extinction coefficient may become so low that the factor $10^{-\epsilon cl}$ in Equation 10 becomes appreciably less than unity and the relation of $\log \frac{I_T}{I_0}$ to $\log c$ then is a curve. Obviously this will occur more at low values of c than at high values. The results shown in Figure 9 demonstrate that this is in fact so; at low concentrations the lines for wavelengths well away from λ_{max} are curves, but at higher concentration values the lines for all wavelengths are parallel.

Effect of Fiber Orientation

The long axes of direct cotton dye molecules in dyed cellulose tend to be orientated parallel to the cellulose molecular chains. The absorption of light by the dye is less intense in a direction *across* its molecule than *along* it. Therefore as the fiber molecules are oriented more closely parallel to the fiber length the weaker the color appears [4, 10, 14]. Baxter et al. [4] (cf. Figure 6 here) found that direct cotton dyes on highly crystalline viscose rayon fabrics gave higher apparent reflectance values than on two rayons of lower crystallinity. (The relative effects shown on the latter vary a little according to conditions and to nature of dye.)

In some cases the curve for the less crystalline fibers has slightly higher slope, implying that with increasing concentration the orientation of dye is less possible in the more amorphous than in the more crystalline fibers.

Acknowledgments

The authors thank Professor P. D. Ritchie for his interest and encouragement, British Cellophane Ltd., Ciba Clayton Ltd., Courtaulds Ltd., and Imperial Chemical Industries Ltd., Dyestuffs Division, for gifts of materials; the Wool Textile Research Council for a financial grant for equipment;

Mrs. P. Catchpole for assistance with some experiments; and Mr. P. E. Knapp for helpful discussions.

Literature Cited

1. Alexander, P., and Stacey, K. A., *Proc. Roy. Soc.* (*London*) **A212**, 274 (1952).
2. Andreasen, A. H. M., Krebs, K., Dalsgaard-Pedersen, N. Aa., Camradt-Petersen, E., and Kjear, B., *J. Soc. Chem. Ind.* **69**, 312 (1950).
3. Atherton, E., *J. Soc. Dyers Colourists* **71**, 389 (1955).
4. Baxter, G., Giles, C. H., McKee, M. N., and Macaulay, N., *J. Soc. Dyers Colourists* **71**, 218 (1955).
5. Campbell, D. S. E., Cathcart, D., Giles, C. H., and Rahman, S. M. K., *Trans. Faraday Soc.* **55**, 1631 (1959).
6. Campbell, D. S. E., and Giles, C. H., *J. Soc. Dyers Colourists* **74**, 164 (1958).
7. Channon, H. J., Renwick, F. F., and Storr, B. V., *Proc. Roy. Soc.* (*London*) **A94**, 222 (1918).
8. Cunliffe, P. W., and Lambert, P. N., *J. Soc. Dyers Colourists* **45**, 313 (1929).
9. Duyckaerts, G., *Analyst* **84**, 201 (1959).
10. Fothergill, F., *J. Soc. Dyers Colourists* **62**, 319 (1946).
11. Giles, C. H., *J. Soc. Dyers Colourists* **66**, 615 (1950); the instrument used here has a cell with characteristics similar to that shown in Figure 12.
12. Guelke, R., and Fitzsimons, M. M., *Trans. Faraday Soc.* **30**, 512 (1934).
13. Kubelka, P., and Munk, F., *Z. tech. Phys.* **12**, 593 (1931); Kubelka, P., *J. Opt. Soc. Amer.* **38**, 448 (1948).
14. Morton, T. H., *J. Soc. Dyers Colourists* **62**, 272 (1946).
15. Pineo, O. W., U. S. Patent 2,218,357 (October 15, 1940).
16. Preston, J. M., and Tsien, P. C., *J. Soc. Dyers Colourists* **62**, 242 (1946).
17. Stokes, G. G., *Proc. Roy. Soc.* (*London*) **11**, 545 (1860–62).
18. Weissbein, L. and Coven, G. E., TEXTILE RESEARCH JOURNAL **30**, 58, 62 (1960), have obtained electron micrographs of aggregates of direct cotton dyes in regenerated cellulose film.

Manuscript received July 7, 1960.

The Influence of Changes in Moisture Content on the Wrinkle Recovery of Fabrics, Part I

A. J. Farnworth[1] and Joel Lindberg

Swedish Institute for Textile Research, Gothenburg, Sweden

Abstract

A study has been made of the effect of rate of drying, and of alternate wetting and drying, on the wrinkle recovery of fabrics of wool, wool blends, and cotton, when wrinkled in the wet state.

Recovery is independent of the rate of drying, but a second-stage rapid recovery occurs at a stage in drying corresponding to loss of water from the internal fiber structure, as distinct from surface evaporation. Repeated, alternate increase and decrease of regain leads to progressive, step-wise recovery from wet wrinkling.

It is probable that the energy required to give these effects originates from the swelling–deswelling associated with changes in regain.

Introduction

One of the major factors to be considered in appearance retention of wash and wear fabrics is the ability to recover from the mechanical deformations imposed during wearing and washing. Wear wrinkles seldom recover at the same relative humidity as that at which they developed, e.g., the fabric in the seat of a pair of trousers, as the wearer sits, may be in an atmosphere approaching 90–95% relative humidity [7], whereas immediately the wearer stands, the humidity may fall to 60%. After a garment is laundered, the conditions of drying may vary to the extent that on one occasion it dries in

[1] Present address: C.S.I.R.O., Division of Textile Industry, Geelong, Victoria, Australia.

TABLE I. Details of Fabrics Used

Fabric No.	Fiber composition	Warp yarn, tex	Weft yarn, tex	Ends/in.	Picks/in.	Weight, oz./sq. yd.	Weave
1136	49% wool; 51% terylene	52	51	53	43	6.2	Plain
1140	46% wool; 54% terylene	44	44	65	61	7.3	2/2 Twill
1141	all wool	52	47	48	47	5.7	Plain
1143	all wool	58	57	30	27	8.1	Hopsack
1149	all wool	37	37	91	96	9.3	Twill
1268	all cotton	14	16	132	69	3.8	Plain

less than an hour and on another it takes several hours. Laundering wrinkles can recover under widely different conditions of relative humidity and, in consequence, at widely different rates.

Most measurements of wrinkle recovery recorded in the literature have been made by one of the standard methods where wrinkling and recovery take place at constant temperature and humidity. As part of the "wash and wear" research program of the Swedish Institute for Textile Research, it was decided to study the wrinkle recovery behavior of fabrics wrinkled in the wet or damp state and allowed to recover at different rates of drying. Subsequently the scope of the study was broadened to include the effect of alternate wetting and drying on the recovery of "wet wrinkles."

Materials and Methods

Fabrics

Fabrics were selected to give a range of weights and types. Details of construction are given in Table I.

Wrinkle Recovery at Different Rates of Drying

As the investigation concerned only recovery rates at unspecified, but different, measurable rates of drying, it was decided to measure recovery angle and drying rate simultaneously on the same sample, thus avoiding the necessity for any elaborate devices for controlling the rate of drying. Hence all experiments were carried out by placing the creased sample over a wire suspended from the arm of a torsion balance, periodically recording the weight and the recovery angle.

Samples for creasing were small (2.5 × 1 cm.) to minimize any influence of the weight of the fabric on the angle when suspended over the wire [1]. Creasing was effected by inserting the sample between two plastic leaves which were riveted together at one end and placing a weight on the upper one. It was found that the upper, thin leaf should not be more than 2–3 mm. wider than the sample or the leaf tilts on the sample leading to uneven distribution of load and irregular results. It was also necessary to ensure that the weight was carefully located longitudinally to obtain reproducible results.

Preliminary investigations showed that, with some cloths, the sample must be immersed in the wetting solution for a least 5 min. to come to equilibrium before creasing. For wetting times intermediate between apparent, almost instantaneous wetting and the 5 min., the initial crease angle increases, presumably the result of swelling or some physical change other than simple wetting. Another source of variable results lay in the fact that with some cloths, particularly warp-faced fabrics, there was a marked difference in initial crease angle depending on whether the fabric was creased with the face inwards or with the face outwards.

By paying attention to these various factors and carefully standardizing the technique, reproducible results were obtained. The sample (2.5 × 1 cm.) was immersed in a 0.1% aqueous solution of a non-ionic wetting agent for 5 min., removed, and squeezed between filter papers. It was then folded exactly in two across the width and always with the face outwards, placed between the plastic leaves, and a 1-kg. weight with a narrow rectangular base placed on the top leaf, directly above the sample. Both the weight and the sample were carefully located in a predetermined position. After 5 min., the weight was removed, the leaves separated, and the sample carefully taken out and suspended from a fine horizontal wire attached to the arm of a torsion balance, the crease lying along the wire. At regular intervals, the weight was recorded and the crease angle measured by means of a protractor with a vernier scale attached to the eyepiece of a cathetometer. In this way the angle could be accurately measured in the immediate vicinity of the crease without

interference from any slight twisting or bending of the sample.

The rate of drying was increased and varied by the simple expedient of placing a heater with a multi-position switch below the sample. The sample and arm of the balance were closed off from convection currents while readings were taken.

Wrinkle Recovery on Alternate Wetting and Drying

For these experiments it was essential to hold the creased sample in such a way that it could recover freely and subsequently be immersed in water, or steamed, without disturbing the crease. This was accomplished by gripping one arm of the creased sample in a holder placed in a clamp which could be rotated to keep the free arm of the sample hanging vertically, as with the conventional Monsanto method [6]. The clamp and holder were arranged in such a way that a beaker of water could be brought up underneath to immerse the sample and holder without disturbing them. The normal metal holder used in the Monsanto method was not satisfactory, as the sample tended to attach itself to the longer leaf when immersed in water, and was no longer free to recover without restraint. A similar holder, but with both leaves the same length, proved to be quite satisfactory.

With this technique, recovery takes place with only one half of the fabric free and hanging vertically, so larger samples (4 × 1.5 cm.) were used. Creasing and measurement of angle were carried out as before, the sample being transferred to the holder immediately after the creasing. The free arm was kept vertical during recovery, immersion in water, or steaming. Immersion and steaming times were 5 min. in each instance, and the alternate drying cycle was carried out with the heater arrangement mentioned previously.

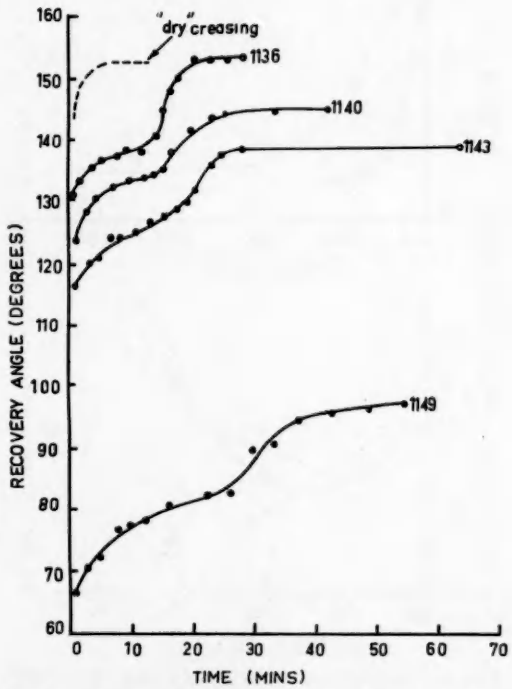

Fig. 1. Recovery-angle–time curves for fabrics creased wet or "dry" and allowed to recover at 65% RH and 21° C.

Results and Discussion

Wrinkle Recovery During Drying

Figure 1 shows recovery-angle–time curves for fabrics which were creased wet and allowed to recover at 65% RH and 21° C. until they reached equilibrium with this atmosphere. A similar curve for fabrics creased "dry" (i.e., at the equilibrium regain for this relative humidity and temperature) is included for comparison. All four fabrics studied gave recovery angles within 2–3 degrees of each other in this instance, so the "dry" recovery curve is an average for the four.

It is seen that with these particular fabrics, only the light weight blend (1136) has an ultimate recovery from wet wrinkling equal to that from dry, and that there is a big difference in the recovery of the two all-wool fabrics from wet wrinkling, Fabric 1149 showing particularly poor recovery.

The most interesting feature of the curves is the two-stage recovery exhibited by all fabrics. The first part of the curve is similar to that for dry creasing, in that there is an initial rapid recovery which flattens off to some extent, but at a later stage of drying a second rapid recovery commences. During the progress of this work, Wilkinson and Hoffman [7] reported similar behavior with fabrics containing cellulosic fibers. These authors found that the weight loss of their fabrics was linear in time until the fabric reached the water retention corresponding to the point at which the second stage of recovery commences, and the results given in the next section (Figures 3–6) are in agreement with this.

The two-stage recovery from wet wrinkling has an important bearing on the wrinkle recovery evaluation

of wash–wear non-iron fabrics. In order to measure the true recovery properties of fabrics wrinkled when wet, the fabric must be allowed to come to equilibrium with the drying atmosphere before recording the recovery angle. Failure to do this could lead to false conclusions when comparing two fabrics. For example, Figure 2 shows recovery curves for an untreated all-wool fabric and for the same fabric after setting with sodium bisulfite [3]. In this particular instance, the second-stage recovery of the set fabric was appreciably greater than the untreated. Therefore, the true difference between the recovery properties of the two fabrics is greater than that indicated by the relative recovery angles after 5 min., the stage at which the angle would normally be taken when using standard methods of measuring wrinkle recovery.

Effect of Varying the Rate of Drying

Samples of each fabric were creased while wet and allowed to recover at different rates of drying, the recovery angle and weight being recorded at various stages of drying. Figures 3–6 show the results for only two drying rates, curves being given for recovery angle as a function of time (Curve A), regain as a function of time (Curve B), and recovery angle as a function of regain (Curve C). The latter curves were constructed from the data of Curves A and B.

It is seen that the second rapid stage of recovery commences at the stage of drying when the regain–time curve departs from linearity. This occurs at a regain of about 15% for the blended fabrics and about 30% for the all-wool. Most probably this corresponds to the stage at which the drying mecha-

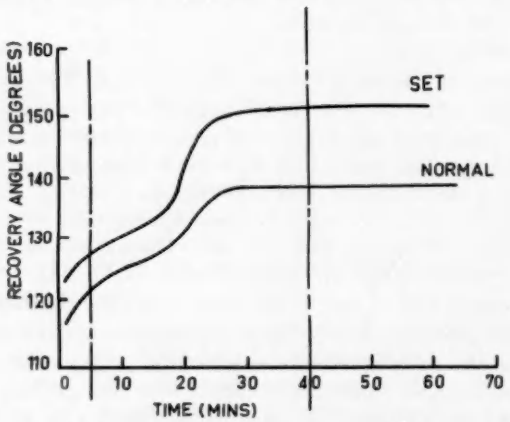

Fig. 2. Recovery-angle–time curves for a normal and a set fabric creased wet and allowed to recover at 65% RH and 21° C.

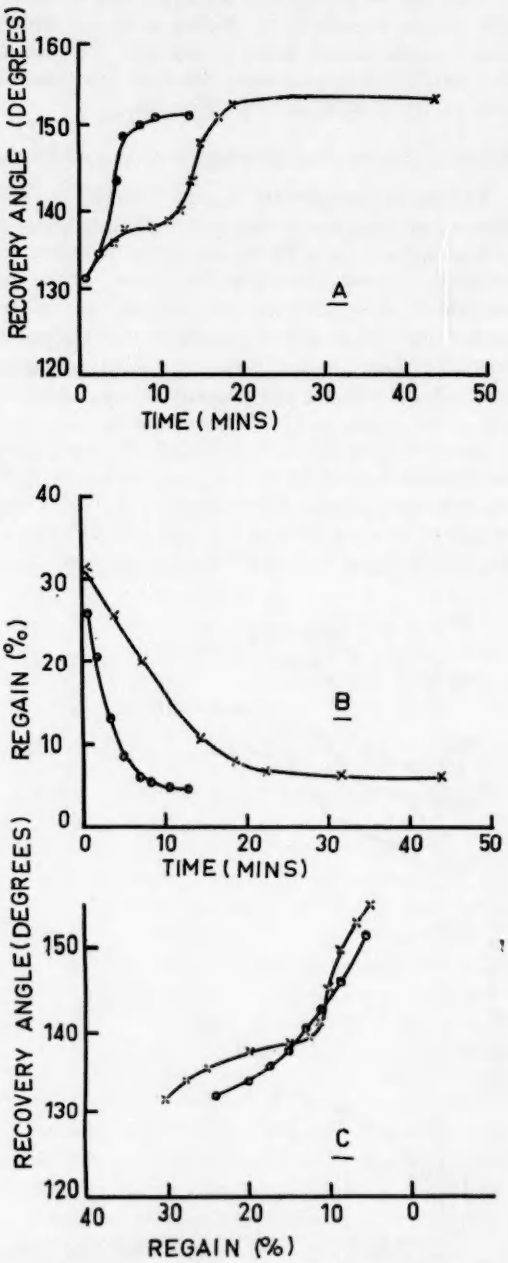

Fig. 3. Curves showing relation between recovery-angle–time (A), regain–time (B), and recovery-angle–regain (C) for Fabric 1136 when creased wet and allowed to recover at two different rates of drying.

nism changes from surface evaporation to loss of water from the internal structure of the fiber, with consequent effects from deswelling.

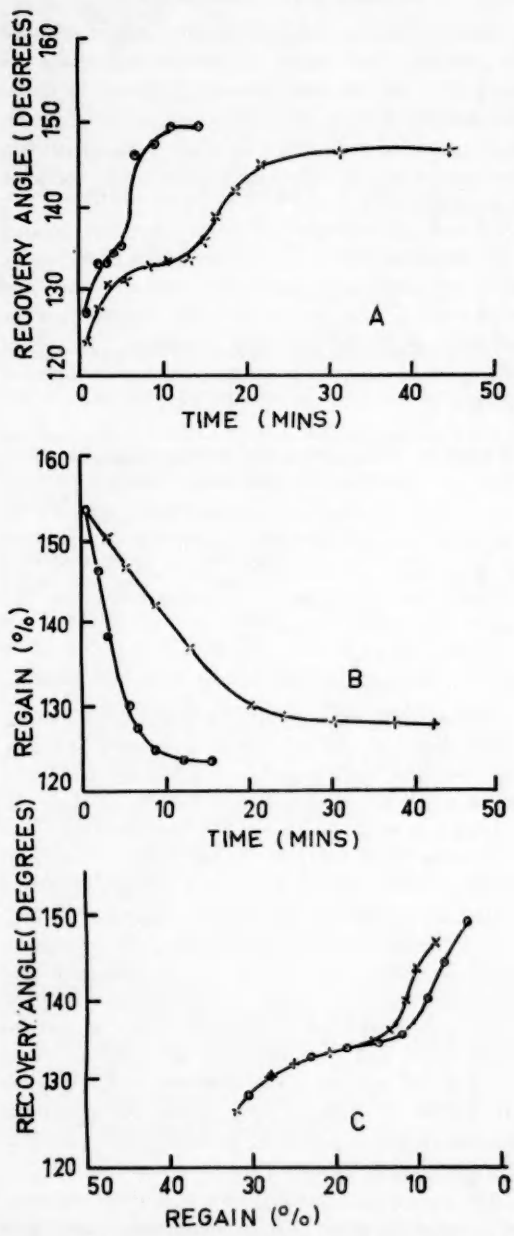

Fig. 4. Curves showing relation between recovery-angle–time (A), regain–time (B), and recovery-angle–regain (C) for Fabric 1140 when creased wet and allowed to recover at two different rates of drying.

The ratio of the two drying rates from which these results were obtained is of the order of 3 to 1. There is very little difference between the recovery-angle–regain curves for the two rates for each fabric, and certainly no significant or consistent trend. It appeared, therefore, that the wrinkle recovery of fabrics after wet creasing is independent of rate of drying. This conclusion was confirmed in a somewhat practical manner by taking fabric samples of fixed size and weight, wetting and blotting them as before, compressing them into a plastic tube and

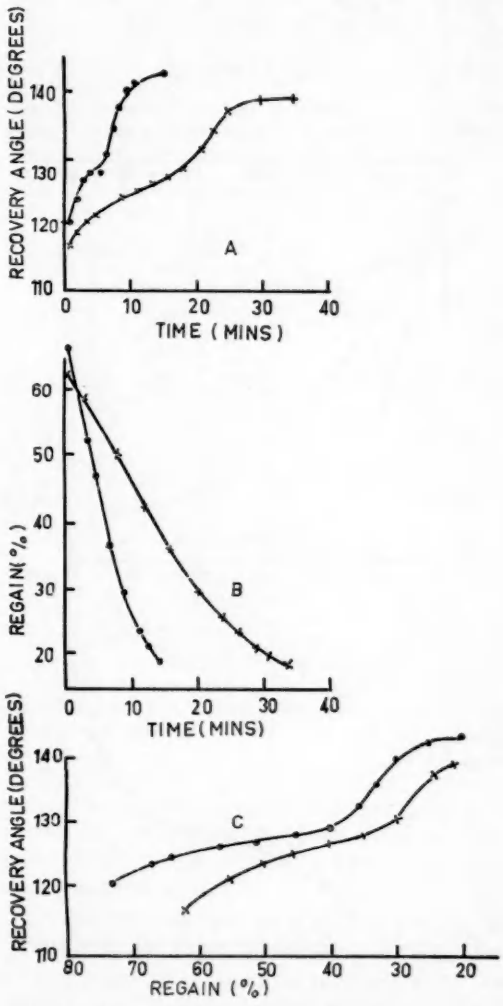

Fig. 5. Curves showing relation between recovery-angle–time (A), regain–time (B), and recovery-angle–regain (C) for Fabric 1143 when creased wet and allowed to recover at two different rates of drying.

leaving them under a fixed weight for 5 min. A device for doing this has been designed by Bernskiöld [4] and enables a fabric to be randomly wrinkled under controlled conditions. After removal, the fabrics were laid out free from restraint and dried at widely different rates. When dry, the various samples of any one fabric were indistinguishable.

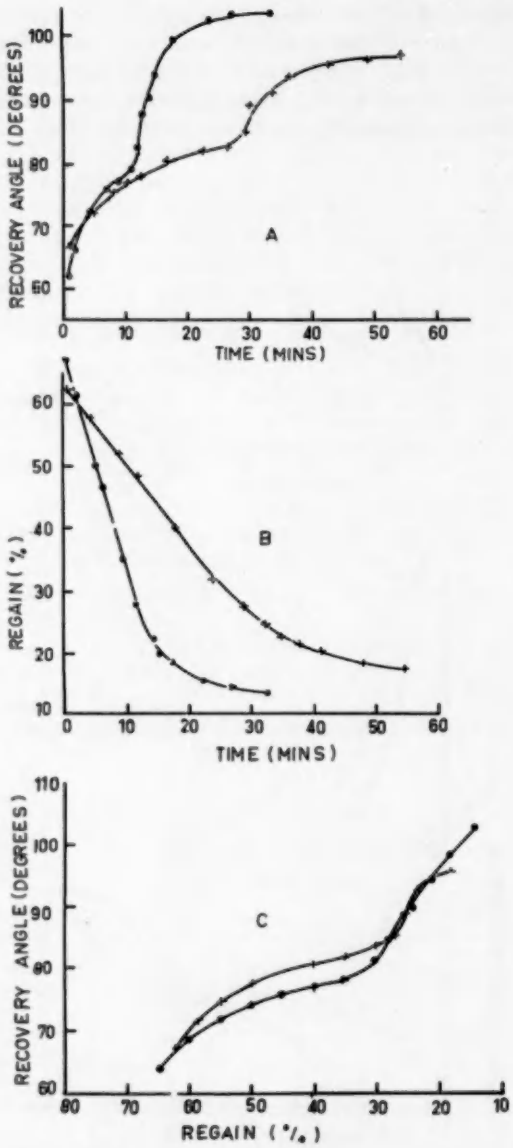

Fig. 6. Curves showing relation between recovery-angle–time (A), regain–time (B), and recovery-angle–regain (C) for Fabric 1149 when creased wet and allowed to recover at two different rates of drying.

Effect of Alternate Wetting and Drying

It is well known that wrinkles or creases developed or put into wool fabrics at normal regain are destroyed by wetting, and this was confirmed by creasing samples at 65% RH, allowing them to recover, and then immersing them in water. In all cases a recovery angle of 180° was obtained, i.e., complete recovery.

Samples of three all-wool fabrics were then creased wet and, after drying and measurement of the stable recovery angle, they were immersed in water and then redried. The results in Table II show that the recovery angle had increased somewhat, the extent of additional recovery being different for the different fabrics.

TABLE II. Effect of Rewetting and Redrying a Crease after Recovery from Initial Creasing

Fabric No.	Recovery angle, degrees	
	After first drying	After rewetting and redrying
1141	147	151
1143	155	161
1149	113	139

These results indicated that it would be of interest to investigate the effect of repeated wetting and drying. Samples were creased wet as before, dried, and the recovery angle measured. They were then immersed in a 0.1% solution of non-ionic wetting agent in water at room temperature for 5 min., dried, and the angle remeasured. This procedure was repeated until the recovery angle reached a constant value.

In a further series of experiments, the immersion step was carried out at 60° C. to overcome any temporary set (see below). For purposes of comparison, samples of each fabric were set with sodium bisulfite [3] and both series of experiments (room temperature and 60° C.) repeated. The results are shown in Figures 7–9, which are drawn as smooth curves rather than following the step-wise changes actually observed.

The curves for normal fabrics with room temperature rewetting show that in some cases there is a remarkable progressive recovery, the ultimate recovery after several rewetting–drying cycles being very high. Fabric 1149, which exhibits very poor

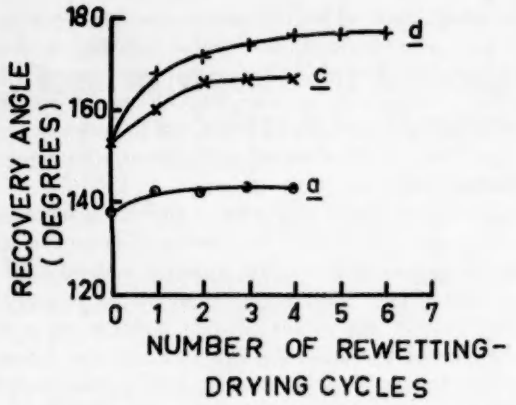

Fig. 7. Effect of alternate rewetting–drying cycles on recovery angle for Fabric 1141 when creased wet. Curve *a* = normal fabric (rewetting at 21° C.); *c* = set fabric (rewetting at 21° C.); *d* = set fabric (rewetting at 60° C.).

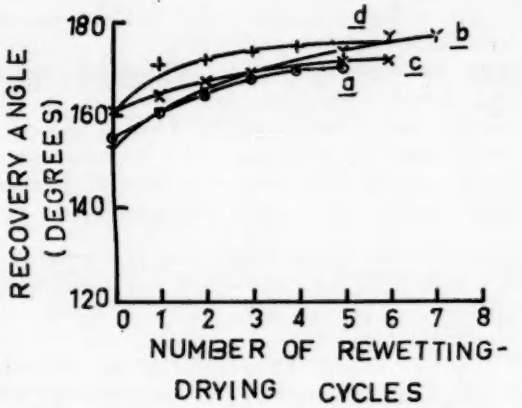

Fig. 8. Effect of alternate rewetting–drying cycles on recovery angle for Fabric 1143 when creased wet. Curve *a* = normal fabric (rewetting at 21° C.); *b* = normal fabric (rewetting at 60° C.); *c* = set fabric (rewetting at 21° C.); *d* = set fabric (rewetting at 60° C.).

initial recovery, shows a considerable increase in recovery angle after one rewetting–drying cycle, and the ultimate recovery after nine such cycles is excellent. The same type of phenomenon was observed by Svenson [5] when studying the shrinkage of wool fabrics. He found that there was a progressive shrinkage, which approached an equilibrium value when fabrics were alternately steamed and dried.

Set fabrics show similar behavior except that the curves lie above the corresponding curves for the normal fabric, i.e., they show better recovery under the same conditions. With Fabric 1149, the set fabric shows complete recovery after only three rewetting–drying cycles.

Immersion in water at 60° C. instead of room temperature gave an increased first-cycle recovery, but thereafter the curves were parallel. This may be due to a small part of the unrecovered angle being temporary set which is stable to water at room temperature but not at temperatures appreciably greater than that at which the fabric was creased. Such behavior has been observed many times when setting wool fibers [2].

Several interesting observations have been made in connection with this phenomenon.

1. The effect is obtained only by alternating the wetting and drying. A sample immersed in water immediately after creasing, without preliminary drying, and then subsequently dried, gave the same recovery angle as a sample dried immediately after creasing.

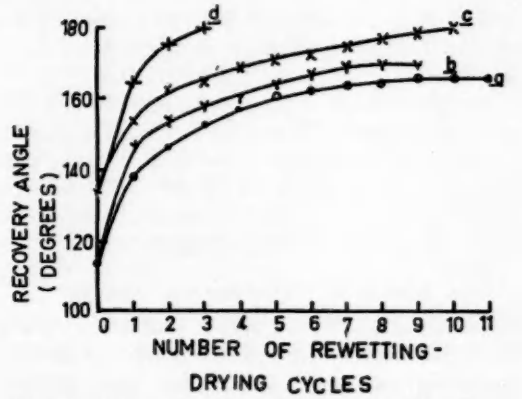

Fig. 9. Effect of alternate rewetting–drying cycles on recovery angle for Fabric 1149 when creased wet. Curve *a* = normal fabric (rewetting at 21° C.); *b* = normal fabric (rewetting at 60° C.); *c* = set fabric (rewetting at 21° C.); *d* = set fabric (rewetting at 60° C.).

2. Prolonged immersion in water (40 hr. in one instance) is no more effective than the 5-min. immersion, i.e., the effect results from drying following wetting, and is independent of the time during which the sample remains wet.

3. Similar behavior was observed when the sample was steamed for 5 min. instead of being immersed in water, although the resultant recovery curve was a little below the water-immersion curve. This is due to the fact that under these conditions, the fabric does not reach saturation point. In a separate experiment, the regain of a fabric after steaming for

5 min. under conditions similar to those used in the creasing experiments was 28%.

4. One cotton fabric (No. 1268) was investigated and showed similar behavior. However, in this instance, samples creased dry did not recover completely with the first wetting as did the wool fabrics, but showed the same progressive recovery on alternate rewetting–drying cycles as samples creased wet.

These results are quite interesting in showing that it is possible for some cloths with poor wet-creasing properties to give excellent recovery after several rewetting–drying, or steaming–drying cycles.

Recovery from wrinkling can be divided into three stages: immediate recovery; delayed recovery; and permanent deformation (unrecovered).

The last stage is associated with interyarn reactions and frictional restraints, and it is probable that the progressive recovery resulting from the rewetting–drying cycles is at least partly due to small forces generated by the swelling–deswelling process overcoming these frictional forces which hold the fabric in a state of deformation. (See Part II.)

The phenomenon of progressive recovery also suggests an interesting alternative to tumble drying for restoring the appearance of non-iron garments after laundering, as it should not be difficult to design a drying cabinet in which the relative humidity is repeatedly cycled from low to high.

Summary

Fabrics of wool, wool blends, and cotton show a two-stage recovery from wet creasing. Following the normal recovery, a second-stage rapid recovery occurs at a regain corresponding to the point at which the rate-of-drying curve ceases to be linear, i.e., when the drying mechanism changes from surface evaporation to loss of water from the internal fiber structure. In evaluating the recovery of fabric from wet wrinkling, therefore, the recovery angle should be measured only after it has come to equilibrium with the atmosphere.

The wrinkle recovery of the fabrics after wet wrinkling is independent of the rate of drying.

Fabrics of wool, wool blends, and cotton which have reached equilibrium wrinkle recovery after wet creasing, show additional, progressive, step-wise recovery when subjected to repeated rewetting–drying cycles. Fabrics which have very poor normal recovery from wet creasing can ultimately exhibit excellent recovery after several such cycles. The same behavior is observed with alternate steaming–drying cycles.

The effect results only from an alternating increase and decrease in regain, as prolonged immersion in water, prolonged drying, or rewetting without intermediate drying, does not give additional recovery. Probably the progressive recovery is due to some of the fiber and yarn interactions and frictional forces responsible for maintaining the fabric deformation being overcome by the small forces generated by the swelling–deswelling process.

Acknowledgments

The work described was carried out while A. J. Farnworth was a guest worker at the Swedish Institute for Textile Research (TEFO). This author would like to express his appreciation to the Executive of C.S.I.R.O. and the Chief of the Division of Textile Industry (Dr. M. Lipson) for enabling him to have this experience, and to Professor Nils Gralén, Docent Joel Lindberg, and the staff of TEFO for helpful discussion and for the wonderful friendship, kindness, and hospitality extended to him and his family during their stay in Gothenburg.

Literature Cited

1. Buck, G. S. and McCord, F. A., TEXTILE RESEARCH JOURNAL **19**, 235 (1949).
2. Farnworth, A. J., TEXTILE RESEARCH JOURNAL **27**, 632 (1957).
3. Farnworth, A. J., Lipson, M., and McPhee, J. R., TEXTILE RESEARCH JOURNAL **30**, 11 (1960).
4. Lindberg, J., Bernskiöld, A., Behre, B., and Dahlberg, B., *Meddelande fr. TEFO,* Nr. 4 (1960). (Swedish Institute for Textile Research.)
5. Lindberg, J., Waesterberg, L., and Svenson, R., *J. Textile Inst.* **51**, T1475–T1491 (1960).
6. Monsanto Chem. Co., "Monsanto Wrinkle Recovery Tester," *Tech. Bull.* T30–45.1; Am. Soc. Testing Materials, Tentative Test Method D1295–53T.
7. Wilkinson, P. R. and Hoffman, R. M., TEXTILE RESEARCH JOURNAL **29**, 652 (1959).

Manuscript received December 27, 1960.

The Influence of Changes in Moisture Content on the Wrinkle Recovery of Fabrics, Part II

Joel Lindberg

Swedish Institute for Textile Research, Gothenburg, Sweden

TWO seemingly contradictory obesrvations are reported in Part I of this paper. If a dry-creased wool fabric is wetted, a complete recovery is obtained. If a wet-creased and dried wool fabric is rewetted, no recovery whatsoever is obtained. A progressive recovery upon alternate drying and wetting is, however, clearly established. A dry-creased cotton fabric does not give complete recovery on wetting, but both a dry-creased and a wet-creased cotton fabric show progressive recovery on alternate drying and wetting.

The question is how these observations can be explained in terms of current theories of crease recovery.

The generally accepted theory has been that poor crease recovery is due to a permanent deformation of fibers (see, for instance, recent work by Abbot et al. [1]. However, on wetting the fibers, one would expect a substantial recovery from the fiber deformation resulting in a recovery from fabric deformation. This is what happens to the dry-creased fabrics and, in the case of wool fabrics, the recovery is complete. The recovery of dry-creased fabric on wetting is therefore compatible with the theory of permanent fiber deformation.

Since there is, to our knowledge, no evidence for a progressive recovery from deformation of fibers on alternate drying and wetting, the theory of permanent fiber deformation is incompatible with the progressive recovery of fabrics on alternate drying and wetting.

There is a growing conviction that frictional restraint on fibers plays an important role in crease recovery. Daniels [2] has shown that some results could be explained by friction between fibers. The elastic forces of the fibers have to overcome the frictional forces between the fibers during recovery. When these two types of forces balance each other, there will be no further fiber movement and there will be, accordingly, a permanent deformation of the fabric.

Lindberg et al. [3] suggested a simple rheological model (Figure 1) to give a qualitative picture of the recovery. The model does not give a quantitative description of what happens because this would require knowledge of, or assumptions about, the statistical distribution throughout the fabric of the frictional forces and the fiber parameters represented in the model by springs and a dash-pot. Figure 2 shows a load–extension curve for the model.

If the model is loaded very rapidly, there would be an immediate increase in load to A ($OA = N\mu$, where N = normal force and μ = coefficient of friction) and a progressive increase with slope k_1 to B. If the model is then held for a long time at this extension, the load falls to C. The slope of the line AC is k_3, where $k_3 = k_1 k_2/(k_1 + k_2)$. If the model is now released, the load will decrease immediately to D ($CD = 2N\mu$) and then to E with a slope k_1. After a long time, the model will contract to F and the slope of the line DF is k_3. The distance OF, which is the permanent deformation of the model, is equal to $N\mu / k_3$.

It can now be shown how this model could be made to behave under conditions similar to those expected in the fabric during alternate wetting and drying.

Olofsson has suggested rheological models for the

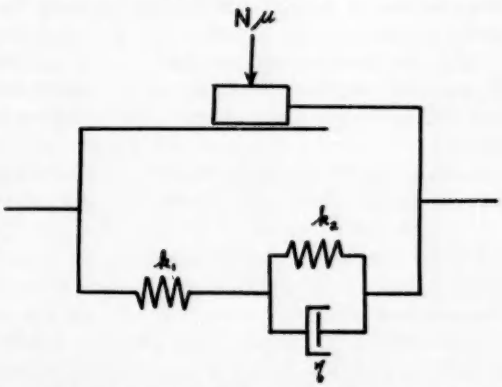

Fig. 1. Simple rheological model for describing qualitatively the recovery of fabrics from deformation.

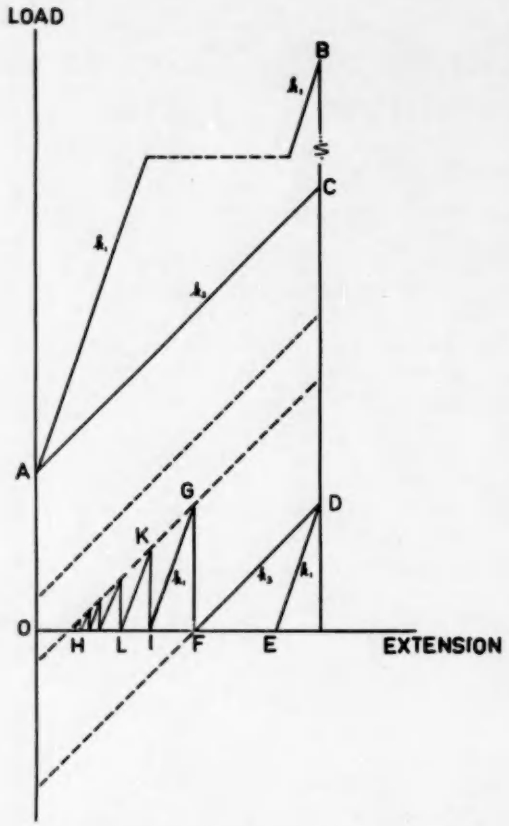

Fig. 2. Load–extension characteristics of the model shown in Figure 1.

behavior of wool fibers under changing humidity and temperature [4]. He introduced into the model a dash-pot and a parallel spring and assumed two extreme values for the viscosity in the dash-pot; $\eta = 0$ at standard atmospheric conditions and $\eta = \infty$ at maximum regain. This part of the model was intended to simulate the cohesive set obtained in drying.

Assume that the model in Figure 1 can have two extreme values of viscosity in the dash-pot; $\eta = 0$ and $\eta = \infty$. Assume further that the frictional force will be $N_1\mu_1$ when $\eta = 0$ and $N_2\mu_2$ when $\eta = \infty$, where $N_1\mu_1 > N_2\mu_2$. The reason for this assumption is that $\eta = 0$ corresponds to the wet, swollen fiber state when both N and μ are almost certain to be higher than when $\eta = \infty$, which corresponds to the dry state.

The model is now extended while $\eta = 0$. The load increases immediately to A ($OA = N_1\mu_1$) and then with slope k_3 to C. The model is then released, and the load drops immediately to D, where $CD = 2N_1\mu_1$. It then decreases with slope k_3 to F. The distance OF will be the permanent deformation of the model corresponding to the wet fabric and, as before, it will be equal to $N_1\mu_1 / k_3$. If it is now assumed that the friction is changed from $N_1\mu_1$ to $N_2\mu_2$ without changing η, the load will increase to G and then decrease with slope k_3 to H where OH will equal $N_2\mu_2 / k_3$. However, in reality, $N_1\mu_1 \rightarrow N_2\mu_2$ when $\eta = 0 \rightarrow \eta = \infty$. Therefore the load will increase to G and decrease with slope k_1 to I. If the system is now changed back to $N_1\mu_1$ and $\eta = 0$, nothing will happen except attainment of force equilibrium between k_1 and k_2. If we change back again to $N_2\mu_2$ and $\eta = \infty$, the system will go from I to K and to L. This can be repeated until point H is reached.

It has been established, therefore, that the theory of frictional restraint is indeed compatible with the progressive recovery on alternate drying and wetting, and in fact gives a far better explanation than the theory of permanent fiber deformation.

Literature Cited

1. Abbott, N. J., Coplan, M. J., and Platt, M. M., *J. Textile Inst.* **51**, T1384 (1960).
2. Daniels, W. W., TEXTILE RESEARCH JOURNAL **30**, 656 (1960).
3. Lindberg, J., Behre, B., and Dahlberg, B., TEXTILE RESEARCH JOURNAL **31**, 99 (1961).
4. Olofsson, B., *J. Textile Inst.* **52**, T272 (1961).

Manuscript received December 27, 1960.

Lightfastness Studies of Basic Dyes on Acid-Modified "Dacron"[1] Polyester Fiber

S. B. Maerov and H. Kobsa

"Dacron" Research Laboratory, Textile Fibers Department, E. I. du Pont de Nemours and Company, Inc.

Abstract

Application of basic dyes to acid-modified polyethylene terephthalate fibers offers such attractive features as brightness of shade, excellent color value, and good solvent and sublimation-fastness. Lightfastness studies of basic dyes on this polymeric substrate indicate that the Critical Fading Region (C.F.R.) is a rather narrow spectral region extending from 350 to 425 mμ. Substituted hydroxybenzophenones such as 2,2′-dihydroxy-4,4′-dimethoxybenzophenone (DHDMBP) act as light screeners with many of these dyes in the C.F.R. and extend their lightfastness in dyed fabrics. Many of these screeners can be applied to the fiber by normal dyeing techniques. The requirements for efficient screening ability of these agents are discussed. Photosensitization of dyes by some screeners with a resultant diminution of lightfastness is ascribed to a radiationless transfer of energy from screener to dye by a resonance transfer mechanism. Chemically modified DHDMBP gave improved lightfastness in dark shades utilizing the tinctorially strong triphenylmethane dyes. The lightfastness improvement due to these modifications can be ascribed to their enhanced bathochromic absorption in the C.F.R. relative to the absorption spectrum of DHDMBP.

Introduction

The basic or cationic dyes are historically among the oldest of the synthetic dyestuffs. Applied to synthetic fibers, this class of dyes offers such attractive features as brightness of shade, high tinctorial power resulting in excellent color value, and fastness to sublimation and solvent bleed. Many of these features have been realized by application of basic dyes to the linear condensation polyester fiber containing metal sulfonate groups [8]. A variety of basic dyes of the "Sevron"[2] type and the recently announced "Dekatyl"[2] dyes recommended expressly for Types 62 and 64 Dacron, may be applied to this fiber substrate with adequate lightfastness in men's and women's wear. Some basic dyes have, however, shown inadequate lightfastness when applied to this fiber. The purpose of these studies was to determine the spectral regions responsible for the fading of these dyes and to determine means for upgrading their lightfastness. The dye lightfastness and fading studies reported below were conducted on Type 62 Dacron (70/34) filament yarn, Type 64 Dacron staple yarn, and films of this modified linear condensation polyester.

[1] Trademark for Du Pont's polyester fiber.
[2] Trademark for Du Pont's cationic dyes.

Fading Studies

Initial experiments were designed to determine the regions in the daylight spectrum which might be responsible for the fading of basic dyes on acid-modified Dacron. Type 64 Dacron fabric was dyed with a number of basic dyes and exposed in late summer at Kinston, North Carolina, in the open, facing south at 45°. The dyed yarns were covered with a series of Corning glass filters designed to "black out" progressively regions of the spectrum below 310, 350, 395, 425, 460, 490, 560, 590, and 610 mμ. Similar techniques have been used by Appel and Smith [1] and more recently by McLaren [9]. Table I shows the results of one such experiment with five different basic dyes. After 48 hr. exposure, all the uncovered dyed samples showed a degree of fade of 1 based on the scale where 5 equals no change and 1 equals very severely changed. Virtually no protection was afforded by filtering out light of wavelengths less than 350 mμ. This was especially true for such classes of basic dyes as the oxazines, cyanines, and xanthenes. In the case of

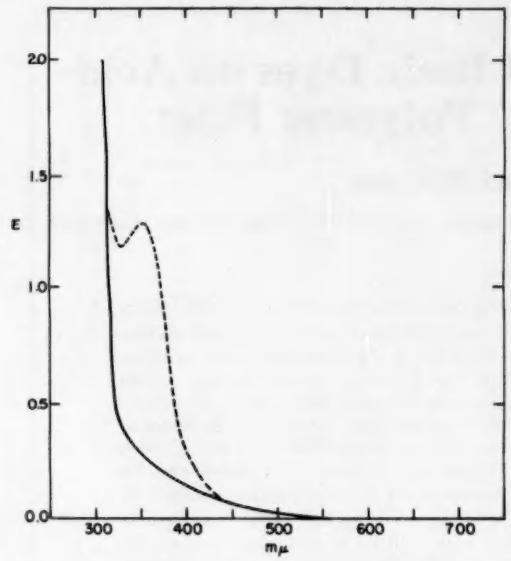

Fig. 1. Absorption spectra of untreated and screener-dyed film: ———— 0.002 in. acid-modified polyethylene terephthalate film, mock-dyed; — — — — 0.002 in. acid-modified polyethylene terephthalate film, dyed with 1% of DHDMBP.

certain triphenylmethane dyes, the fading region extended beyond 390 mμ to 425 mμ. The spectral region from 350 to 425 mμ is apparently the Critical Fading Region (C.F.R.) for these basic dyes on this fiber substrate. It is believed that this behavior results from the interplay of several factors, three of which are particularly important: the dependence of the quantum yield of fading on wavelength; the spectral distribution of sunlight; the absorption characteristics of the polymer substrate. At long wavelengths (above 390 or 425 mμ, depending on the dye) the quantum yield of the fading reaction drops to very low values and such light causes little or no fading. Light of wavelengths shorter than 350 mμ, on the other hand, is of relatively small abundance in natural sunlight. A rough calculation based on the data given by Forsythe [6] shows that for cloudless weather at sea level and a zenith distance of the sun of 0°, the intensity of the light incident in the wavelength region below 350 mμ is only about one-third of the intensity incident between 350 and 400 mμ; for a zenith distance of 60°, this ratio drops to one-sixth. In addition, the polymer substrate absorbs increasingly strongly at wavelengths below 350 mμ (see Figure 1) and therefore absorbs much of the light incident in this region. While light of less than 350 mμ wavelength is photochemically active and does cause fading, the amount of light in this spectral region that reaches the dyes is so much lower than that of the light of longer wavelengths that it contributes but little to the overall fading rate. This is in agreement with our findings that a filter cutting off wavelengths below 350

TABLE I. Critical Fading Region for Some Basic Dyes on T-64 Dacron Polyester Fiber

Filter used*		Degree of fade rating† after 48 hr. exposure to sunlight (2.0% dye on weight of fiber)				
		Dye color index, application class				
		C. I. Basic Violet 10	C. I. Basic Blue 4	C. I. Basic Green 1	C. I. Basic Blue 7	C. I. Basic Violet 14
		Dye, structural class				
Filter wavelength cut-off, mμ	Glass code number	Xanthene	Oxazine	Triphenyl-methane	Triphenyl-methane	Triphenyl-methane
None		1	1	1	1	1
310	0160	1	1	1	1	1
350	7380	1	2	1	1	1
390	3060	5	5	4	4–3	4
420	3389	5	5	5	5	5
460	3387	5	5	5	5	5

* Corning glass color filters: Catalogue Form No. C-248 Rev. 5–11–53. The glass code number refers to the molded glass from which the color filter was produced. The molded glass was polished to thickness specifications such that the percent transmittancy at the stated filter cut-off wavelength was 20 ± 5%.

† Degree of Fade Rating: 5 = unchanged; 4 = slightly changed; 3 = moderately changed; 2 = considerably changed; 1 = very severely changed.

TABLE II. Screening Effect of Polyester Films Containing Substituted Hydroxybenzophenones

Substituted hydroxybenzophenone			Wavelength, mμ, at 50% transmittancy for film plus screener cover*	Degree of Fade Rating† after 20 hr. Fade-Ometer exposure (2.0% dye on weight of fiber)	
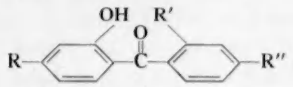				C. I. Basic Red 14 (Cyanine)	C. I. Basic Green 1 (Triphenylmethane)
Uncovered			—	1	1
Untreated film			350	2	1
R	R′	R″			
OCH_3	H	H	382	2–3	1
H	OH	H	388	3	1
OCH_3	OH	OCH_3	410	5–4	2–3
OCH_3	OH	OCH_3 nickel complex‡	426	5	5–4

* 2.0 mil film containing 1.0 ± 0.1% screener on weight of film.
† Degree of Fade Rating: 5 = unchanged; 4 = slightly changed; 3 = moderately changed; 2 = considerably changed; 1 = very severely changed.
‡ See Figure 5A for the structure of this nickel complex.

mμ gives hardly any protection at all to basic dyes on a Type 62 or 64 Dacron substrate.

The C.F.R. is, then, that region of the spectrum which causes most of the fading, because both the quantum yield of fading and the intensity of the incident light are high at those wavelengths. For the fading of basic dyes on acid-modified Dacron in sunlight, this is the region between 350 and 390 or 350 and 425 mμ. The spectral distribution of the Fade-Ometer radiation does not approximate the spectral distribution of sunlight very well. However, the radiation of the Fade-Ometer does show a drop-off in intensity below 350 mμ and, perhaps somewhat fortuitously, gave C.F.R. results comparable to those obtained in sunlight. It should be pointed out, however, that this will not always be the case. Artificial light sources should not be used for the evaluation of UV absorbers without prior ascertainment that they show, for the system under investigation, the same C.F.R. as sunlight.

The hyopthesis that protection against fading could be obtained by screening out the wavelengths in the C.F.R. was further tested with a number of organic compounds having strong light absorption properties in this spectral region. The substituted hydroxybenzophenones were especially useful for this purpose since their absorption properties could be progressively shifted to longer wavelengths by varying the degree of substitution on the benzophenone nucleus. A number of recent publications have indicated the effectiveness of these hydroxybenzophenones in preventing photodegradation of polymeric substrates in the form of clear or pigmented films [2, 7, 10]. Films of polyethylene terephthalate containing such organic compounds[3] were exposed in the Fade-Ometer over Type 62 Dacron yarns dyed with a variety of basic dyes. The relative effectiveness of these screener combinations in preventing the fading of a cyanine dye (C.I. Basic Red 14) and a triphenylmethane dye (C.I. Basic Green 1) is shown in Table II. Both these dyes were very severely faded (Degree of Fade Rating = 1) after 20 hr. exposure in the Fade-Ometer. The cyanine dye was very slightly protected when covered by the untreated film or by film containing 2-hydroxy-4-methoxybenzophenone; the triphenylmethane dye showed no improvement with these combinations. 2,2′-Dihydroxybenzophenone with increased screening ability from 350 to 388 mμ afforded some protection to C.I. Basic Red 14 (C.F.R. 350 to 390 mμ) but was ineffective for the triphenylmethane dye (C.F.R. 350 to 420 mμ). 2,2′-Dihydroxy-4,4′-dimethoxybenzophenone (DHDMBP) gave almost complete protection to the cyanine dye for this exposure period but was only partially effective for the triphenylmethane dye. The nickel complex of DHDMBP (Figure 5) with enhanced bathochromic absorption relative to DHDMBP was able to protect the cyanine and the triphenylmethane dyes. Similar techniques with substituted hydroxybenzophenones on cellulose acetate film were reported

[3] U. S. Patent 2,920,978, granted Jan. 12, 1960, disclosed the strong affinity of many of these hydroxybenzophenones for polyethylene terephthalate fibers. Rapid "dyeing in" of these screeners into Dacron polyester fiber resulted after brief exposure in diethylene glycol solution at elevated temperature.

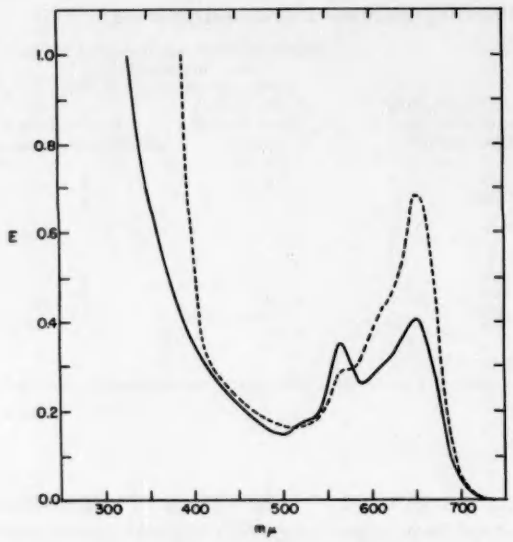

Fig. 2. Methylene Blue in presence of co-dyed screener: ———— 0.002 in. acid-modified polyethylene terephthalate film, dyed with 0.05% of Methylene Blue. – – – – Same + 1.0% DHDMBP on film weight.

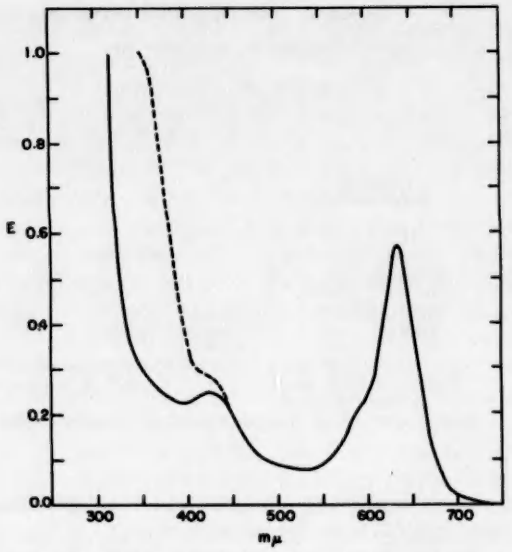

Fig. 3. Brilliant Green in presence of co-dyed screener: ———— 0.002 in. acid-modified polyethylene terephthalate film, dyed with 0.05% Brilliant Green. – – – – Same + 1.0% DHDMBP on film weight.

to give increased protection to a variety of dyes on cotton and wool [3]. The absorption cut-off for these organic screeners [3] was not as sharp as that observed for the glass filters; however, the relative improvement in dye lightfastness observed with a number of dyes on the acid-modified polyester correlated well with the previously determined C.F.R.'s for these same dyes obtained with sharp cut-off filters.

If a UV absorber is to be employed for protecting dyes on fabrics in actual use, the absorber must be evaluated on the fiber substrate in the presence of dye. Absorbers were applied to the fabric by the dyeing procedures described below. The fact that a compound absorbs strongly in the C.F.R. does not necessarily make it a good screener. Differences in effectiveness were often observed for a given absorber depending on whether it was used as a screen in front of the dyed substrate or was within the dyed substrate. Of a considerable number of potential screening agents tested, only a few conferred protection upon basic dyes when applied directly to the fabric. The others were ineffective or even caused accelerated fading. For instance, 2,4-dibenzoylresorcinol was found to cause severe light sensitization of a number of dyes.

The explanation of the ability of some of these compounds to accelerate dye fading rather than inhibit it requires the postulation of two opposing forces. On the one hand, any compound absorbing strongly in the near ultraviolet region of the spectrum will be effective in screening out some of the light incident in the C.F.R. and will, therefore, tend to prolong the useful life of the dyes. On the other hand, some compounds simultaneously photosensitize the dyes. Depending on which effect predominates, the net result will then be either one of protection or of sensitization.

Obviously it would be of great interest to elucidate the nature of this photosensitization. During the course of this work no obvious correlation could be found between chemical structure and the presence or absence of sensitizing propensity in many classes of compounds. For this and other reasons, the authors do not believe that sensitization is usually chemical in nature, i.e., a reaction between dye and screener upon illumination. Rather, the most probable mechanism of sensitization consist of radiationless transfer of energy from the screener to the dye. The specific process involved would most likely be a resonance transfer or a virtual photon transfer of the type described by Förster [4, 5]. Since a detailed discussion of this matter is outside the scope of this article, the following remarks will suffice:

1. A high extinction coefficient in the C.F.R. of the spectrum is a necessary but not sufficient requirement for a good screener.[4]

2. In order to be effective as a screener, a compound must be able, not only to absorb harmful light, but also to dissipate it in a harmless fashion. That is, a screener must not transfer absorbed energy to the dyes.

3. The probability of energy transfer is determined by the spectral properties of both screener and dye [4, 5]. Some potential screening agents will be more likely than others to enter into energy transfer reactions; such compounds are of little practical utility. Other compounds show energy transfer only on rare occasions; those will be more useful in prolonging the life of dyes.

While radiationless energy transfers may occur over considerable distances [4, 5], their probability is greatly enhanced if the two participating molecules are in close proximity to each other. For this reason, complex formation between a dye and a UV-screener should increase the likelihood of energy transfer and consequent sensitization of the dye. Fortunately, complex formation does not seem to be a general phenomenon. In our work, it was observed only in the case of C.I. Basic Blue 9 (Methylene Blue). The spectrum of this dye on a polyethylene terephthalate film is shown in Figure 2, both in the absence of an added UV-screener and in the presence of 1%, on fiber weight, DHDMBP. From the considerable change in the relative intensity of the two visible absorption peaks of the dye it is quite apparent that some sort of interaction with the UV-screener must have taken place. We believe that it is significant that this dye was found to be sensitized by all screening agents tried so far, including DHDMBP. For comparison purposes, a typical example in which there is no apparent interaction between dye and UV-screener is shown in Figure 3.

Application of Screening Agents to Type 64 Dacron

The foregoing indicated what were the prerequisites for an agent to inhibit basic dyes from fading on the polymeric fiber or film substrate. One of the most efficient agents which satisfied many of these requirements was 2,2′-dihydroxy-4,4′-dimethoxybenzophenone (DHDMBP).[5] This agent could be satisfactorily applied to Type 64 Dacron by the usual techniques for application of disperse dyes; it can be satisfactorily applied by predyeing, co-dyeing with the basic dyes, or afterdyeing into fabric or yarn. Figure 4 shows the exhaustion characteristics of DHDMBP applied at the boil to staple fabric of acid-modified Dacron. Gantz and Sumner have reported similar application techniques for hydroxybenzophenones on nylon fabric [7]. Although no carriers were necessary for adequate penetration of this screener or other screeners of the substituted *o*-hydroxybenzophenone type, they proved compatible with the usual commercial polyester carriers when co-applied in the same bath. These agents proved relatively sublimation-fast to the usual Dacron heat-setting conditions and were also exceptionally washfast and solvent-fast to commercial laundering and drycleaning, respectively.

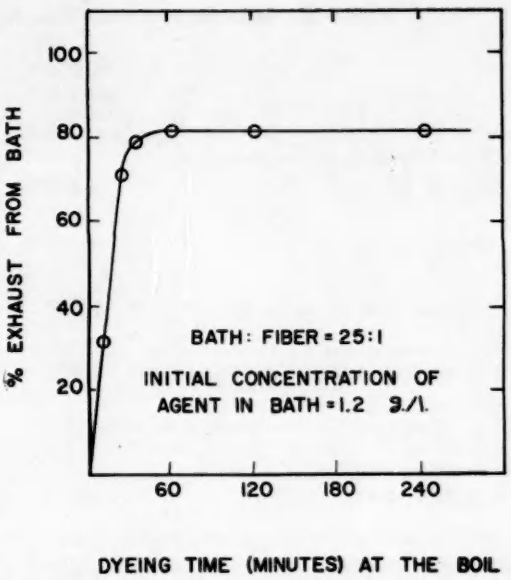

Fig. 4. Percent exhaust from bath of 2,2′-dihydroxy-4,4′-dimethoxybenzophenone on Type 64 Dacron.

The ultraviolet screener DHDMBP proved extremely efficient in extending the lightfastness of a number of self-shade dyes at loadings of 0.6% to 1.5% of absorber on fiber weight. Table III summarizes results for a number of basic dyes on T-64

[4] A corollary to this requirement is that absorption in the C.F.R. be strong enough to allow commercial application of the agent to the dyed fiber at low enough levels to be economically practical.

[5] This compound is one of the active ingredients of the commercial ultraviolet screeners, "Uvinul" D-49 and "Uvinul" 490, marketed by the Antara Chemicals Division of the General Aniline and Film Corporation.

TABLE III. Lightfastness of Some Basic Dyes on T-64 Dacron—Effect of Co-Dyed DHDMBP

Dye	% Dye on wt. of fiber	% DHDMBP on wt. of fiber	Fade-Ometer hours for degree of fade rating of:* 4	3	2
A. Dyes showing significant protection					
"Sevron" Red GL	1.2	None	10	15	20
		0.6	15	25	40
"Sevron" Bordeaux G	1.75	None	10	15	20
		0.7	15	25–30	35
C. I.Basic Violet 14 (Fuchsine)	0.6	None	8	12–15	
		1.5	30–35	35–40	
C. I. Basic Green 1 (Brilliant Green)	0.6	None	0.75	1.25	3
		1.15	3	5	7
"Sevron" Blue BR	2.0	None	7	13	24
		1.5	16	28	49
C. I. Basic Red 14	2.0	None	6	10	15
		1.0	20	25	40
		1.0 Ni complex†	30	45	60
Cationic Black: "Sevron" Yellow 3RL / Basic Violet 14 / Basic Green 1	0.75 / 0.40 / 0.75	None	10	15	20
		1.5	18	22	28
Cationic Navy: "Sevron" Yellow 3RL / Basic Violet 14 / Basic Green 1 / Basic Blue 4	0.26 / 0.30 / 0.42 / 1.0	None		12	20
		1.5		20	25
		1.5 Thioketone mixture‡		35	45
B. Dyes showing no protection or sensitization					
C. I. Basic Green 4 (Victoria Green)	0.5	None	0.5	0.7	1.0
		1.25	0.55	0.8	1.25
C. I. Basic Blue 9 (Methylene Blue)	0.35	None	0.8	1.25	2
		1.05	0.25	0.5	0.8

* Degree of Fade Rating: 4 = slightly changed; 3 = moderately changed; 2 = considerably changed.
† DHDMBP–Ni(II) complex; see Figure 5A.
‡ Mixture containing 95% DHDMBP and 5% of its thioketone derivative, see Figure 5B.

Dacron with and without co-dyed DHDMBP. In the case of self-shade dyes the presence of the screener served to decrease the rate of dye fading or to extend the Fade-Ometer exposure hours required to reach a given degree of fade rating. In many cases the absolute increase in exposure hours to a given degree of fade amounted to a 200% to 300% improvement. It should be pointed out, however, that some of these dyes would be unacceptable in commercial application for self-shades even with the improved lightfastness obtained with a screener. In other cases the improvement with a screener is sufficient to raise them from the submarginal class to the rank of a commercially useful dyestuff. Two cationic dark shade formulations (navy and black) utilizing the triphenylmethane dyes are also included in Table III. Only a marginal improvement resulted in these dark shade formulations in the presence of DHDMBP. This was believed to be due to the fact that DHDMBP supplied insufficient screening ability for these dyes in the region extending from 390 to 420 mμ. When the absorption ability of DHDMBP was extended, by chemical modifications, to include the longer wavelengths, improved fading protection in these formulations resulted. These modifications, shown in Figure 5, which gave enhanced bathochromic absorption relative to that of DHDMBP, without apparently impairing its screen-

ing ability or promoting sensitization were (a) the nickel (II) complex of DHDMBP and (b) a mixture of DHDMBP and its thioketone derivative. Table III shows the improvement afforded the cyanine dye, Basic Red 14, when 1.0% of the nickel (II) complex was substituted for 1.0% of DHDMBP. Similarly, the cationic navy improved an average of 2.47-fold versus 1.46-fold when 1.5% of a mixture of DHDMBP containing 5% of its thioketone derivative was substituted for 1.5% DHDMBP. The absorption spectra of DHDMBP and its two modifications are shown in Figure 6.

Both of these modifications were more deeply colored than DHDMBP (in the yellow to orange region) and caused some darkening of the shade in navy blues or blacks. However, compensation for the color of these agents could be made in the dark shade dye formulation to give the required shade.

In conclusion, it has been shown that ultraviolet absorbers may be useful in upgrading the lightfastness of basic dyes on Types 62 and 64 Dacron. This approach has been little exploited commercially at the present time but offers promising possibilities especially for dyes whose lightfastness is marginal in specific end uses. The screener approach is only one solution to this problem since more lightfast basic dyes have already been commercialized and dyes with inherently improved light stability are currently being developed.

A. 2,2′-dihydroxy-4,4′-dimethoxybenzophenone nickel (II) complex. A probable structure for the complex formed from DHDMBP and Ni (II) salts is:

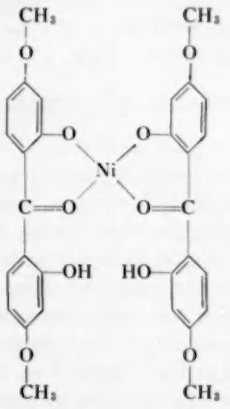

B. 2,2′-dihydroxy-4,4′-dimethoxythiobenzophenone

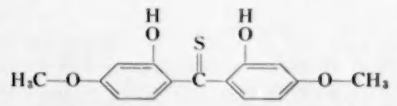

Fig. 5. New screeners derived from DHDMBP.

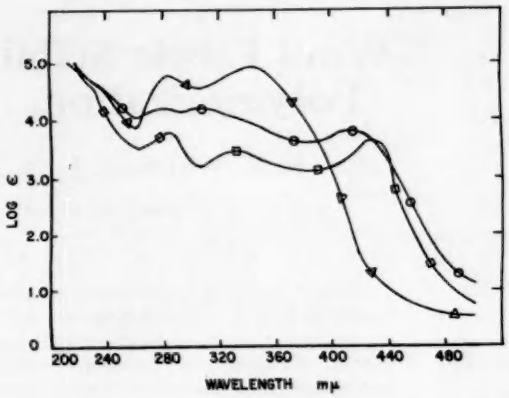

Fig. 6. Absorption spectra of various screeners (in methanol): △ 2,2′-dihydroxy-4,4′-dimethoxybenzophenone (DHDMBP); □ DHDMBP thioketone derivative; ○ DHDMBP nickel (II) complex.

Acknowledgment

The authors express their appreciation to many colleagues in the Du Pont Company for the cooperation received in these endeavors. In particular, we would like to mention the many helpful discussions held with Drs. R. H. Terss and H. P. Landerl of the Organic Chemicals Department.

Literature Cited

1. Appel, W. D. and Smith, W. C., *Am. Dyestuff Reptr.* **17**, 410 (1928).
2. Batdorf, S. B. and Gantz, G. W., *Offic. Dig.* **28**, No. 2, 65 (1956).
3. Coleman, R. A. and Peacock, W. H., TEXTILE RESEARCH JOURNAL **28**, 784 (1958).
4. Förster, T., *Ann. Physik* **2**, 55 (1948).
5. Förster, T., *Discussions Faraday Soc.* **27**, 7 (1959).
6. Forsythe, W. E., "Measurement of Radiant Energy," New York, McGraw-Hill Book Co., Inc., 1937, Table II, p. 77.
7. Gantz, G. W. and Sumner, W. G., TEXTILE RESEARCH JOURNAL **27**, 244 (1957).
8. Griffing, J. M. and Remington, W. R. (to E. I. du Pont de Nemours and Co.) Belgium Patent Number 594,179 (July 14, 1956); *idem.*, Belgium Patent Number 562,460 (May 19, 1958).
9. McLaren, K., *J. Soc. Dyers Colourists* **72**, 86 (1956).
10. Weth, R. J. and Signore, A. C., *Am. Paint J.* **42**, No. 6 (Oct. 1957).

Manuscript received October 10, 1960.

Wool Fabric Stabilization by Interfacial Polymerization. Part I: Polyamides

R. E. Whitfield, L. A. Miller, and W. L. Wasley

Western Regional Research Laboratory,[1] Albany 10, California

Abstract

A new technique is presented for making wool fabrics shrink resistant. Through interfacial polymerization polyamides, e.g., poly(hexamethylene sebacamide), are formed on the surface of the textile fibers. Fabric is padded consecutively through an aqueous solution of a diamine and a water-immiscible solution of a diacid chloride. Polymerization is extremely rapid and no heating or curing is required. Following the two-step padding, the fabric is simply washed and dried. Less than 5% resin on the fabric is required for dimensional stability in laundering. The wool fabrics treated are essentially unchanged in hand, flexural rigidity, break strength, percent elongation, and chemical resistance; they are improved in wrinkle recovery and smoothness after tumble drying.

Introduction

The present paper reports the general scope of treatment of wool fabrics with polyamides by interfacial polymerization, demonstrates the effect of several reaction variables on the treatment, and describes the effect of the treatment on various chemical and physical properties of the wool.

Interfacial polymerization has been highly successful for the preparation of a variety of condensation polymers [4, 7, 13, 14, 15, 16, 19, 20, 21, 23, 25, 26]. This technique consists in bringing a solution of a diacid chloride in an inert, water-immiscible, organic solvent, into contact with an aqueous solution of a diamine; polymer is formed almost instantaneously at or near the interface of the two liquid phases. The polymerization is based on the Schotten–Baumann reaction of an acid chloride with a compound containing an active hydrogen such as $-OH$, $-NH_2$, $-SH$ (Figure 1).

The polymers prepared by interfacial polymerization are not new ones, but their formation by the interfacial method is new and unique. The technique is of interest because of its general simplicity and versatility compared with the more conventional procedures for the preparation of condensation polymers.

The method of applying polymers by the interfacial polymerization technique to produce shrink-resistant wool fabrics has not been reported previously. It is a promising new method for preparing shrink-resistant wool fabrics, with little or no impairment of the desirable physical properties, and promises to have advantages over resin treatment methods previously reported.

The use of preformed polyamides and polyamide derivatives to impart shrink resistance to wool has been reported previously [6, 9–12], as has the use of synthetic polypeptides [1, 3, 5]. However, none of these workers used the interfacial polymerization procedure being reported here.

[1] A laboratory of the Western Utilization Research and Development Division, Agricultural Research Service, U. S. Department of Agriculture.

Materials and Procedures

Wool Fabric

A 6.12-oz./yd.[2] undyed worsted wool flannel containing 64 ends and 55 picks/in. was used. Before treatment, unless otherwise stated, the flannel was extracted in a Soxhlet extractor with ether for 8 hr., and then with ethanol for 8 hr., then rinsed with tap water, dried at room temperature, and conditioned to equilibrium at 70° F. and 65% RH (standard conditions). Swatches, about 5 in. sq., conditioned and weighed before and after treatment, were used to determine polymer uptake.

Reagents and Solvents

Adipoyl chloride. A mixture of 300 g. of adipic acid (2.05 moles) and 512 g. of thionyl chloride (4.3 moles) was heated slowly to reflux with stirring.

Reflux was continued for 3 hr. and 10 min., until evolution of HCl ceased; then dry nitrogen was bubbled through the solution for 1½ hr. The resulting adipoyl chloride distilled at 80° C. under a pressure of 0.4 mm. Hg.

Azelaoyl chloride. Azelaoyl chloride was obtained from Trubek Laboratories [2] and used without further purification.

Pimeloyl chloride. The procedure was that used for adipoyl chloride, with the exception that the mixture of pimelic acid and thionyl chloride was held at 80° C. for 3 hr. After removal of excess thionyl chloride, the pimeloyl chloride distilled at 79° C. at 0.2 mm. Hg.

Sebacoyl chloride. The procedure was the same as used for adipoyl chloride, using sebacic acid with an excess of thionyl chloride. The sebacoyl chloride distilled at 106° C. at 0.25 mm. Hg.

Terephthaloyl chloride. Eastman, practical grade, was used without further purification.

1,6-Hexamethylene diamine. An 85% aqueous solution obtained from Du Pont.

Meta-xylylene diamine. A development sample obtained from California Chemical Company.

Piperazine. Eastman, practical grade, was used without further purification.

The solvents used were carbon tetrachloride (Baker Reagent Grade), Skellysolve "B" (Skelly Oil Company), toluene (Baker Reagent Grade), methyl chloroform (The Dow Chemical Company), Stoddard solvent (Standard Oil Company of California—thinner grade).

Interfacial Formation of Polymer

Weighed and conditioned wool flannel swatches are immersed for varying lengths of time up to 60 sec. in an aqueous solution of the diamine, then passed through squeeze rolls to remove excess solution. Subsequently the cloth is immersed in a non-aqueous solution of the diacid chloride for varying lengths of time up to 60 sec. and again passed through squeeze rolls to remove excess solution. The immersion of the diamine-treated fabric into the acid chloride solution results in almost instantaneous formation of a polyamide resin at the fiber surface (Figure 1). The fabric is finally rinsed thoroughly with water and dried at 100° C. for 15–20 min. or

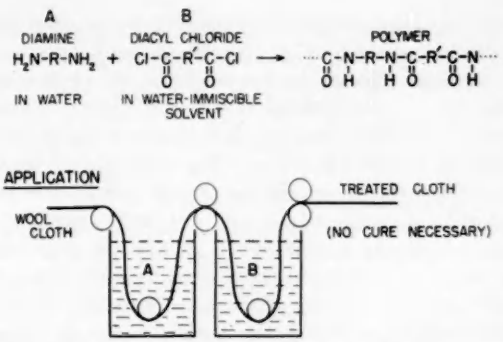

Fig. 1. Interfacial polymerization. Schematic representation of chemistry and application.

at room temperature, if preferred. The order of treatment may be reversed by simply applying the non-aqueous solution of diacid chloride first and the aqueous amine solution second, though this is not the preferred of the two procedures because it is not as effective and resin deposition is generally not as uniform.

Testing Methods

Wrinkle recovery. ASTM test method D 1295-53T was employed, using the Monsanto Wrinkle Recovery Tester.

Flexural rigidity. The Cantilever Procedure, ASTM D 1388-55T, was used to determine flexural rigidity of the resin-treated wool flannel swatches.

Shrinkage tests. The Accelerotor [22] was used to test the shrinkage resistance of the polymer-treated flannel swatches. The conditions were 1780 r.p.m., 2 min., 200 ml. of 1 % sodium oleate, 40° C., 6 × 5 in., preconditioned in 1% sodium acetate, 10 cm. marks. One 2-min. Accelerotor wash under the specified conditions is equal to about fifteen home launderings [17, 18].

Fabric breaking strength. ASTM Method D 39-40, cut strip method; 6 × 1 in.; 3-in. gauge; 20 sec. to break.

Moisture regain. Wool flannel swatches were conditioned at 70° F. and 65% RH; equilibrium was approached from the dry side. The weight of the dry sample was determined on material dried for 4 hr. at 105° C.

Rate of drying. Wool swatches weighing about 0.9 g. were wet out in water containing 0.1% non-ionic detergent. Wetted swatches were merely removed from the water with no squeezing, and the

[2] Mention of specific products or manufacturers does not imply recommendation by the Department of Agriculture over others not mentioned.

rate of loss in weight was followed by hanging the swatches on a multiple-unit relaxometer [24].

Soiling. The soiling test employed is a qualitative one for comparing the soiling tendency of untreated and treated wool fabrics. The soiling mixture consists of 10 parts by weight Norite C carbon black and 90 parts by weight anhydrous sodium sulfate, or vacuum sweeper soil only. A test swatch and control swatch, each about 4 in. sq., are placed in a jar (8 cm. diameter by 20 cm. height) with $\frac{1}{10}$ their weight of soiling mixture and $\frac{1}{2}$ lb. of lead shot and shaken vigorously by hand for 1 min. The swatches are then vacuum cleaned, and visual comparison of their relative soiling tendency is made.

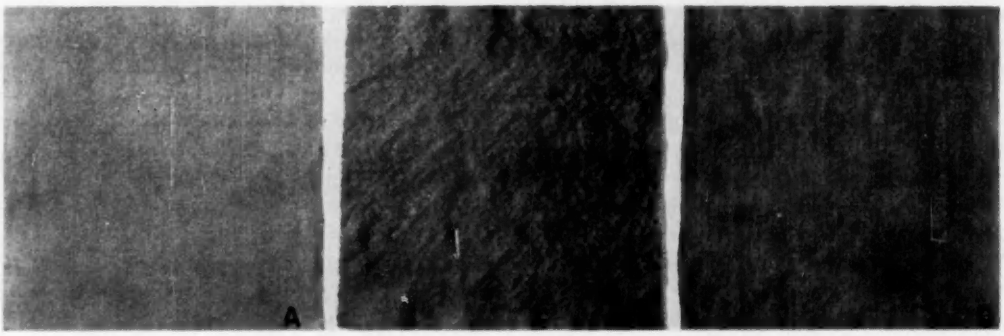

Fig. 2. Samples that illustrate smooth drying of treated wool fabric. A, control, untreated; B, untreated but wetted in detergent solution, squeezed to cause wrinkling, and tumble dried; C, treated (3% polyhexamethylene sebacamide on fabric), wetted in detergent solution, squeezed and tumble dried along with sample B.

Color. Color was measured with a Gardner Color and Color Difference Meter. Results are expressed in terms of Hunter coordinates = $R_{d,\,a,\,b}$.

Acid solubility. The sample is exposed to 4 *M* HCl at 65° for 1 hr. The loss in weight is used as a measure of the acid solubility [27].

Peracetic acid solubility. Weighed samples of the wool fabric were exposed to 100 ml. of 2% peracetic acid for 25 hr. and treated subsequently with 0.3% ammonia. The loss in weight was taken as a measure of the solubility in this medium [2].

Alkali solubility. Weighed samples of wool were immersed in 0.1 *M* NaOH for 1 hr. at 65° C. and the loss in weight was measured to estimate the solubility [8].

Results and Discussion

While interfacial polymerization is sensitive to a range of reaction variables, including concentration of reagents, monomer type and reactivity, solvent used, time fabric remains in treating solutions, solubility of polymer, and order of application of reagents to the fabric, the treatment effectively stabilizes the fabric from shrinking when it is applied under carefully controlled conditions. Because of the simplicity of operation, the technique is attractive. It consists simply in padding the cloth through the respective treating solutions, rinsing, and drying. No curing of resin is required, since the polymer forms almost instantaneously at or near the interface of the aqueous-organic phases during the second immersion and padding step. This rapid treatment, complete in 1 min. or less and operating at room temperature is readily adaptable to a continuous process. Although the second treating step normally is given immediately following the first treating step (within a minute or so), the time interval between steps does not appear to be crucial. Good results have been obtained with times between steps as long as 1 hr. However, since extended contact with amines tends to yellow wool, it is better to keep the over-all treatment time to a minimum and to rinse as soon as possible after the second treatment to remove unreacted reagent.

The treated fabric has good shrink resistance and handle, and shows a marked non-iron effect after laundering and tumble drying (Figure 2).

The polyamide systems studied are summarized in Table I. These include various amine-acid chloride combinations, selected to provide significant variations in polymer structure, including aliphatic-aliphatic, aliphatic-aromatic, aromatic-aliphatic, and aromatic-aromatic structural combinations. It is possible to secure fairly good shrink-resistant fabric

TABLE I. Polyamide Systems Studied

A. Aliphatic diamine	Aliphatic diacid chloride
1,6-Hexamethylene	Adipoyl
1,6-Hexamethylene	Pimeloyl
1,6-Hexamethylene	Azelaoyl
1,6-Hexamethylene	Sebacoyl
Piperazine	Adipoyl
Piperazine	Sebacoyl
B. Aliphatic diamine	Aromatic diacid chloride
1,6-Hexamethylene	Terephthaloyl
Piperazine	Terephthaloyl
C. Aromatic diamine	Aliphatic diacid chloride
Meta-xylylene	Sebacoyl
Meta-xylylene	Adipoyl
D. Aromatic diamine	Aromatic diacid chloride
Meta-xylylene	Terephthaloyl

with a variety of polyamides. The optimum conditions for each polyamide have to be ascertained by systematically studying variation in reaction conditions and correlation with properties of the treated fabric. The optimum conditions vary from one polyamide to another and have not been ascertained for most of the polyamides in Table I. Table II, for example, presents the comparative results for a variety of polyamides, all formed under reaction conditions favorable for good results with poly(hexamethylene sebacamide). It will be noted that these conditions are not favorable for the piperazine–acid chloride combinations and only moderately favorable for metaxylylene diamine–sebacoyl chloride. Although the amount of resin deposition appeared adequate, the shrink resistance of the treated fabric was poor. Quite possibly, in these cases, the polymer was not formed uniformly throughout the fabric and the conditions selected were not conducive to the formation of high molecular weight polymer with good film-forming properties. Supporting this interpretation, it was observed that extremely poor films were formed under these conditions when interfacial polymerization was carried out in the absence of wool.

The best results have consistently been obtained with sebacoyl chloride–hexamethylene diamine, and for that reason this polyamide has been studied in greater detail than others. (Table III). Good results have also been obtained with poly(hexamethylene adipamide) (Table VI), poly(hexamethylene pimeloylamide) (Table IV), and poly(hexamethylene azelaoylamide) (Table V).

The effects of the order of application of the reagents are illustrated in Table III. It will be noted that a smaller quantity of resin is deposited when the solution of sebacoyl chloride is applied to the fabric first, all other conditions being the same. Good shrinkage protection results in either case, independently of the order of application of the reagents. In general, however, it is advantageous to apply the aqueous solution of diamine to the cloth first and the non-aqueous solution of acid chloride second. A more uniform treatment of the fabric results, there is better penetration of the resin into the fabric, and a better handle for a given resin uptake is observed.

Table III also shows the feasibility of using a variety of organic solvents for the acid chloride. These include carbon tetrachloride, methyl chloro-

TABLE II. Shrink-Resistant Wool Flannel by Interfacial Formation of Polyamides*

Polymer system	Percent resin deposited on fabrics			Percent area shrinkage of treated fabrics, Accelerotor washing		
	As is†	Bleached‡	Extracted**	As is	Bleached	Extracted
None				52.0		
Hexamethylene diamine–Sebacoyl chloride	3.4	3.9	2.4	5.0	2.0	7.9
Piperazine–Sebacoyl chloride	4.5	4.0	2.7	32.8	12.6	32.8
Piperazine–Sebacoyl chloride	4.5	3.2	4.4	45.2	36.8	45.2
Piperazine–Terephthaloyl chloride	3.1	5.6	3.5	46.7	31.1	42.2
meta-Xylylene diamine–Sebacoyl chloride (benzene solvent)	5.7	7.2	3.9	5.0	10.7	10.8
meta-Xylylene diamine–Sebacoyl chloride	6.0	6.0	3.2	21.7	28.7	31.2

* Methyl chloroform used as the non-aqueous solvent unless otherwise specified. 20 sec. in each dip; amine concentration 4.0 gm./100 cm³. of H_2O plus 8 gm. Na_2CO_3 plus 0.1% non-ionic surfactant; acid chloride concentration, 4 cm³./100 cm³. of solvent.

† Used as received. No pretreatment or extraction.

‡ 0.6% H_2O_2, 0.8% tetrasodium pyrophosphate; wool/solution, 1:25; 1 hr. at 50° C.; rinsed in H_2O.

** As described under Materials and Procedure.

form, and aromatic and aliphatic hydrocarbons. The preferred solvent will vary from one polyamide system to another, depending on such factors as the solubility of the polymer in the solvent, the molecular weight, the film-forming properties of the polymer formed, and the physical characteristics of the polymer, as well as price and safety of an operable process. Variation in reaction time and in reagent concentrations affect the amount of polymer formed; more polymer is formed with longer exposures to the reagent solutions for a given concentration (Tables III and IX), or with increasing reagent concentration and given immersion time (Table VIII).

The durability of the shrinkage protection of the treated fabric to repeated accelerated washings is good, as measured in consecutive wash tests in the Accelerotor (Table VII).

The resistance of the treated fabric to alkali, acid, and oxidizing solution such as peracetic acid is about the same as for untreated fabric, though there is some indication of slight improvement in resistance in certain cases (Table X).

The physical properties of fabric treated by the interfacial formation of poly(hexamethylene sebacamide), poly(hexamethylene adipamide), poly(*meta*-xylylene sebacamide), and poly(hexamethylene te-

TABLE III. Shrink-Resistant Wool Flannel by Interfacial Formation of Poly(Hexamethylene Sebacamide)

Organic solvent for acid chloride	Order of treatment		Immersion time,* sec.	Percent resin uptake	Percent area shrinkage, Accelerotor†
	1	2			
—	—	—	—	None	52.0
CCl_4	Am‡	Ac**	90	8.3	3.0
CCl_4	Am	Ac	30	4.4	1.0
CCl_4	Am	Ac	15	4.6	4.0
CCl_4	Am	Ac	5	4.4	4.0
CCl_4	Ac	Am	90	3.2	2.0
CCl_4	Ac	Am	15	1.3	3.0
Toluene	Am	Ac	30	5.9	0
Toluene	Ac	Am	15	1.5	5.9
Skellysolve B	Am	Ac	30	5.1	13.5
Skellysolve B	Am	Ac	15	4.3	15.4
Skellysolve B	Ac	Am	15	2.2	3.0
Methyl chloroform	Am	Ac	20	2.4	7.9
Methyl chloroform	Am	Ac	10	3.6	3.0

* Time test fabric remains immersed in each treating solution.
† Two-minute wash.
‡ Am = Hexamethylene diamine solution (4.4 g. amine + 8 g. Na_2CO_3 + 0.1% Triton X-100/100 cm^3. H_2O).
** Ac = Sebacoyl chloride (2.0 cm^3./100 cm^3. solvent).

TABLE IV. Interfacial Formation of Poly(Hexamethylene Pimeloylamide) on Wool Flannel

Reagent concentration					
Amine,* g./100 cm^3. H_2O	Acid chloride, cm^3./100 cm^3. solvent	Order of treatment†		Percent resin uptake	Percent area shrinkage, Accelerotor
		1	2		
—	—	—	—	None	49.0
4.0	3.0 in CCl_4	Am	Ac	2.0	2.0
4.0	3.0 in CCl_4	Ac	Am	1.0	1.0
4.0	3.0 in CCl_4	Am	Ac	1.4	4.9
2.0	1.5 in CCl_4	Am	Ac	<1	17.2
2.0	1.5 in CCl_4	Ac	Am	<1	5.9
1.0	0.75 in CCl_4	Am	Ac	<1	26.1
4.0	3.0 Stoddard solvent	Am	Ac	<1	19.9
4.0	3.0 Stoddard solvent	Ac	Am	<1	26.9
2.0	1.5 Stoddard solvent	Am	Ac	<1	21.7
1.0	0.75 Stoddard solvent	Am	Ac	<1	36.8

* The aqueous amine solution contained twice as much sodium carbonate, in grams, as amine, also 0.1%, Triton X-100 to assist in wetting the fabric.
† Time fabric remained immersed in each treating solution, 15 sec. for all but sample on line 2, which was 60 sec.

TABLE V. Interfacial Formation of Poly(Hexamethylene Azelaoylamide) on Wool Flannel

Reagent concentration					
Amine,* g./100 cm³. H_2O	Acid chloride, cm³./100 cm³. solvent	Order of treatment† 1	Order of treatment† 2	Percent resin uptake	Percent area shrinkage, Accelerotor
—	—	—	—	None	52.0
4.0	3.0 in CCl_4	Am†	Ac	2.7	2.0
4.0	3.0 in CCl_4	Am	Ac	1.5	3.0
4.0	3.0 in CCl_4	Ac	Am	1.0	6.9
2.0	1.5 in CCl_4	Am	Ac	<1	14.4
2.0	1.5 in CCl_4	Ac	Am	<1	12.6
1.0	0.75 in CCl_4	Am	Ac	<1	19.9
4.0	3.0 in Stoddard solvent	Am	Ac	2.0	11.7
4.0	3.0 in Stoddard solvent	Ac	Am	1.3	24.3
2.0	1.5 in Stoddard solvent	Am	Ac	<1	19.0
1.0	0.70 in Stoddard solvent	Am	Ac	<1	25.2

* Aqueous solution of amine contained twice as much sodium carbonate, in grams, as amine; also 0.1% Triton X-100 to assist in wetting the fabric.

† Time fabric remained immersed in each treating solution, 15 sec. for all but the sample of line 2, which was 60 sec.

TABLE VI. Shrink-Resistant Wool Flannel by Interfacial Formation of Poly(Hexamethylene Adipamide)

Organic solvent	Order of treatment* 1	Order of treatment* 2	Percent resin uptake	Percent area shrinkage, Accelerotor†
—	Untreated		None	52.0
CCl_4	Am 2‡	Ac 2‡	7.5	2.0
CCl_4	Ac 2	Am 2	4.3	3.0
CCl_4	Am**	Ac††	4.7	13.6
CCl_4	Ac	Am	2.6	31.2
CCl_4	Am(½)‡	Ac(½)‡	2.4	10.7
CCl_4	Ac(½)	Am(½)	1.6	17.2
CCl_4	Am(¼)†	Ac(¼)‡	2.0	16.3
CCl_4	Ac(¼)	Am(¼)	1.5	40.7
Toluene	Am	Ac	5.5	3.0
Toluene	Ac	Am	1.5	32.8

* Time test fabric remained immersed in each treating solution, 15 sec.

† Two-minute wash.

‡ ¼, ½ and 2 refer to reagent concentrations changed by these factors from the concentrations specified in ** and ††.

** Aqueous solution of hexamethylene diamine, 8.8 g./100 cm.³ H_2O, 0.1% Triton X-100.

†† Solution of adipoyl chloride, 2.0 cm.³/100 cm.³ solvent.

TABLE VII. Durability of Resin to Repeated Accelerotor Tests

Polyamide from hexamethylene diamine	Percent resin on fabric	Percent area shrinkage, Accelerotor* Wash 1	Wash 2	Wash 3	Wash 4
None	None	52.	—	—	—
Sebacoyl chloride	8.3	3.0	3.0	5.9	11.7
Sebacoyl chloride	3.2	2.0	9.8	—	—
Sebacoyl chloride	4.4	1.0	9.8	—	—
Sebacoyl chloride	4.1	4.0	11.7	—	—
Sebacoyl chloride	2.2	3.0	18.1	—	—
Sebacoyl chloride	5.9	0	1.0	3.0	4.0–9.8 (5th)
Adipoyl chloride	5.5	3.0	11.7	—	—
Adipoyl chloride	7.5	2.0	6.9	16.3	—
Adipoyl chloride	4.3	3.0	15.4	—	—

* Each wash, 2 min.

rephthalamide) are summarized in Table XI. The conditions under which the fabrics were treated are given for reference, since these play an important part in the resultant fabric properties—more than does the actual amount of resin deposited. Treated fabrics do not differ significantly from the untreated in handle (as indicated by flexural rigidity), wrinkle recovery, color, break strength, and percent elongation. Good shrinkage resistance is noted for these fabrics when the resin formation is properly controlled. Rates of drying of fabric containing 0–6% resin were almost identical. Apparently the amount of resin required for shrinkage protection has little or no effect on the rate of drying of the fabric. The moisture regain is essentially unchanged for treated samples with this range of resin uptake. Dry soiling tests on treated fabrics using vacuum cleaner soil showed that the treated fabrics soil slightly less than the untreated control fabric; with carbon black, slightly more.

In additional larger-scale experiments, the interfacial polymerization procedure has been used to treat 14 different types of wool fabric, yielding materials with good shrinkage control and good handle, and with other physical qualities unimpaired. The

TABLE VIII. Effect of Variation of Reagent Concentration on Amount of Resin Deposited on Fabric

(Adipoly chloride–Hexamethylene diamine)

Reagent concentration		Order of treatment*		Percent resin uptake	
Diamine, g./100 cm³. H_2O	Acid chloride, cm³./100 cm³. CCl_4	First	Second	As is†	Extracted‡
17.6	4.0	Amine	Ac. chloride	7.3	7.5
8.8	2.0	Amine	Ac. chloride	4.9	4.7
4.4	1.0	Amine	Ac. chloride	3.6	2.4
2.2	0.5	Amine	Ac. chloride	2.0	2.1
17.6	4.0	Ac. chloride	Amine	4.8	4.3
8.8	2.0	Ac. chloride	Amine	3.5	2.7
4.4	1.0	Ac. chloride	Amine	2.5	1.6
2.2	0.5	Ac. chloride	Amine	1.5	1.6

* 15 sec. immersion in each treating solution.
† Used as received. No extraction or scouring prior to treatment.
‡ Extracted as described under Materials and Procedure.

results of these developmental investigations will be reported in a future paper.

The interfacial polymerization technique is suitable for other polycondensation reactions, such as the formation of polyesters, polycarbonates, polyurethanes, and polyethers. Exploratory experiments in progress are attempting to use the technique to apply these polymers to wool. The process should also be applicable to a variety of textile materials besides wool, as well as to paper, films, and to many other materials where polymer surface coatings may be of interest.

TABLE IX. Effect of Immersion Time on Amount of Resin Formed on Fabric*

Order of treatment		Duration of treatment,† sec.	Percent resin uptake on fabric (duplicates)	
First	Second			
Amine	Acid chloride	90	8.3	6.0
Amine	Acid chloride	30	4.4	4.7
Amine	Acid chloride	15	4.6	4.1
Amine	Acid chloride	5	4.4	4.2
Acid chloride	Amine	90	3.2	3.5
Acid chloride	Amine	15	1.3	1.4

* Resin was poly(hexamethylene sebacamide) formed using 4% aqueous amine solution and 3% acid chloride in carbon tetrachloride.
† Fabric remained immersed in each solution for the time interval shown.

TABLE X. Solubility of Wool Flannel Treated with Poly(Hexamethylene Sebacamide)

Percent resin on fabric	Acid* solubility, percent	Alkali† solubility, percent	Peracetic‡ acid solubility, percent
None	11.0	10.2	86.9
1.9	7.6	10.5	83.3
3.5	7.9	9.6	80.9
4.7	11.0	11.9	82.4
6.0	10.3	14.4	88.7

* 4 *M* HCl, 65° C., 1 hr. [24].
† 0.1 *M* NaOH, 65° C., 1 hr. [26].
‡ 2% peracetic acid, 24 hr., 25° C.; treated [25] subsequently with 0.3% ammonia, 24 hr.

Conclusion

A new technique for preparing shrink-resistant wool fabrics makes use of interfacial polymerization reactions to form polyamides on the surface of textile fibers. Dimensionally stable through repeated accelerated washings, the wool fabrics treated by this method are essentially unchanged in hand, flexural rigidity, break strength, percent elongation, and chemical resistance, and are also improved in wrinkle recovery and smoothness after tumble drying.

Although the technique is applicable to a variety of polyamides, the best results have been consistently obtained with poly(hexamethylene sebacamide). This polyamide may be formed with chlorinated solvents, such as carbon tetrachloride, or high-boiling hydrocarbon solvents, such as Stoddard solvent, for the non-aqueous phase. One minute or less is adequate for the two-step treating procedure, the polymer being formed almost instantaneously, at room temperature, during the second step. No curing of the resin is required. Following the treatment, the fabric is rinsed thoroughly to remove unreacted or excess reagent and finally dried. The technique gives promise of being readily adaptable

TABLE XI. Properties of Fabrics Treated with Polyamides by Interfacial Polymerization*

Conditions of interfacial polymerization													
Organic solvent	First reagent applied†	(Am)‡	(Ac)**	Time,†† sec.	Wt. % resin on fabric	% Area‡‡ shrinkage	Flexural rigidity, mg-cm.	Wrinkle recovery (Warp), deg.	Fabric break strength, lb.	% Elongation	Color Rd	Color a	Color b
Poly(hexamethylene sebacamide)													
—	—	—	—	—	None	52.0	143	146	36.4	33.4	69.5	−3.0	14.9
Skeylly-solve B	Ac	8.8	2.0	15	1.8	3.0	—	150	33.1	30.8	64.1	−3.8	13.3
Skelly-solve B	Am	8.8	2.0	15	4.6	15.4	—	148	36.4	32.0	64.4	−3.1	14.8
CCl_4	Ac	8.8	2.0	15	1.4	3.0	—	149	35.2	35.2	61.8	−3.4	13.9
CCl_4	Am	8.8	2.0	5	4.2	4.0	—	146	38.8	39.1	61.6	−2.7	15.1
CCl_4	Ac	8.8	2.0	90	3.5	2.0	296	146	39.0	36.0	61.3	−3.4	14.2
CCl_4	Am	8.8	2.0	15	4.1	4.0	210	146	40.1	34.6	61.5	−3.2	15.4
CCl_4	Am	8.8	2.0	30	4.7	1.0	160	149	38.0	32.0	58.9	−3.1	15.1
CCl_4	Am	8.8	2.0	90	6.0	3.0	194	149	37.6	33.9	60.7	−2.8	15.0
CCl_4	Ac	8.8	2.0	90	3.2	3.0	133***	152	35.1	31.5	62.2	−3.0	15.0
CCl_4	Am	8.8	2.0	15	4.1	4.0	128***	154	31.3	30.5	61.2	−2.6	14.8
CCl_4	Am	8.8	2.0	30	4.4	1.0	110***	157	30.9	25.7	60.6	−2.6	14.6
Poly(hexamethylene adipamide)													
Toluene	Am	8.8	2.0	120	5.9	3.0	264	138	40.2	38.3	63.4	−3.4	14.0
CCl_4	Am	8.8	2.0	5	3.6	22.6	149	150	35.4	32.2	63.6	−3.3	14.6
CCl_4	Am	8.8	2.0	15	4.9	—	126	152	34.1	32.2	62.1	−2.9	14.1
CCl_4	Am	8.8	2.0	120	5.2	4.9	188	154	34.7	27.1	63.4	−3.4	14.8
Poly(meta-xylylene sebacamide)													
CCl_4	Am	4.5	1.0	15	1.3	20.8	191	152	37.5	29.0	64.8	−3.6	15.1
CCl_4	Am	9.0	2.0	5	3.4	20.8	180	147	40.3	34.4	64.4	−3.7	14.7
Poly(hexamethylene terephthalamide)													
CCl_4	Am	8.8	1.25	15	4.4	20.8	324	147	35.3	27.0	61.9	−2.7	15.7
CCl_4	Am	17	2.5	30	6.7	21.7	184	143	39.5	39.2	63.0	−3.0	14.5
CCl_4	Am	17	2.5	60	7.9	19.0	173	136	37.4	31.8	63.2	−3.0	14.3
CCl_4	Ac	17	2.5	60	1.8	6.0	316	138	40.4	39.7	60.4	−2.9	14.2

* Unless otherwise specified all properties were measured on treated fabric which had no mechanical conditioning following the treatment. Treated swatches were merely rinsed, dried at room temperature, and evaluated without further processing.

† Refers to the order of application of the reagents.

‡ (Am) = concentration of diamine in grams per 100 cm^3. H_2O.

** (Ac) = concentration of acid chloride in cm^3. per 100 cm^3. organic solvent.

†† Time refers to the immersion time of the fabric in each of the treating solutions.

‡‡ Two-minute wash in Accelerotor.

*** These swatches were Accelerotor-washed for 2 min. prior to measurement of the other properties.

to continuous operation. It has been found suitable for a wide variety of wool fabrics and merits further development and extension to other polymer systems, as well as to other textiles.

Acknowledgment

The authors gratefully acknowledge the encouragement and advice of Harold P. Lundgren and the technical assistance of Lura Brown, T. J. Coe, Iva Montgomery, and Mary Sawyer in carrying out most of the physical tests required in this study.

Literature Cited

1. Alexander, P., Bailey, J. L., and Carter, D., TEXTILE RESEARCH JOURNAL **20**, 385–399 (1950).
2. Alexander, P., Fox, M., Stacey, K. A., and Smith, L. F., *Biochem. J.* **52**, 177–184 (1952).
3. Baldwin, A. W., Barr, T., and Speakman, J. B., *J. Soc. Dyers Colourists* **62**, 4–9 (1946).
4. Beaman, R. G., Morgan, P. W., Koller, C. R., Wittbecker, E. L., Magat, E. E., *J. Polymer Sci.* **40**, 329–336 (1959).
5. Bradbury, J. H. and Leeder, J. D., TEXTILE RESEARCH JOURNAL **30**, 118–127 (1960).

6. Delmenico, J., Jackson, D. L. C., and Lipson, M., TEXTILE RESEARCH JOURNAL **24**, 828–834 (1954).
7. Eareckson, W. M., *J. Polymer Sci.* **40**, 399–406 (1959).
8. Harris, M. and Smith, A. L., *J. Research Natl. Bur. Standards* **17**, 577–583 (1936).
9. Jackson, D. L. C., TEXTILE RESEARCH JOURNAL **21**, 655–659 (1951).
10. Jackson, D. L. C., TEXTILE RESEARCH JOURNAL **23**, 616–622 (1953).
11. Jackson, D. L. C., TEXTILE RESEARCH JOURNAL **24**, 624–629 (1954).
12. Jackson, D. L. C. and Lipson, M., TEXTILE RESEARCH JOURNAL **21**, 156–163 (1951).
13. Katz, M., *J. Polymer Sci.* **40**, 337–342 (1959).
14. Lyman, D. J. and Lup Jung, S., *J. Polymer Sci.* **40**, 407–418 (1959).
15. Magat, E. E. and Strachan, D. R., U. S. Patent 2,708,617 (May 17, 1955).
16. Morgan, P. W. and Kwolek, S. L., *J. Polymer Sci.* **40**, 299–327 (1959).
17. Pardo, C. E., *J. Textile Inst.* **51**, P842–853 (1960).
18. Pardo, C. E. and O'Connell, R. A., *Am. Dyestuff Reptr.* **47**, No. 10, P 333–8 (1958).
19. Schaefgen, J. R., Koontz, F. H., and Tietz, R. F., *J. Polymer Sci.* **40**, 377–387 (1959).
20. Shashoua, V. E. and Eareckson, W. M., *J. Polymer Sci.* **40**, 343–358 (1959).
21. Stephens, C. W., *J. Polymer Sci.* **40**, 359–366 (1959).
22. Stiegler, H. W., Glidden, H. E., Mandikos, G. J., and Thompson, G. R., *Am. Dyestuff Reptr.* **45**, 685–700 (1956).
23. Sundet, S. A., Murphey, W. A., and Speck, S. B., *J. Polymer Sci.* **40**, 389–397 (1959).
24. Thorsen, W. J., TEXTILE RESEARCH JOURNAL **24**, 899–902 (1954).
25. Wittbecker, E. L. and Katz, M., *J. Polymer Sci.* **40**, 367–375 (1959).
26. Wittbecker, E. L. and Morgan, P. W., *J. Polymer Sci.* **40**, 289–297 (1959).
27. Zahn, H. and Würz, A., *J. Textile Inst.* **45**, P88–92 (1954).

Manuscript received December 23, 1960.

Adsorption of Direct Cotton Dyes by Chemically Modified Celluloses

E. H. Daruwalla, P. J. Kangle, and G. M. Nabar

Department of Chemical Technology, University of Bombay, Bombay 19, India

Abstract

Equilibrium adsorption of two direct cotton dyes on cellulose oxidized with specific oxidizing agents and by the products of reduction of these oxycelluloses, under standard conditions of dyeing has been studied. It is shown that conversion of hydroxyl groups of cellulose to carbonyl groups does not influence dye adsorption, but formation of ionizable carboxyl groups in cellulose chain molecules brings about an appreciable reduction in dye uptake, the extent of reduction being independent of the position in the glucose units of cellulose at which the carboxyl group is formed. Based on a theoretical treatment, it is shown that only a fraction of the total carboxyl groups is responsible for the reduction in dye adsorption under specific conditions of dyeing, and with progressive increase in the total carboxyl content of cellulose, the value of this fraction goes on decreasing continuously.

Introduction

Adsorption of direct cotton dyes on different cellulosic fibers has been studied extensively by a number of workers mainly from the point of view of developing the kinetic as well as thermodynamic interpretations for understanding the mechanism of dyeing of cellulose with these dyes [10, 17]. In comparison, work reported in the literature on the adsorption of these dyes on chemically modified celluloses and on the part played by the hydroxyl groups of cellulose during the dye uptake is rather limited. The only detailed treatments on this subject have been given by Neale and Stringfellow [21], Standing and co-workers [27], Rochas and Daneyrolle [24], and Sadov and Kalinina [26]. The present investigation was undertaken with a view to studying the

changes in equilibrium adsorption of two direct cotton dyes on cellulose oxidized with specific oxidizing agents which would oxidize preferentially selective groups in the cellulose chain molecules to carbonyl or carboxyl groups and by the reduced oxycelluloses prepared from the corresponding oxycelluloses. An attempt has also been made to investigate the contribution of carboxyl groups formed at different positions in the glucose unit of the cellulose chains towards reduction in dye adsorption.

Experimental Materials and Methods

Dyes: Chrysophenine G (C.I. Direct Yellow 12); Chlorazol Sky Blue FF (C.I. Direct Blue 1). The dyes were purified by the method recommended by Robinson and Mills [23]. Purity of the dye was determined from the analysis of the elements present. All other chemicals used were of Analar quality.

Preparation of Oxycelluloses and their Reduced Products

For the preparation of oxycelluloses, carefully purified 20's single yarn prepared from Indian cotton was used. Periodate oxycelluloses were prepared by steeping cotton cellulose in 0.01 *M* potassium metaperiodate at 30° C. for different periods according to the method suggested by Davidson [3], while the dichromate-sulfuric acid oxycelluloses were prepared by treatment of cotton cellulose with an aqueous solution containing 0.1 *N* $K_2Cr_2O_7$ and 0.2 *N* H_2SO_4 for different periods at 30° C. according to the method recommended by Davidson [4]. For the preparation of dichromate-oxalic acid oxycelluloses, cotton cellulose was suspended in an aqueous solution of 2 *N* oxalic acid at 30° C. and to this was added different amounts of 2 *N* $K_2Cr_2O_7$ depending on the extent of oxidation desired as suggested by Nabar and Padmanabhan [19]. Hypochlorite oxycelluloses were prepared by the method recommended by Birtwell, Clibbens, and Ridge [2] in which cotton cellulose was treated for 4 hr. with an aqueous solution of sodium hypochlorite containing 3 g./l. active chlorine buffered to a suitable pH. All oxycelluloses were further oxidized with a standard solution of sodium chlorite in aqueous phosphoric or acetic acid according to the method recommended by Davidson and Nevell [5]. Reduced oxycelluloses were prepared by reduction of the corresponding oxycelluloses under standard conditions with sodium borohydride solution according to the method suggested by Head [11]. All the samples were air dried and preserved under constant condition of RH and temperature away from light.

Copper number and carboxyl content of the oxycelluloses were determined according to the methods suggested by Clibbens and Geake as modified by Heys [13] and Nabar and Padmanabhan [19], respectively.

Dyeing Procedure

In all the experiments 0.025 g. of the material (allowance made for moisture regain) was dyed in 250 ml. of the dye liquor at 90° ± 1° C. till equilibrium conditions between the dye in the fiber and that in solution were attained. The large volume of the dyebath in comparison with the small amount of substrate used corresponds to an infinite dyebath. Dyeings were carried out in 250-ml. round bottom Pyrex flasks fitted with water condensers to prevent the loss of liquor due to evaporation and with loop type stirrers passing through the condensers and revolving at a speed of 240 r.p.m. for proper agitation. In all the experiments, the dye liquor consisted of 0.05 g./l. dye and 5 or 10 g./l. Analar sodium chloride. Dye liquors were buffered to pH 7 with a suitable buffer system. At the end of appropriate dyeing periods, dyed samples were removed from the liquor, washed on sintered glass crucibles (AG 3X4) with ice-cold water till the washings did not show any coloration, blotted between filter papers to remove the excess of water, dried over P_2O_5, and then conditioned in an atmosphere of 65% RH at 30° ± 1° C. Dye from accurately weighed dyed samples was extracted with 25% aqueous pyridine at 30° C. by allowing the samples to remain in contact with pyridine solution overnight in the dark to prevent complications arising from *cis-trans* transformation in the case of Chrysophenine G, which is a stilbene derivative. Optical density of the extract was determined in the dark on a Hilger Spekker Photoelectric Absorptionmeter which had been previously calibrated with standard solutions of dye in 25% aqueous pyridine. Results are expressed in terms of grams of dye adsorbed per kilogram bone dry sample.

Experimental Results and Discussion

It is well known that under standard conditions, periodic acid or potassium metaperiodate preferentially oxidizes the hydroxyl groups at carbon atoms 2 and 3 of the glucose units to dialdehyde groups

with a carbon–carbon bond cleavage at the points of oxidative attack, and during this conversion no appreciable breakdown of cellulose chains takes place if potassium metaperiodate is used as the oxidizing agent and the reaction is carried out at neutral pH [14]. With dichromate-sulfuric acid or dichromate-oxalic acid oxidation, the reaction has been shown to be mainly confined to the oxidation of primary alcoholic groups to aldehyde or carboxylic acid groups [*20, 22*], while during oxidation with sodium hypochlorite there is no selective oxidation of the hydroxyl groups of cellulose, and it is suggested that oxidation of hydroxyl groups at carbon atoms 2, 3, and 6 takes place simultaneously to the aldehyde or carboxyl state [18].

Results of the present investigation indicate that conversion of the hydroxyl groups, whether at *2*, *3*, or *6* position in the glucose units of cellulose chains, to the carbonyl stage does not alter the equilibrium adsorption of either of the dyes studied at either of the two dyebath salt concentrations (Table I); and in case of periodate oxidation there is very little change in the equilibrium dye adsorption even though oxidation has been carried to an appreciable extent, *viz.*, oxycelluloses with copper number of the order of *22* (Figure 1). In the case of dichromate-sulfuric acid, dichromate-oxalic acid, and hypochlorite oxycelluloses, it is not possible to convert the hydroxyl groups to the carbonyl stage without simultaneous formation of carboxylic acid groups to some extent. Thus, the reduction in dye uptake observed in the case of these oxycelluloses, as dis-

TABLE I. Equilibrium Adsorption of Chrysophenine G and Chlorazol Sky Blue FF by Different Oxycelluloses

		Chryso-phenine G, g./kg.		Sky Blue FF, g./kg.				Chryso-phenine G, g./kg.		Sky Blue FF, g./kg.				Chryso-phenine G, g./kg.		Sky Blue FF, g./kg.	
Copper No.	Carboxyl content, eq./kg.	NaCl, 5 g./l.	NaCl, 10 g./l.	NaCl, 5 g./l.	NaCl, 10 g./l.	Copper No.	Carboxyl content, eq./kg.	NaCl, 5 g./l.	NaCl, 10 g./l.	NaCl, 5 g./l.	NaCl, 10 g./l.	Copper No.	Carboxyl content, eq./kg.	NaCl, 5 g./l.	NaCl, 10 g./l.	NaCl, 5 g./l.	NaCl, 10 g./l.
Cotton cellulose						Borohydride treated cotton cellulose						Chlorite treated cotton cellulose					
0.005	0.004	1.76	2.34	4.20	5.79	0.005	0.004	1.76	2.34	4.19	5.79	0.005	0.004	1.76	2.34	4.2	5.79
Periodate oxycelluloses						Borohydride treated periodate oxycelluloses						Chlorite treated periodate oxycelluloses					
1.49	0.004	1.76	2.34	4.20	5.79	0.005	0.004	1.74	2.35	4.22	5.79	0.005	0.068	0.75	1.19	1.36	2.55
3.98	0.004	1.76	2.33	4.21	5.79	0.005	0.004	1.77	2.34	4.21	5.78	0.010	0.139	0.56	0.91	0.88	1.62
5.56	0.004	1.75	2.33	4.22	5.80	0.005	0.004	1.77	2.34	4.25	5.80	0.050	0.180	0.48	0.80	0.77	1.40
8.88	0.004	1.76	2.32	4.22	5.79	0.005	0.004	1.74	2.34	4.22	5.79	0.200	0.270	0.45	0.66	0.61	1.04
14.89	0.004	1.75	2.32	4.20	5.78	0.005	0.004	1.74	2.32	4.22	5.79	0.550	0.460	0.44	0.65	0.58	0.85
20.95	0.005	1.76	2.33	4.20	5.79	0.010	0.005	1.73	2.30	4.20	5.80	0.700	0.594	0.43	0.64	0.58	0.80
21.98	0.005	1.75	2.32	4.21	5.79	0.010	0.005	1.73	2.30	4.20	5.80	0.780	0.617	0.43	0.64	0.58	0.80
Dichromate-sulfuric acid oxycelluloses						Borohydride treated dichromate-sulfuric acid oxycelluloses						Chlorite treated dichromate-sulfuric acid oxycelluloses					
1.11	0.009	1.49	2.04	3.60	5.15	0.005	0.009	1.54	2.04	3.59	5.19	0.12	0.024	1.14	1.75	2.23	4.40
2.67	0.013	1.35	1.90	3.14	4.90	0.005	0.013	1.38	1.92	3.15	4.92	0.47	0.048	0.85	1.34	1.50	3.09
5.09	0.019	1.29	1.82	2.50	4.50	0.020	0.019	1.30	1.83	2.47	4.49	1.00	0.083	0.74	1.10	1.18	2.20
9.57	0.034	1.00	1.50	2.02	3.44	0.060	0.034	1.00	1.47	2.05	3.48	1.49	0.155	0.54	0.85	0.75	1.49
11.80	0.048	0.85	1.30	1.62	2.98	0.170	0.048	0.85	1.31	1.63	2.96	2.04	0.196	0.50	0.75	0.72	1.26
17.74	0.079	0.75	1.10	1.17	2.30	0.230	0.079	0.75	1.13	1.17	2.28	3.05	0.307	0.44	0.58	0.58	0.87
Dichromate-oxalic acid oxycelluloses						Borohydride treated dichromate-oxalic acid oxycelluloses						Chlorite treated dichromate-oxalic acid oxycelluloses					
1.62	0.006	1.62	2.20	3.84	5.50	0.005	0.006	1.69	2.33	3.89	5.56	0.05	0.023	1.24	1.76	2.28	4.31
3.12	0.014	1.34	1.98	3.20	5.00	0.005	0.014	1.43	2.00	3.26	4.99	0.12	0.048	1.09	1.32	1.48	3.10
6.98	0.020	1.05	1.78	2.44	4.44	0.005	0.020	1.10	1.75	2.40	4.45	0.49	0.091	0.74	1.10	1.06	2.10
10.24	0.026	0.95	1.62	2.14	3.96	0.005	0.026	0.96	1.62	2.14	3.98	0.82	0.132	0.59	0.94	0.77	1.70
13.63	0.041	0.88	1.42	1.63	3.30	0.010	0.041	0.82	1.38	1.45	3.28	1.00	0.176	0.48	0.76	0.68	1.45
17.06	0.060	0.75	1.27	1.32	2.79	0.010	0.060	0.75	1.28	1.30	2.72	1.42	0.228	0.46	0.69	0.62	1.17
Hypochlorite oxycelluloses						Borohydride treated hypochlorite oxycelluloses						Chlorite treated hypochlorite oxycelluloses					
0.15	0.012	1.30	2.07	3.23	5.00	0.005	0.012	1.30	2.03	3.23	5.03	0.005	0.020	1.00	1.66	2.41	4.38
2.89	0.030	0.89	1.60	1.95	3.80	0.040	0.030	0.90	1.60	1.95	3.85	1.47	0.076	0.71	1.15	1.20	2.45
7.55	0.035	0.85	1.48	1.79	3.48	0.320	0.035	0.85	1.49	1.78	3.44	3.09	0.130	0.60	0.94	0.80	1.75
8.30	0.039	0.81	1.39	1.72	3.28	0.420	0.039	0.81	1.38	1.72	3.27	3.21	0.149	0.55	0.88	0.76	1.55

cussed later, is mainly due to such carboxyl groups ionizing in the aqueous dyebath and repelling the negatively charged dye anions and not to the conversion of hydroxyls to the carbonyl stage. This conclusion is substantiated by the fact that all these oxycelluloses after borohydride reduction, where the aldehyde groups have been converted to primary alcoholic groups, do not show an increase in the equilibrium dye adsorption (Table I).

Adsorption of direct dyes on cellulose has been partly attributed to the hydrogen bonding between hydroxyl groups of cellulose chain molecules in the noncrystalline accessible regions and electron donating or proton donating groups in the dye molecule [25]. When these hydroxyl groups are converted to the aldehyde state, as is the case with the oxycellulose studied, the oxygen atom of the carbonyl group would possess an unshared pair of electrons as compared with the two pairs on the hydroxyl oxygen, and, therefore, the tendency to form hydrogen bonds with suitable groups in the dye molecule would be less in the case of oxycellulose than in the case of cellulose. With the dye Chrysophenine G, which has no proton donor in its molecule for hydrogen bond formation with the lone pair of electrons in the carbonyl of oxycelluloses, the chances of hydrogen bond formation between dye and oxycellulose will be very few. Hence, under such circumstances, dye adsorption should have decreased continuously with progressive oxidation of cellulose. The possibility of $-NH_2$ groups in the dye molecule combining chemically with the $-CHO$ of the oxycelluloses by chemical bonding of the type cellulose $-CH=N-$ dye cannot be considered, because if that were so, the energy of association of dye molecules with cellulose would have been very high. Heats of reaction between these dyes and cotton cellulose and oxycelluloses prepared from it were therefore determined by the method of Gilbert [6] as modified by Lemin [16] in which a fiber containing a constant amount of the dye is brought to equilibrium at different temperatures with solutions containing varying amounts of dye, as these values are likely to indicate to some extent the strength of the dye–fiber bonding. It was found that heats of dyeing for cotton cellulose and periodate oxycellulose were very close, *viz.*, 14.2 and 14.0 kcal./mol. for Chrysophenine G and 24.8 and 24.9 kcal./mol. for Chlorazol Sky Blue FF, indicating that the possibility of chemical combination between the dye and oxycellulose can safely be ruled out. Another possibility that might be envisaged is that oxidation might have resulted in only a few of the total number of available hydroxyl groups being converted to the carbonyl state, with the result that a large proportion of the hydroxyls may still be available for hydrogen bonding with the dye. In this connection, results of Goldfinger, Mark, and Siggia [9], who have used periodate oxidation as a method of determining crystalline–noncrystalline portions in cellulosic materials, have been considered. According to their results, for an oxygen consumption of about 0.06 atoms per glucose unit, most of the secondary alcoholic groups in the amorphous regions of cotton linters have been converted to the carbonyl groups. In the present investigation, as oxidation with potassium metaperiodate has been continued till the stage of oxygen consumption of the order of 0.08 atoms of oxygen per glucose unit, it is certain that most of the accessible secondary alcoholic groups have been oxidized. Furthermore, it is also found that there is no change in the noncrystalline portions of the fiber substance during oxidation with the oxidizing agents studied, under the conditions of oxidation employed, or during the reduction of the oxidized products as evidenced by Kangle's [15] determination of cellulose crystallinity by the iodine adsorption method of Hessler and Power [12]. Thus, it can be concluded that conversion of hydroxyl groups in cellulose to the carbonyl groups makes no difference to the equilibrium adsorption of the direct dyes studied irrespective of whether oxidation of the hydroxyl groups at carbon atoms 2, 3, or 6 of the

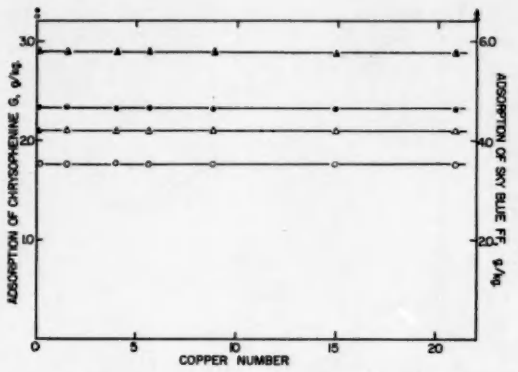

Fig. 1. Equilibrium adsorption of Chrysophenine G, circles, and Chlorazol Sky Blue FF, triangles, by periodate oxycelluloses. ○, △, NaCl 5 g./l.; ●, ▲, NaCl 10 g./l.

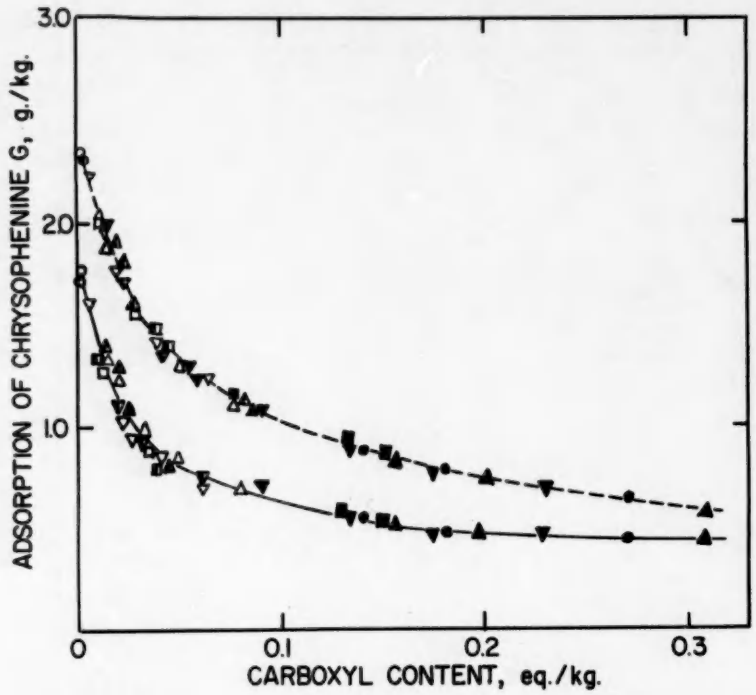

Fig. 2. Relation between carboxyl content of oxycelluloses and equilibrium adsorption of Chrysophenine G. ———— NaCl, 5 g./l.; ———— NaCl, 10 g./l. Open circle, periodate oxycellulose; half dark circle, borohydride periodate oxycellulose; dark circle, chlorite-periodate oxycellulose. Open triangle (point up) $K_2Cr_2O_7$-H_2SO_4 oxycellulose; half dark triangle, borohydride-$K_2Cr_2O_7$-H_2SO_4 oxycellulose; dark triangle, chlorite - $K_2Cr_2O_7$ - H_2SO_4 oxycellulose. Open inverted triangle, $K_2Cr_2O_7$-oxalic acid oxycellulose; half dark inverted triangle, borohydride $K_2Cr_2O_7$-oxalic acid oxycellulose; dark inverted triangle, chlorite-$K_2Cr_2O_7$-oxalic acid oxycellulose. Open squares, hypochlorite oxycellulose; half dark squares, borohydride hypochlorite oxycellulose; dark squares, chlorite hypochlorite oxycellulose.

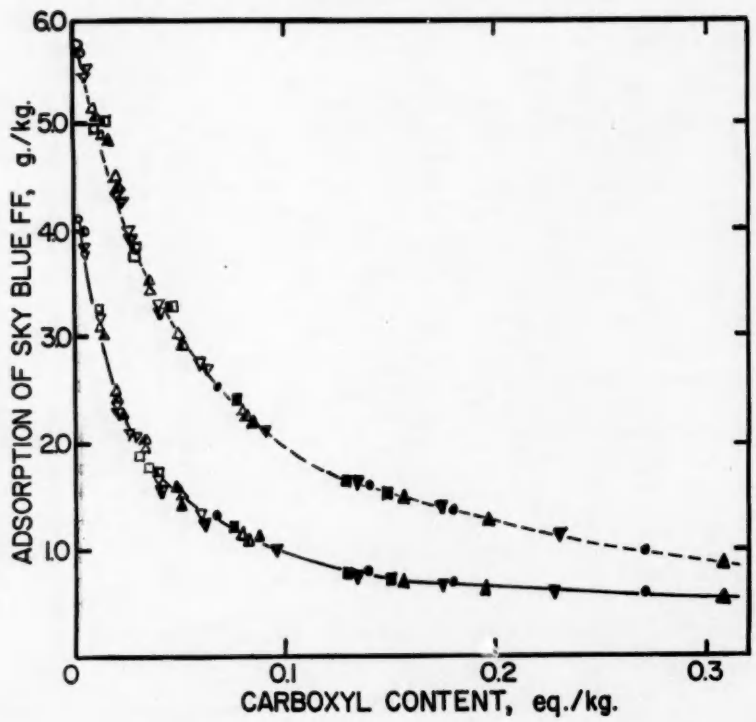

Fig. 3. Relation between carboxyl content of oxycellulose and equilibrium adsorption of Chlorazol Sky Blue FF. ———— NaCl, 5 g./l. ———— NaCl, 10 g./l. Symbols same as Figure 2.

glucose units has taken place. The importance of the hydroxyl groups for the adsorption of direct cotton dyes is, therefore, questionable. In this connection it may be noted that Giles and co-workers [7, 8], on the basis of results of the measurement of the substantivity of model organic compounds for cellulose, and experiments with dyes in monolayers and adsorption of organic compounds from non-aqueous media, have shown that in aqueous solutions the hydroxyl groups of cellulose are too firmly solvated by water to enter into bond formation with external solutes; they have put forward positive evidence for attributing the adsorption of direct dyes on cellulose to van der Waals forces.

When equilibrium adsorption of the two dyes on different types of oxycellulose, on their products of reduction with borohydride, or on their products of further oxidation with sodium chlorite are plotted against their respective carboxyl contents, a unique relationship has been obtained between dye uptake and carboxyl content at 5 and 10 g./l. electrolyte concentration in the dyebath (Figures 2 and 3). These results indicate that irrespective of the position in the glucose unit at which a carboxyl group is formed, it is effective to the same extent in reducing the equilibrium dye adsoption by virtue of its ionization into COO^- ions. The reduction in dye uptake has been attributed to the ionizable carboxyl groups, which, on account of their negative charge, increase the negative surface potential of the substrate and enhance the repulsion of the negatively charged dye ions approaching the fiber surface. The reduction in dye uptake depends on the extent of ionization of the carboxyl groups present, and, as seen from the results plotted in Figures 2 and 3, although the total carboxyl content of an oxycellulose may increase, the fraction which directly influences the equilibrium adsorption is generally less than the total number of carboxyl groups present in the oxidized celluloses. This reduction in dye uptake may be due to the negative charge on the ionized carboxyl groups repelling the dye anion, as shown by Standing and Warwicker [27], who found that changes in the pH of the dye bath brought about changes in the ionization of the carboxyl groups in cellulose and consequently affected the equilibrium dye uptake by the oxycelluloses. Sadov and Kalinina [26] also found that when the ionization of carboxyl groups in nitrogen dioxide oxycelluloses was suppressed by formation of calcium or aluminum salts, adsorption of dyes by these oxycelluloses was nearly the same as in the case of unoxidized cellulose. With all the oxycelluloses examined, equilibrium dye adsorption is greater at higher electrolyte concentration in the bath (Table I), the decrease in equilibrium adsorption resulting from an increase in ionizable groups of the oxycelluloses is more marked from dyebaths containing 5 g./l. sodium chloride than from those containing 10 g./l., and at each specific stage of oxidation, the reduction in dye uptake is more prominent in the case of Chlorazol Sky Blue FF than in the case of Chrysophenine G (Table II). These observations can be explained

TABLE II. Reduction in Equilibrium Dye Adsorption by Oxycellulose at Different Electrolyte Concentrations in Dyebath

Carboxyl content, eq./kg.	Percent reduction			
	Chrysophenine G		Chlorazol Sky Blue FF	
	NaCl, 5 g./l.	NaCl, 10 g./l.	NaCl, 5 g./l.	NaCl, 10 g./l.
0.010	17	10	18	11
0.020	38	23	40	23
0.030	46	33	52	35
0.050	55	44	64	48
0.100	63	56	73	65
0.150	69	62	82	73
0.200	73	68	84	78
0.300	74	78	86	85

on the following basis. Under the dyebath conditions of electrolyte concentration of 5 g./l., the effect of the negative surface potential due to the ionization of carboxyl groups in oxycelluloses will be more marked than will be the case when the electrolyte concentration is high, *viz.*, 10 g./l., and is sufficiently large to suppress the negative charge. In the case of Chlorazol Sky Blue FF, due to the greater number of negative charges in the dye molecule, the repulsive forces will be operative to a greater extent, at each stage of oxidation and under identical conditions of salt concentration, than in case of Chrysophenine G.

With a view to studying quantitatively the influence of ionizable carboxyl groups formed at different carbon atoms in the glucose units of cellulose chain molecules on the equilibrium adsorption of Chrysophenine G and Chlorazol Sky Blue FF, the following theoretical treatment of the results, taken from the work of Standing and Warwicker [27], has been adopted.

$[Na]_f$, $[Cl]_f$, and $[D]_f$ represent the sodium ions, chloride ions, and dye ions in the fiber phase, and $[Na]_s$, $[Cl]_s$, and $[D]_s$, represent the ionic concentrations of sodium, chloride, and dye ions in solution phase in terms of moles/kg. fiber and moles/l. solution respectively. According to Donnan equilibrium the ionic concentrations in the two phases will be related as follows:

$$\left(\frac{[Na]_s}{[Na]_f}\right)^z = \left(\frac{[Cl]_f}{[Cl]_s}\right)^z = \frac{[D]_f}{[D]_s} = \lambda^z \qquad (1)$$

where λ is the Donnan coefficient and z is the basicity of the dye anion. Thus,

$$[Na]_f = \frac{[Na]_s}{\lambda}; \quad [Cl]_f = \lambda[Cl]_s$$

and

$$[D]_f = \lambda^z[D]_s \qquad (2)$$

According to Hanson, Neale, and Stringfellow [10], the concentration of the adsorbed dye on cellulose is directly proportional to the concentration of the free dye ions in the cellulose phase.

$$[D]_\phi = K[D]_f \qquad (3)$$

where $[D]_\phi$ is the concentration of dye ions adsorbed by cellulose in terms of moles/kg. dry fiber and K is a constant. Substituting the value of $[D]_f$ from Equation 2, one obtains

$$[D]_\phi = K\lambda^z[D]_s \qquad (4)$$

For maintaining electrical neutrality in the cellulose phase,

$$[Na]_f = [Cl]_f + z[D]_f + \frac{1}{W}(z[D]_\phi + [COO]) \qquad (5)$$

where W represents the volume of water in cellulose phase in terms of l./kg. dry fiber and [COO] represents carboxyl content in terms of eq./kg. and

$$[Na]_s = [Cl]_s + z[D]_s \qquad (6)$$

Combining Equations 2, 5, and 6, one obtains the following equation

$$\frac{[Cl]_s + z[D]_s}{\lambda} = \lambda[Cl]_s + z\lambda^z[D]_s + \frac{1}{W}(z[D]_\phi + [COO]) \qquad (7)$$

In the present experiments, the concentration of dye in solution is small as compared with that of salt and therefore as an approximation the term $z[D]_s$ can be neglected in comparison with $[Cl]_s$. This leads to Equation 7 being reduced to

$$\lambda^2 + \frac{1}{W}\lambda\frac{z[D]_\phi + [COO]}{[Cl]_s} - 1 = 0 \qquad (8)$$

This quadratic equation can be solved for λ for a given salt concentration $[Cl]_s$ by substituting the

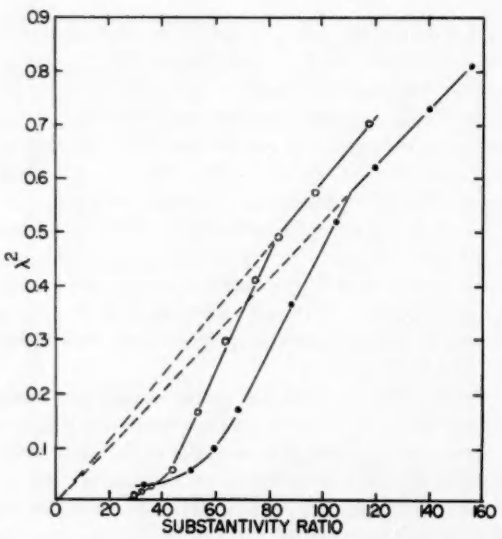

Fig. 4. Relation between substantivity ratio and λ^2 for Chrysophenine G. ○, NaCl, 5 g./l.; ●, NaCl, 10 g./l.

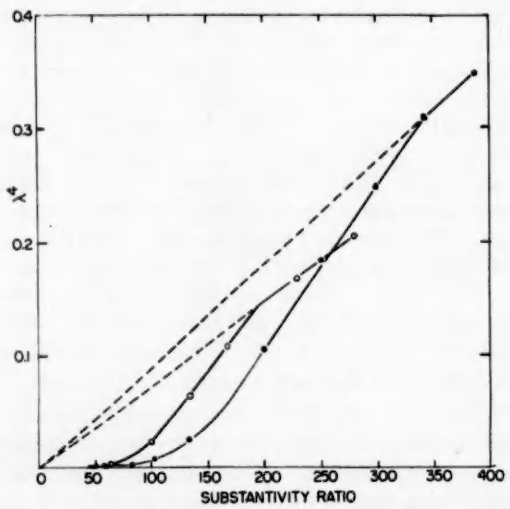

Fig. 5 Relation between substantivity ratio and λ^4 for Chlorazol Sky Blue FF. ○, NaCl, 5 g./l.; ●, NaCl, 10 g./l.

TABLE III. Determination of Donnan Coefficient and Ionized Carboxyl Groups at Different Stages of Oxidation for Chrysophenine G

W = 0.3 l./kg.; $[D]_s = 7.3 \times 10^{-5}$ moles/l.

Total [COO], eq./kg.	Dye adsorption, g./kg.	$[D]_\phi$, moles/kg.	Substantivity ratio $\frac{[D]_\phi}{W[D]_s}$	λ	Calculated [COO], eq./kg.	$\frac{\text{Calculated [COO]}}{\text{Total [COO]}}$
			NaCl, 5 g./l.			
0.004	1.76	0.00259	117	0.8370	0.0040	1.00
0.010	1.46	0.00215	97	0.7592	0.0098	0.98
0.015	1.25	0.00184	83	0.7007	0.0147	0.95
0.020	1.10	0.00162	73	0.6448	0.0182	0.91
0.030	0.95	0.00140	63	0.5480	0.0231	0.77
0.050	0.80	0.00118	53	0.4085	0.0287	0.58
0.100	0.66	0.00097	44	0.2380	0.0349	0.35
0.150	0.55	0.00081	37	0.1640	0.0417	0.29
0.200	0.48	0.00071	32	0.1260	0.0460	0.23
0.300	0.45	0.00066	30	0.0850	0.0483	0.16
			NaCl, 10 g./l.			
0.004	2.34	0.00344	156	0.9000	0.0040	1.00
0.010	2.10	0.00309	140	0.8542	0.0099	0.99
0.020	1.80	0.00264	120	0.7835	0.0192	0.96
0.030	1.57	0.00231	105	0.7178	0.0270	0.90
0.050	1.32	0.00194	88	0.6045	0.0373	0.75
0.100	1.02	0.00150	68	0.4130	0.0528	0.53
0.150	0.88	0.00129	59	0.3200	0.0617	0.41
0.200	0.76	0.00112	51	0.2390	0.0710	0.36
0.300	0.50	0.00074	33	0.1655	0.1012	0.34

TABLE IV. Determination of Donnan Coefficient and Ionized Carboxyl Groups at Different Stages of Oxidation for Chlorazol Sky Blue FF

W = 0.3 l./kg.; $[D]_s = 5.0 \times 10^{-5}$ moles/l.

Total [COO], eq./kg.	Dye adsorption, g./kg.	$[D]_\phi$, moles/kg.	Substantivity ratio $\frac{[D]_\phi}{W[D]_s}$	λ	Calculated [COO], eq./kg.	$\frac{\text{Calculated [COO]}}{\text{Total [COO]}}$
			NaCl, 5 g./l.			
0.004	4.19	0.00422	280	0.6725	0.0040	1.00
0.010	3.43	0.00346	229	0.6378	0.0099	0.99
0.020	2.50	0.00252	167	0.5730	0.0182	0.91
0.030	2.00	0.00202	133	0.5030	0.0235	0.78
0.050	1.50	0.00151	100	0.3890	0.0299	0.60
0.100	0.95	0.00096	63	0.2335	0.0397	0.40
0.150	0.75	0.00076	50	0.1625	0.0444	0.30
0.200	0.65	0.00066	43	0.1245	0.0473	0.24
0.300	0.58	0.00059	39	0.0850	0.0495	0.17
			NaCl, 10 g./l.			
0.004	5.79	0.00584	386	0.7682	0.0040	1.00
0.010	5.15	0.00520	343	0.7442	0.0097	0.97
0.020	4.50	0.00453	300	0.7048	0.0159	0.80
0.030	3.75	0.00378	250	0.6527	0.0239	0.80
0.050	3.00	0.00303	200	0.5640	0.0331	0.66
0.100	2.00	0.00202	133	0.3990	0.0488	0.49
0.150	1.55	0.00156	103	0.2990	0.0582	0.39
0.200	1.25	0.00126	83	0.2400	0.0660	0.33
0.300	0.87	0.00088	58	0.1640	0.0792	0.27

value of 0.3 l./kg. for W (it is assumed that the value of W does not change with changes in dye or salt concentration of the bath), experimentally determined values of $[D]_\phi$, and total carboxyl content of the oxycellulose determined by iodimetric method for [COO]. Values of λ thus obtained at different salt concentrations of the bath and for the two dyes examined are given in Tables III and IV. As expected theoretically, the value of λ decreases as [COO] increases. From Equation 4 it can be seen that $\frac{[D]_\phi}{[D]_s}$ is directly proportional to λ^z if all [COO] determined experimentally ionize completely and all these groups become directly effective for the reduction in dye adsorption. Under such conditions the plot of λ^z against $\frac{[D]_\phi}{[D]_s}$ should give a straight line passing through the origin. These curves for Chrysophenine G and Chlorazol Sky Blue FF at each of the two salt concentrations are given in Figures 4 and 5. It is found that with both the dyes, only at low amounts of [COO] do the points lie close enough to the theoretical straight line, and as the proportion of [COO] in the oxycelluloses increases, the deviation also increases.

In order to determine the proportion of the total [COO] groups which are responsible for the reduction of the dye uptake, values of K were obtained for each dye at each of the two salt concentrations for a value of [COO] of 0.004 eq./kg. For each set of conditions, using the appropriate value of K, different values of λ were obtained for the corresponding values of substantivity ratios, and the proportion of [COO] responsible for the repulsion of the dye for each of the dyes studied, at 5 and 10 g./l. salt concentration in the dyebath, has been calculated from Equation 8. The fraction of the total [COO] responsible for reduction in dye uptake at each stage of oxidation has also been calculated. These values are presented in the last two columns of Tables III and IV. It may be possible that only in the very initial stages of oxidation may more than 95% of the total [COO] groups be responsible for reduction in dye uptake, and with progressive increase in the total [COO], the fraction of the total [COO] groups ionizing in the dyebath may go on decreasing progressively. An alternate explanation for this behavior may be that although at high concentration of carboxyl groups all these groups may be ionized, they may not all be effective in reducing the equilibrium dye uptake because they may be located in regions of cellulose inaccessible to the molecules of the dye. However, under such circumstances, changes in pH of the dyebath should not influence the dye uptake. Bilsbury, Martin, and Standing [1] have clearly indicated the effect of dyebath pH on equilibrium adsorption, and, therefore, in interpreting the results of the present investigation, the first explanation appears to be more valid. As expected theoretically, with both the dyes studied, the proportion of [COO] responsible for the repulsion of dye is higher at a dyebath salt concentration of 10 g./l. than at 5 g./l. because at the salt concentration of 10 g./l., the extent of ionization of [COO] of the oxycellulose will be higher than would be the case at a concentration of 5 g./l.

Summary

Equilibrium adsorption of Chrysophenine G and Chlorazol Sky Blue FF on cellulose oxidized with potassium metaperiodate, dichromate-sulfuric acid, dichromate-oxalic acid, and sodium hypochlorite and on their corresponding borohydride reduced products and sodium chlorite treated samples have been determined under standard conditions of dyeing. Conversion of hydroxyl groups at 2, 3, or 6 position in the glucose units of cellulose chain molecules to carbonyl groups does not alter the dye uptake, but formation of carboxyl groups reduces dye adsorption markedly. The extent of reduction in dye adsorption at a specific stage of oxidation and electrolyte concentration in the bath is the same irrespective of the position in the glucose unit at which the carboxyl group has been formed. With an increase in the total carboxyl groups in cellulose, the increase in carboxyls which are responsible for the reduction in dye adsorption is not proportional. Based on a theoretical treatment, the fraction of the total carboxyl groups responsible for this reduction has been calculated.

Literature Cited

1. Bilsbury, M. M., Martin, J. T., and Standing, H. A., *J. Textile Inst.* **45**, T1 (1954).
2. Birtwell, C., Clibbens, D. A., and Ridge, P., *J. Textile Inst.* **16**, T13 (1925).
3. Davidson, G. F., *J. Textile Inst.* **31**, T81 (1940).
4. Davidson, G. F., *J. Textile Inst.* **32**, T132 (1941).
5. Davidson, G. F. and Nevell, T. P., *J. Textile Inst.* **46**, T407 (1955).

6. Gilbert, G. A., *Proc. Roy. Soc.* (*London*) **A183**, 167 (1944).
7. Giles, C. H., "XXVII Congrès International de Chimie Industrielle, Bruxelles," 1954.
8. Giles, C. H., Jain, S. K., and Hussain, A. S. A., *Chemistry & Industry*, No. 22, 629 (May 28, 1955).
9. Goldfinger, G., Mark, H., and Siggia, S., *Ind. Eng. Chem.* **35**, 1083 (1943).
10. Hanson, J., Neale, S. M., and Stringfellow, W. A., *Trans. Faraday Soc.* **31**, 1718 (1935).
11. Head, F. S. H., *J. Textile Inst.* **46**, T400 (1955).
12. Hessler, L. E. and Power, R. E., TEXTILE RESEARCH JOURNAL **24**, 822 (1954).
13. Heyes, T. F., *J. Soc. Chem. Ind.* (*London*) **47**, T90 (1928).
14. Jackson, E. L. and Hudson, C. S., *J. Am. Chem. Soc.* **59**, 2049 (1937); **60**, 989 (1938).
15. Kangle, P. J., Ph.D. Thesis, University of Bombay, 1960.
16. Lemin, D. R., *vide* Vickerstaff, T., "The Physical Chemistry of Dyeing," London, Oliver and Boyd, 1954, p. 95.
17. Marshall, W. J. and Peters, R. H., *J. Soc. Dyers Colourists* **63**, 446 (1947).
18. Mehta, M. T., M.Sc. (Tech.) Thesis, University of Bombay, 1958.
19. Nabar, G. M. and Padmanabhan, C. V., *Proc. Indian Acad. Sci.* **31A**, 370 (1950).
20. Nabar, G. M. and Padmanabhan, C. V., *J. Soc. Dyers Colourists* **69**, 295 (1953).
21. Neale, S. M. and Stringfellow, W. A., *J. Soc. Dyers Colourists* **56**, 17 (1940).
22. Nevell, T. P., *J. Textile Inst.* **39**, T118 (1948).
23. Robinson, C. and Mills, H. A. T., *Proc. Roy. Soc.* (*London*) **A131**, 596 (1931).
24. Rochas, P. and Daneyrolle, C., *Bull. inst. textile France* **76**, 21 (August 1958).
25. Rose, F. L., *vide* Vickerstaff, T., "The Physical Chemistry of Dyeing," London, Oliver and Boyd, 1954, p. 180.
26. Sadov, F. I. and Kalinina, K. G., *Nauch. Issledovatel., Trudy, Moskov. Tekstil Inst.* **13**, 18 (1954), *vide C. A.* **48**, 4842 (1954).
27. Standing, H. A. and Warwicker, J. O., *J. Textile Inst.* **40**, T175 (1949).

Manuscript received December 23, 1960.

Stress-Strain Relationships in Yarns Subjected to Rapid Impact Loading.

Part VII: Stress-Strain Curves and Breaking-Energy Data for Textile Yarns

Jack C. Smith, Paul J. Shouse, Josephine M. Blandford, and Kathryn M. Towne

National Bureau of Standards, Washington 25, D. C.

Abstract

Stress–strain curves at rates of straining up to 440,000%/min. have been obtained for a number of textile yarns by a technique involving high-speed photography of the yarn following transverse impact. These curves and others obtained at conventional speeds are presented for samples of acetate, triacetate, cotton, polyester, glass fiber, human hair, vinal, nylon, acrylic, rayon, saran, and silk yarns. Also given are specific breaking energies obtained from the areas under the stress–strain curves and by direct measurements involving longitudinal impact speeds of the order of 50 m./sec. These data show how stress–strain curves depend upon rate of straining and provide ratings for the yarns with respect to ability to survive impact and to resist impact without appreciable deformation.

Introduction

The Textiles Section of the National Bureau of Standards during the past five years has accumulated a considerable body of impact data on various textile yarns. Included in these data are stress–strain curves obtained at rates of straining of over 5000%/sec. by a method in which the yarn specimens were impacted transversely at speeds of the order of

40 m./sec. Stress–strain curves for these yarns were also obtained at 1%, 10%, and 100%/min. rates of straining by use of a commercial tester. These stress–strain data show how the breaking tenacity, breaking elongation, and initial tensile modulus for the yarns change when the rate of testing is varied over a wide range.

The ability of a yarn to withstand impact is characterized by its specific breaking energy, or work per unit mass required to break the yarn.[1] This quantity, which is proportional to the area under the stress–strain curve up to the rupture strain, was calculated for each yarn from the stress–strain data obtained under impact conditions. The specific breaking energies for the yarns were also measured directly using a longitudinal-impact tester operating at impact speeds between 20 and 70 m./sec.

By collecting data, such as those just described, for a variety of textile yarns, it becomes possible to discover similarities in the reactions of different yarns to impact loading. The effects of differences in the yarns also suggest themselves. It was with this purpose in mind that the following data were obtained.

Tests at Slow Speeds

The yarn specimens were tested at low rates of straining with a class 3 (constant-rate-of-straining) machine, ASTM Designation: D 76-53. Stress–strain curves were plotted from average data of five tests on specimens 10 in. long. The specimens were tabbed at each end with masking tape to prevent slippage in the jaws of the tester. The heavier specimens were tabbed with two strips of heavy cloth held together with a rubber-base adhesive. Two-turns/in. twist was added to most of the yarns prior to testing in order to minimize interfiber slippage and strand-by-strand breakage. Conditioning and testing of the specimens were carried out at a temperature of 23° C. and 50% RH.

Transverse-Impact Tests

The apparatus and technique used in the transverse-impact tests have been described elsewhere [8], and will be only briefly outlined here. A specimen 40–60 cm. in length was clamped to a rigid massive table on which a reference grid was inscribed. The specimen was impacted at the midpoint by a freely flying projectile that had been struck by a rapidly rotating, spring-actuated hammer. In most of the tests, the velocity of the projectile was approximately 40 m./sec., but in a few tests velocities up to 65 m./sec. were employed. The subsequent configurations of the specimen after impact were recorded by means of a high-speed camera which took 15,000 pictures per second.

When the yarn specimen is struck by the projectile, longitudinal strain-waves are initiated and propagated along the yarn, one in each direction away from the point of impact. In the region between the two wave fronts, material of the yarn is set into motion towards the point of impact. This inward flowing material forms itself into a transverse wave shaped like an inverted "V" with the impacting projectile at the vertex. The front of this transverse wave travels along the yarn at a slower velocity than that of the preceding longitudinal-strain-wave front. Reflections of the transverse wave occur at the clamps and at the projectile until the yarn breaks. It is these successive positions of the transverse-wave front that are recorded photographically.

The photographic records obtained in the transverse-impact tests were analyzed as follows. The distance along the yarn specimen from the impact point to one of the clamps was measured in each picture. This provided strain–time data for the test. The position of the transverse-wave front was measured in each picture and the position–time curve plotted. Slopes taken from this position–time curve provided data for the velocity–time curve of the transverse-wave front. The velocity at which the transverse-wave front travels depends in a simple manner upon the stress and strain in the yarn, so that the stress–time data for the test were easily calculated. The stress–strain curve was then plotted from the strain–time data and the stress–time data. The rate of straining in these tests was not constant, in fact, the strain–time curves were always convex to the time axis. The strain rates given are computed by dividing the breaking strain by the time required to break the specimen.

In order to obtain a distinct photographic record, it was necessary to ply some of the yarns to obtain a test specimen of the order of 100 tex. The plied specimens were given a small twist, usually ½ turn/cm., in order to prevent spreading of the specimen after impact. From 2 to 5 specimens of each

[1] In previous publications in this series the term "breaking-energy density" was used instead of "specific breaking energy." Both terms have the same meaning.

yarn material were tested. On the 40-cm. specimens it was possible to record yarn configurations on each side of the projectile. In this way data for two stress–strain curves were obtained from each test. The temperature and relative humidity were not controlled in the laboratory in which the transverse-impact tests were conducted.

Longitudinal-Impact Tests

The apparatus and techniques used in the longitudinal-impact tests have also been described elsewhere [5, 7, 9], but will be briefly discussed here. The yarn specimens impacted were approximately 70 cm. long. A head mass weighing approximately 20 g. was attached to one end of the specimen, and a tail mass was attached to the other end. The size of the tail mass used depended upon the mass of the specimen and the velocity of impact. Thus for heavy specimens impacted at high velocity, aluminum masses weighing as much as 6 g. were employed, but for lighter specimens of approximately 10 tex, ½-g. tail masses made from strips of masking tape were used.

The longitudinal-impact apparatus consisted primarily of a rotating disc with a pair of hammers affixed to it, one on either side. The head mass, specimen, and tail mass were inserted in a metal tube which was mounted horizontally, above and in the plane of the rotating disc. While the disc was being brought up to impact speed, the hammers passed to either side of the tube and protruding head mass. When impact was desired, the tube was rapidly rotated through a 90° angle so that the hammers would strike projections on the head mass, thus subjecting the specimen to a sudden longitudinal pull. The head mass, specimen, and tail mass were propelled into free flight and caught in a catch box located a few feet away.

When the impact velocity was high enough, the inertia of the tail mass was sufficient to break the specimen. When the impact velocity was too low the specimen was not broken. After a series of tests it was possible to determine the velocity, W_{mn}, just sufficient to break a specimen to which a given tail mass was attached. The specific breaking energy was then computed from the formula

$$E_b = \tfrac{1}{2}\,\frac{(n+\tfrac{1}{2})(m+\tfrac{1}{2})}{n+m+1}\,W_{mn}^{2} \times 10^{-3} \qquad (1)$$

where E_b is the specific breaking energy in joules/g., n is the ratio of the tail mass to the mass of the specimen, m is the ratio of the head mass to the mass of the specimen, and W_{mn} is the head-mass velocity in m./sec. that is just sufficient for the specimen to be broken. A derivation of this formula is given in a previous paper [7]. Several different values of W_{mn} corresponding to different tail masses were found for each yarn sample and the corresponding values of E_b were averaged to obtain the final value. The temperature and relative humidity were not controlled in the laboratory in which the longtiudinal-impact tests were conducted.

An illustration of this method is provided by the results of a test on acetate yarn given in Table I.

TABLE I. Break, No-Break Data for Acetate Sample

Hammer velocity, m./sec.	Breaks	No breaks	Number of specimens tested
28		/	1
29		/	1
30	/	/	2
31	///	///	6
32	///	/	4
33	///		3

In this test various one-ply specimens with masking-tape tail masses attached were impacted at different hammer velocities, and the results of the impact noted. From these data a hammer velocity of 31 m./sec. was chosen as the velocity just sufficient to cause rupture of the specimen. The impact of the hammers and head mass was a semi-elastic collision, and the velocity of the head mass was greater than that of the hammers. The head-mass velocity, therefore, was found by multiplying the hammer velocity by a correction factor found by a previous calibration. A value of 45.6 m./sec. for W_{mn} was obtained.

The aluminum head mass weighed 16.180 g., and the masking-tape tail masses 0.317 g. apiece. Each specimen was 76.5 cm. long and weighed 0.0129 g. Thus $m = 16.180/0.0129 = 1254$, and $n = 0.317/0.0129 = 24.6$. Substituting the above values into Equation 1 gave a value of 25.6 joules/g. for the specific breaking energy. Similar tests were performed at two other impact velocities by using different tail masses. Specific breaking energies obtained from these tests were 31.9 joules/g. and 27.8 joules/g. The average of these tests was 28.4 joules/g., which is the value reported in Table III.

Results

Table II lists the yarn samples tested. These yarns were obtained from various sources and the details of their manufacture are not known. Most of the yarns were of regular commercial production, but triacetate, vinal, and some of the rayon tire yarns were spun experimentally. The sample of human hair used was purchased from a local hair emporium. It was in the natural state and had not been subjected to any setting treatment.

Stress–strain curves for these textile yarns are given in Figures 1 through 19 inclusive. The curves corresponding to 1%, 10%, and 100%/min. rates of straining were obtained with a commercial tensile tester. The curves corresponding to strain rates of the order of 5000%/sec. were obtained by the transverse-impact technique. Test data for the yarns are given in Table III. Here are tabulated the modulus, breaking-tenacity, and breaking-elongation values for the stress–strain curves. Specific breaking energies were found by multiplying the areas under the stress–strain curves by an appropriate conversion factor. Specific breaking energies obtained by direct measurement with the longtiudinal-impact apparatus are also tabulated.

Certain features are common to all of the stress–strain curves. Thus stress–strain curves obtained at

TABLE II. Description of Yarns Tested

A. Acetate, bright, 16.7 tex, 16 filament, stretch ratio 1.09
B. Triacetate, 16.7 tex, 40 filament
C. Cotton sewing thread, Karnak-3, 1 $\frac{7}{16}$ in. staple length, 22 S yarn twist, 19 Z ply twist, undyed, regular finish, 11.6 cotton count, 50.9 tex.
D. Cotton sewing thread, Acala 4–42, 1$\frac{1}{4}$ in. staple length, 22 S yarn twist, 19 Z ply twist, undyed, regular finish, 11.7 cotton count, 50.5 tex.
E. Polyester, bright, 6.7 tex, 34 filament, 3.61 X draw ratio
F. Glass fiber, D 450–4/3, 141 tex, continuous filament, 4.4 S twist
G. Human hair, 50 hairs per specimen, 5 tex per hair, 250 tex total
H. Vinal, 54.3 tex, 600 filament
I. Vinal, 83 tex, 600 filament
J. Nylon, high tenacity, bright, 93.3 tex, 140 filament, $\frac{1}{2}$ Z twist
K. Acrylic, semi-dull, 16.7 tex, 80 filament, 8 X draw ratio
L. Rayon, low tenacity, bright, 100 tex, 50 filament
M. Rayon, medium tenacity, bright, 16.7 tex, 60 filament
N. Rayon, high tenacity, 183 tex, 720 filament
O. Rayon tire yarn, 207 tex, 980 filament, 4.4 Z twist
P. Rayon tire yarn (experimental), 199 tex, 980 filament, 4.2 Z twist
Q. Rayon tire yarn (experimental), 185 tex
R. Saran, 22.2 tex, 12 filament, 1 Z twist
S. Braided silk fish line, 24# test, approximately 330 tex

TABLE III. Test Data on Yarns

Yarn sample and method of test	Initial tensile modulus, g./tex	Breaking tenacity, g./tex	Breaking elongation, %	Specific breaking energy, joules/g.
A. Acetate				
Slow speed				
1%/min.	320	10.1	35.7	24.3
10%/min.	340	10.8	35.6	27.2
100%/min.	370	11.2	32.0	25.8
Transverse impact				
20 cm. half-length, 42 m./sec., 7300%/sec.	350	14.6	30.7	34.9
Longitudinal impact				
76.5 cm. length, 45–64 m./sec.				28.4
B. Triacetate				
Slow speed				
1%/min.	370	11.0	24.5	19.5
10%/min.	410	11.8	24.7	21.4
100%/min.	450	12.7	24.2	22.5
Transverse impact				
15 cm. half-length, 40 m./sec., 7300%/sec.	400	16.8	15.6	18.9
Longitudinal impact				
77.0 cm length, 50 m./sec.				20.6
C. Cotton, Karnak-3				
Slow speed				
1%/min.	490	23.2	6.1	8.0
10%/min.	510	24.8	6.4	8.7
100%/min.	570	28.0	6.4	9.7
Transverse impact				
20 cm. half-length, 40 m./sec., 4100%/sec.	860	34.5	6.8	13.6
Longitudinal impact				
76.5 cm. length, 36–47 m./sec.				9.9
D. Cotton, Acala 4–42				
Slow speed				
1%/min.	450	16.4	4.7	4.3
10%/min.	500	16.7	4.7	4.6
100%/min.	520	19.3	5.1	5.4
Transverse impact				
20 cm. half-length, 41 m./sec., 3500%/sec.	710	30.6	4.6	7.1
Longitudinal impact				
76.5 cm. length, 35 m./sec.				5.0
E. Polyester				
Slow speed				
1%/min.	940	39.9	24.1	74.5
10%/min.	990	42.6	24.8	83.6
100%/min.	1100	44.0	22.3	80.3
Transverse impact				
20 cm. half-length, 42 m./sec., 4100%/sec.	1100	60.5	8.0	24.3
Longitudinal impact				
77.0 cm. length, 34–54 m./sec.				15.5

TABLE III.—Continued

Yarn sample and method of test	Initial tensile modulus, g./tex	Breaking tenacity, g./tex	Breaking elongation, %	Specific breaking energy, joules/g.
F. Glass fiber				
Slow speed				
1%/min.	2310	58.0	2.6	7.2
10%/min.	2370	62.6	2.7	8.3
100%/min.	2430	64.5	2.7	8.5
Transverse impact				
30 cm. half-length,				
39 m./sec., 1800%/sec.	2470	63.1	2.6	8.1
G. Human hair				
Slow speed				
1%/min.	330	9.8	30.8	38.7
10%/min.	360	13.1	36.8	55.6
100%/min.	380	14.4	36.7	60.9
Transverse impact				
20 cm. half-length,				
38 m./sec., 7000%/sec.	420	17.3	33.6	71.8
H. Vinal				
Slow speed				
1%/min.	1960	75.2	6.2	20.9
10%/min.	1820	80.9	6.2	22.6
100%/min.	2430	81.9	5.8	21.8
Transverse impact				
20 cm. half-length,				
38 m./sec., 3000%/sec.	2760	82.0	5.3	23.3
Longitudinal impact				
70.7 cm. length,				
41 m./sec.				17.1
I. Vinal				
Slow speed				
1%/min.	700	53.1	17.0	43.0
10%/min.	770	56.2	16.0	41.4
100%/min.	940	58.3	15.1	41.0
Transverse impact				
20 cm. half-length,				
40 m./sec., 5000%/sec.	1130	68.9	14.3	48.2
Longitudinal impact				
70.7 cm. length,				
38 m./sec.				45.2
J. Nylon				
Slow speed				
1%/min.	390	65.7	15.5	48.1
10%/min.	430	71.1	15.4	51.5
100%/min.	480	75.8	15.5	55.4
Transverse impact				
20 cm. half-length,				
41 m./sec., 4800%/sec.	860	81.4	11.1	38.5
Longitudinal impact				
75–78 cm. length,				
32–61 m./sec.				32.1

TABLE III.—Continued

Yarn sample and method of test	Initial tensile modulus, g./tex	Breaking tenacity, g./tex	Breaking elongation, %	Specific breaking energy, joules/g.
K. Acrylic				
Slow speed				
1%/min.	800	39.4	18.4	35.7
10%/min.	870	44.6	18.1	40.8
100%/min.	980	50.6	17.0	43.2
Transverse impact				
20 cm. half-length,				
41 m./sec., 5100%/sec.	1020	60.6	14.6	46.5
Longitudinal impact				
76.5 cm. length,				
45–74 m./sec.				49.2
L. Rayon, low tenacity				
Slow speed				
1%/min.	460	14.9	20.4	18.9
10%/min.	550	16.4	20.3	21.4
100%/min.	610	18.3	20.7	24.6
Transverse impact				
20 cm. half-length,				
39 m./sec., 5500%/sec.	590	22.8	19.3	28.3
Longitudinal impact				
73–77 cm. length,				
32–54 m./sec.				30.6
M. Rayon, medium tenacity				
Slow speed				
1%/min.	800	23.0	15.1	21.6
10%/min.	950	24.2	14.9	22.7
100%/min.	1080	26.6	15.3	25.5
Transverse impact				
20 cm. half-length,				
38 m./sec., 4500%/sec.	1360	33.0	13.1	25.8
Longitudinal impact				
76.5 cm. length,				
37–57 m./sec.				30.6
N. Rayon, high tenacity				
Slow speed				
1%/min.	1020	35.3	9.9	20.8
10%/min.	1080	37.7	9.3	20.1
100%/min.	1120	39.6	9.2	21.0
Transverse impact				
30 cm. half-length,				
37 m./sec., 2500%/sec.	1420	45.5	8.8	24.1
Longitudinal impact				
74–78 cm. length,				
37–66 m./sec.				21.6
O. Rayon tire yarn				
Slow speed				
1%/min.	390	24.5	20.8	27.5
10%/min.	490	26.0	19.6	28.9
100%/min.	500	26.0	19.0	28.1
Transverse impact				
20 cm. half-length,				
41 m./sec., 5900%/sec.	650	38.8	19.1	44.8
Longitudinal impact				
73–77 cm. length,				
40–72 m./sec.				44.1

(continued)

TABLE III.—Continued

Yarn sample and method of test	Initial tensile modulus, g./tex	Breaking tenacity, g./tex	Breaking elongation, %	Specific breaking energy, joules/g.
P. Rayon tire yarn (experimental)				
Slow speed				
1%/min.	330	30.5	27.2	43.6
10%/min.	370	30.4	24.7	39.8
100%/min.	430	32.8	25.0	43.7
Transverse impact				
20 cm. half-length, 41 m./sec., 6500%/sec.	550	42.1	22.9	55.5
Longitudinal impact				
75–77 cm. length, 43–72 m./sec.				45.0
Q. Rayon tire yarn (experimental)				
Slow speed				
1%/min.	960	39.1	12.2	27.4
10%/min.	1040	42.1	11.6	27.4
100%/min.	1140	45.4	12.4	32.4
Transverse impact				
20 cm. half-length, 40.9 m./sec., 4700%/sec.	1530	57.8	10.7	36.8
Longitudinal impact				
74–77 cm. length, 44–61 m./sec.				32.9
R. Saran				
Slow speed				
1%/min.	100	18.9	22.7	21.2
10%/min.	120	19.5	19.5	18.3
100%/min.	130	18.7	18.3	16.9
Transverse impact				
20 cm. half-length, 41 m./sec., 5300%/sec.	170	21.7	15.3	17.4
Longitudinal impact				
76.5 cm. length, 34–62 m./sec.				21.2
S. Braided silk fishing line				
Slow speed				
1%/min.	400	31.5	18.5	35.6
10%/min.	410	34.3	18.8	39.3
100%/min.	470	36.5	19.0	43.6
Transverse impact				
20 cm. half-length, 39 m./sec., 5300%/sec.	490	42.3	17.9	46.4
Longitudinal impact				
61 cm. length, 45–66 m./sec.				44.3

the higher rates of straining have steeper initial slopes. The initial linearity of these higher-rate curves tends to persist to higher values of stress. The breaking tenacities are usually higher, but the breaking elongations may be greater or less than the values obtained at conventional rates of testing depending upon the material tested.

The breaking elongation for acetate (Figure 1)

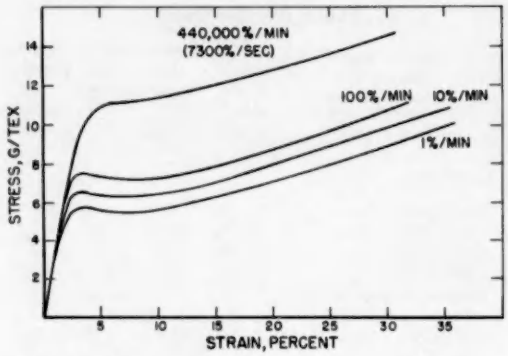

Fig. 1. Stress–strain curves for acetate (A) yarn.

is only slightly less at the 7300%/sec. rate of straining than at the lower testing rates, but the breaking tenacity is comparatively high. Thus, for acetate the specific breaking energy, which is proportional to the area under the stress–strain curve, is slightly higher at high rates of straining than at the lower ones. This means that the ability of acetate to withstand impact is unimpaired at speeds up to 50 m./sec. In fact, acetate performance is slightly better at the higher speeds.

The test results for triacetate (Figure 2) are similar to those of acetate except that the specific breaking energies for triacetate are slightly lower and the values under impact conditions remain about the same as the low-speed values.

The specific breaking energy for acetate calculated from the area under the stress–strain curve obtained by transverse impact is 34.9 joules/g., whereas the value obtained directely by the longitudinal-impact method is 28.4 joules/g. The latter value compares better with the 24–27-joules/g. range obtained from tests with a commercial tester. Similar discrepancies will be noted for several others of the fibers tested. The value obtained by transverse impact would seem to be too high, possibly because of an overestimate of the breaking elongation. If the breaking elongation were 27% instead of the 30.7% given in Table III, the specific breaking energy would be reduced to 29.7 joules/g., a more reasonable value.

The 30.7% breaking elongation for acetate was determined by visually examining the photographic records of the tests made. It was usually possible in this way to determine when the breakage occurred to within one or two pictures. As the acetate specimens elongated at a rate of 1% per picture for strains near the breaking strain, the uncertainty in

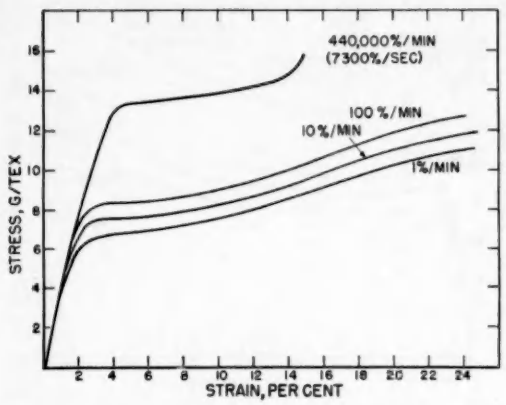

Fig. 2. Stress–strain curves for triacetate (B) yarn.

the value of the breaking strain was of the order of $\pm 2\%$. It is also likely that strand-by-strand breakage occurred in the heavily plied specimens tested. This type of breakage cannot be detected visually until many of the strands have been broken. From the foregoing discussion it seems likely that the value of 34.9 joules/g. specific breaking energy found for acetate by transverse-impact tests is too high. The magnitude of the overestimate, however, is exceptional, and better accuracies are obtained in the values given for other textile yarns.

Two samples of cotton sewing thread were tested, Karnak (Figure 3) and Acala (Figure 4). For each of these samples the breaking tenacity at the high rate of straining is greater than the breaking tenacity obtained at conventional strain rates, but the breaking strain does not change much. Therefore the specific breaking-energy value determined from the transverse-impact stress–strain curve is higher than the values obtained from the curves corresponding to the slower testing rates. It should be noted that the transverse-impact values given, 13.6 joules/g. for Karnak and 7.1 joules/g. for Acala, are higher than the corresponding longitudinal-impact values of 9.9 and 5.0. Although the transverse-impact values may have been overestimated, it is also possible in this case that the longitudinal-impact values are slightly low. The measurement of specific breaking energies less than 10 joules/g. involves tail-mass to specimen-mass ratios of magnitude 10 or less, and this introduces an uncertainty of the order of 10% into the measurement. Despite this, the tests indicate that these two cotton samples retain their ability to withstand impact up to strain rates of 4000%/sec.

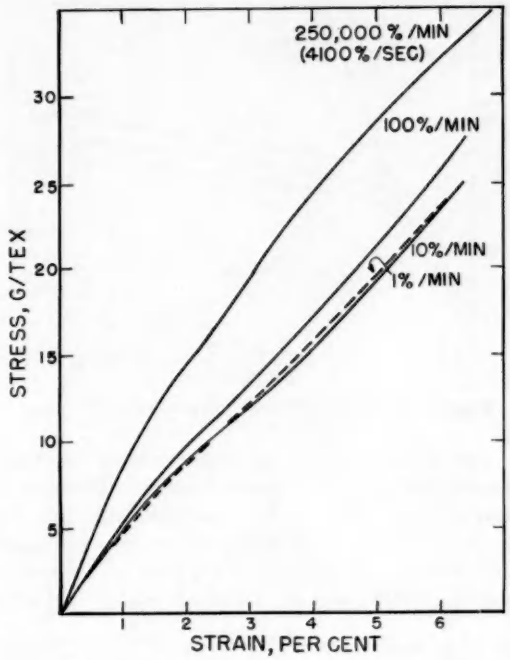

Fig. 3. Stress–strain curves for Karnak cotton (C) yarn.

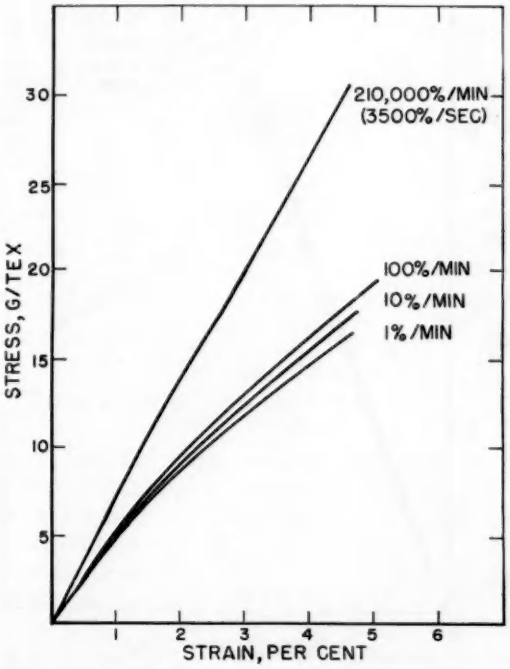

Fig. 4. Stress–strain curves for Acala cotton (D) yarn.

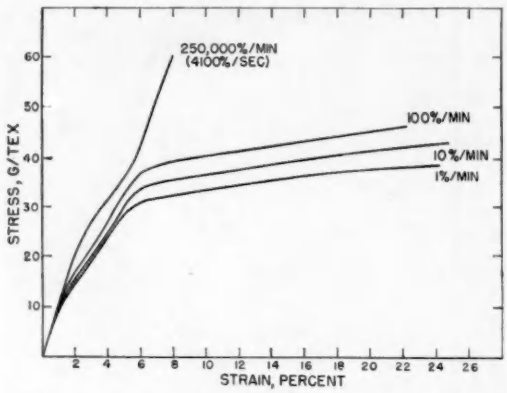

Fig. 5. Stress–strain curves for polyester (E) yarn.

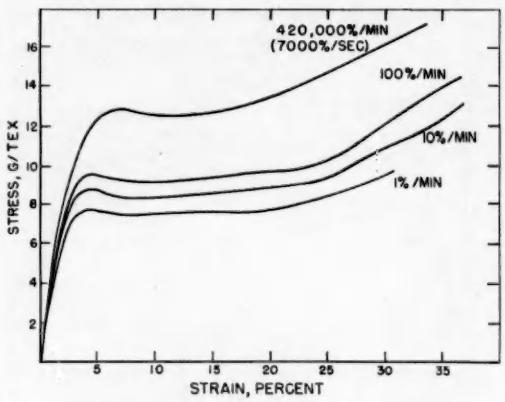

Fig. 7. Stress–strain curves for human hair (G) yarn.

The behavior of the polyester sample contrasts sharply with that of acetate and cotton. The stress–strain curves (Figure 5) show that although the breaking tenacity obtained by the transverse-impact test is high, the breaking elongation is drastically reduced. The specific breaking energy of 24.3 joules/g. obtained from the transverse-impact data is considerably less than the value of 80 joules/g. obtained at the lower testing rates, but higher than the value of 15.5 joules/g. obtained by longitudinal-impact tests. It is possible that the value of 24.3 joules/g. is too high because of overestimate of the breaking elongation. It can be seen from the corresponding stress–strain curve that a small change in breaking elongation in this case would greatly affect the area under the curve and hence the specific breaking energy. It should be noted that the polyester yarn used was of regular tenacity. If a high-tenacity yarn, having a breaking tenacity of 67 g./tex and a breaking elongation of 15% at conventional test rates [10], had been used, the difference in specific breaking energies from high- and low-speed tests would probably not have been so pronounced.

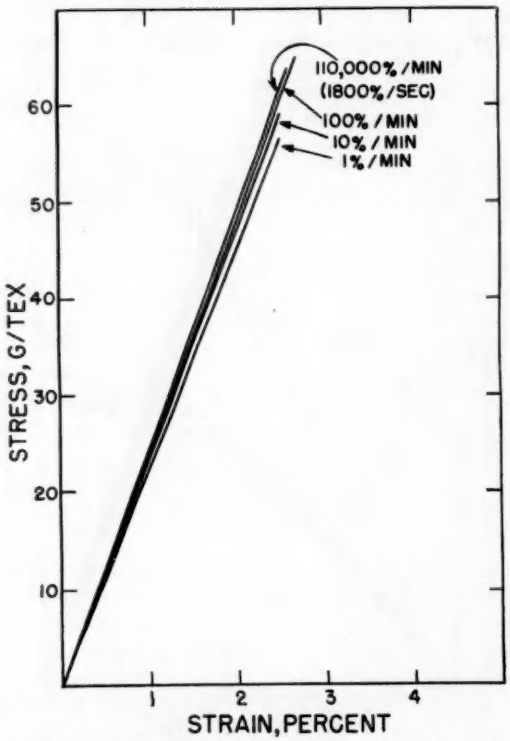

Fig. 6. Stress–strain curves for glass fiber (F) yarn.

According to the curves (Figure 6) and the data of Table III, the stress–strain behavior of glass fiber does not change much with the rate of straining. The stress–strain curve obtained by transverse impact is practically the same as that obtained at a straining rate of 1%/min. Specific breaking energies are also unchanged over the wide range of straining rates used. Longitudinal-impact data were not obtained on this yarn sample because of the difficulty of making the tail weights required for accurate results. The specific breaking energy of glass fiber, 8.1 joules /g., and the comparable values for cotton are the lowest obtained from all the samples tested.

The stress–strain behavior of human hair (Figure 7) is similar over a range of straining rates up to 7000%/sec. At the 7000%/sec. rate the breaking tenacity is high and the breaking elongation remains

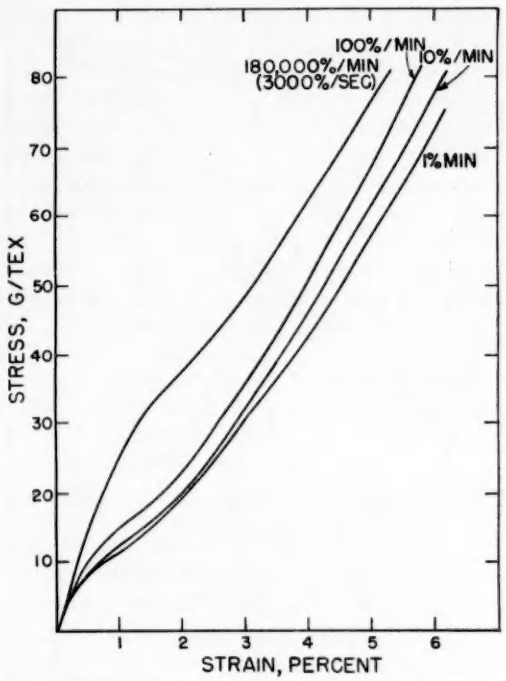

Fig. 8. Stress–strain curves for vinal (H) yarn.

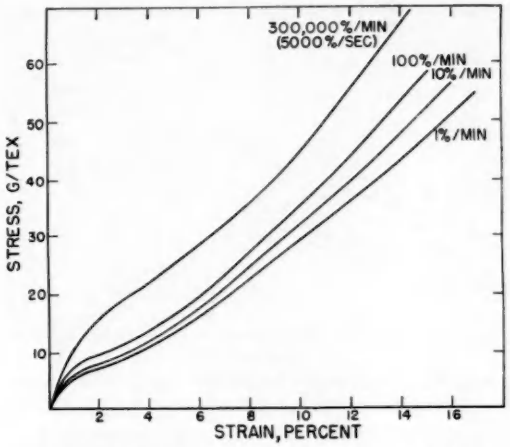

Fig. 9. Stress–strain curves for vinal (I) yarn.

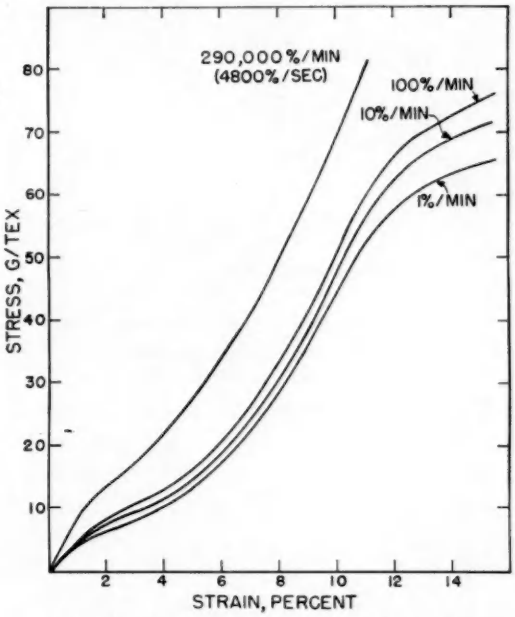

Fig. 10. Stress–strain curves for high-tenacity nylon (J) yarn.

at the same value as that obtained at the lower straining rates. The specific breaking energy increases as the test rate increases, and attains a value of 71.8 joules/g. when tested by a 38-m./sec. transverse impact. This value of specific breaking energy is the highest value obtained under impact conditions of all the samples tested.

Stress–strain curves for two vinal samples are given in Figures 8 and 9. In each of these samples the breaking elongation decreases only slightly as the speed of testing is increased. This decrease in breaking elongation is accompanied by an increase in breaking tenacity. The specific breaking energy therefore remains practically independent of the rate of straining. The specific breaking energy of 17.1 joules/g. obtained by a longitudinal-impact test on the vinal (H) sample is probably too low. Only a small amount of this sample was available, so the value obtained could not be checked by a second test.

Figure 10 gives curves obtained from tests on a high-tenacity nylon sample. The breaking elongation for this sample decreases significantly under impact conditions, and the increase in tenacity is only moderate. The specific breaking energy for nylon, therefore, decreases at high rates of straining. This effect has previously been noted by Meredith [6] and confirmed in an earlier publication [7].

Stress–strain curves for a continuous-filament acrylic fiber are given in Figure 11. At high rates of straining the breaking elongation is decreased slightly, but this decrease is accompanied by an increase in breaking tenacity. The specific breaking

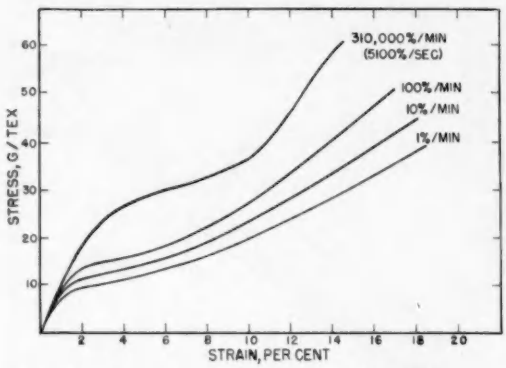

Fig. 11. Stress–strain curves for acrylic (K) yarn.

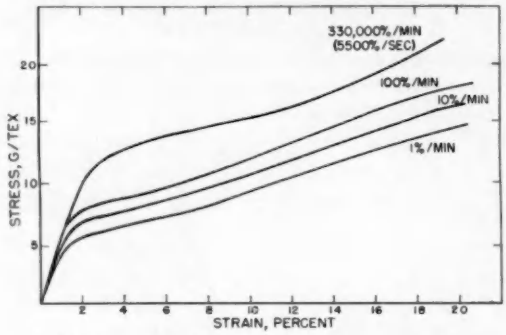

Fig. 12. Stress–strain curves for low-tenacity rayon (L) yarn.

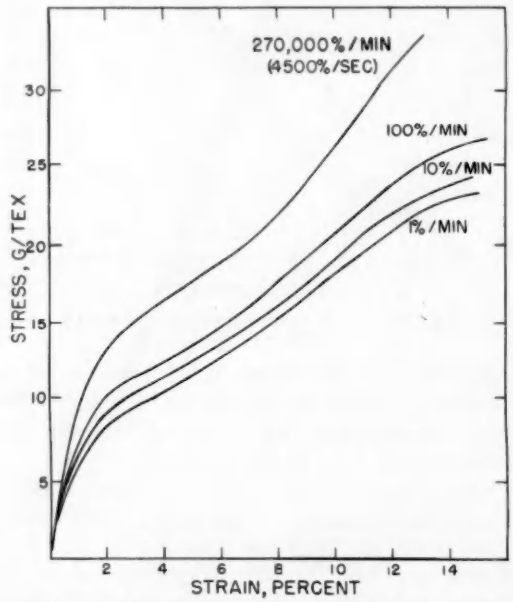

Fig. 13. Stress–strain curves for medium-tenacity rayon (M) yarn.

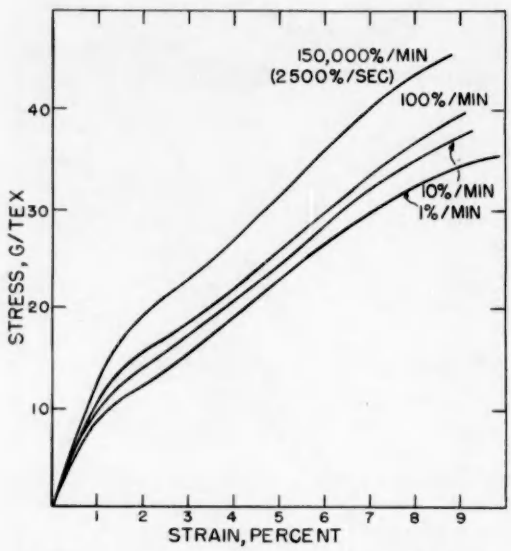

Fig. 14. Stress–strain curves for high-tenacity rayon (N) yarn.

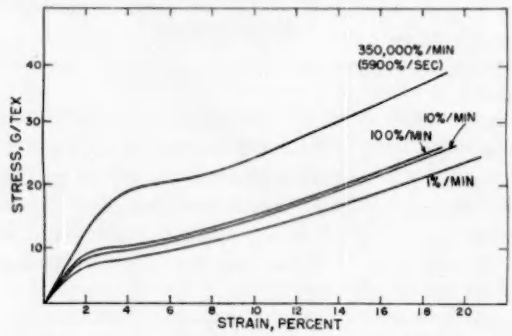

Fig. 15. Stress–strain curves for rayon (O) tire yarn.

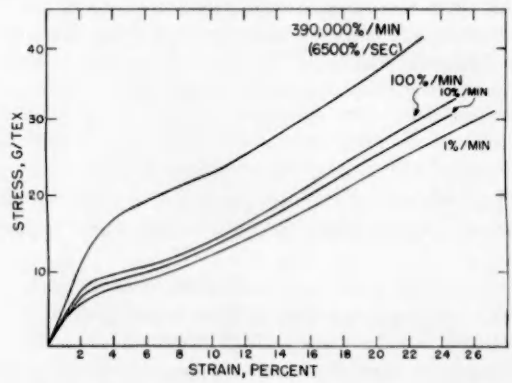

Fig. 16. Stress–strain curves for rayon (P) tire yarn.

energy increases slightly as the rate of straining is increased.

Data on a number of different rayon samples are given in Figures 12–17. The first three sets of curves are for low-tenacity (L), medium-tenacity (M), and high-tenacity (N) rayons. In each of these samples the breaking elongation is only slightly decreased at high rates of straining, and the breaking tenacities are increased. The specific breaking energies in each case are slightly higher under impact conditions. It is interesting to note that similar behavior is observed for the other cellulosic fibers, acetate and cotton.

The high-tenacity rayon (N) is representative of commercial tire yarn production of the year 1955. Rayon (O) is a commercial tire yarn of the year 1956 made by a different manufacturer. Rayon (P) and Rayon (Q) are experimental tire yarns. The changes in the stress–strain curves with rate of straining are similar in all of these samples. The specific breaking energies increase at the high rates of straining, indicating that these yarns exhibit improved behavior under impact conditions.

Stress–strain curves for saran are given in Figure 18. Here again the breaking elongation is decreased at the highest rate of straining but the breaking tenacity is increased by a compensating amount. The specific breaking energy remains essentially constant with rate of straining.

The curves for braided silk fishing line are given in Figure 19. It is seen from these curves and the data of Table III that the specific breaking energy remains high and increases slightly with increase in the rate of straining up to longitudinal-impact speeds of the order of 50 m./sec.

Discussion of Results

The ability of a textile material to extract energy from an impactor is measured by the specific break-

TABLE IV. Textile Yarns with Specific Breaking Energies Exceeding 40 joules/g.

Yarn	Specific breaking energy, joules/g.	
	Low strain rate	High strain rate
Polyester (E)	80	20
Hair (G)	61	72
Nylon (J)	55	35
Rayon (P)	44	50
Acrylic (K)	43	48
Silk (S)	44	45
Vinal (I)	41	46
Rayon (O)	28	44

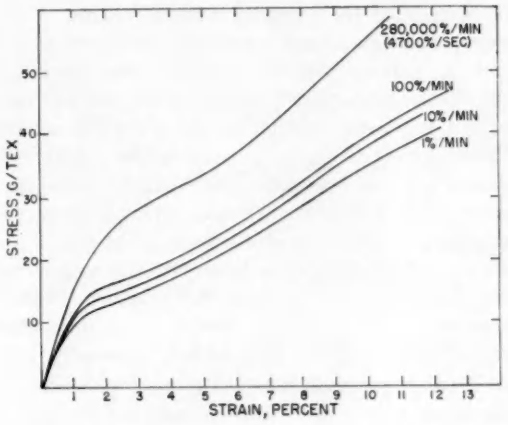

Fig. 17. Stress–strain curves for rayon (Q) tire yarn.

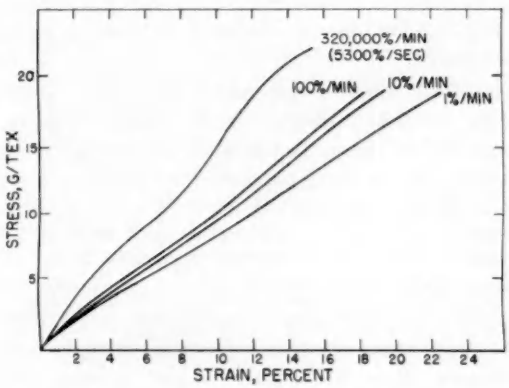

Fig. 18. Stress–strain curves for saran (R) yarn.

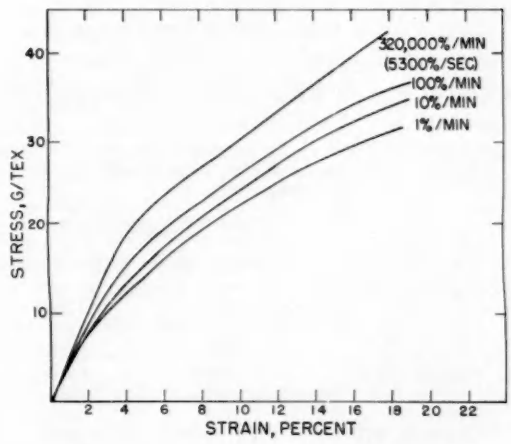

Fig. 19. Stress–strain curves for braided silk (S) fishing line.

ing energy of the component textile yarns. This energy, therefore, characterizes the ability of a textile yarn to survive impact. Textile yarns having a specific breaking energy exceeding 40 joules/g. may be said to possess superior ability to survive impact. The choice of 40 joules/g. as a criterion, although arbitrary, seems reasonable from a study of the data presented in Table III. Textile yarns whose specific breaking energies exceed 40 joules/g. at low strain rates or under impact conditions have been selected from Table III and are listed in Table IV. Several facts become immediately obvious from this table. For instance, high-tenacity nylon, ordinarily considered to have superior impact properties, is actually inferior to several other fibers usually not thought of in connection with impact. The impact-absorbing ability of human hair is outstanding. The polyester sample, although possessing high specific breaking energy at low test speeds, fails under impact conditions.

In many practical applications the quantity sought is not the energy absorbed by the fiber in breaking, since rupture cannot be tolerated. A more desirable quantity is the energy absorbed by the fiber for a small strain of the order of 2% or less. This energy measures the ability of a textile yarn to resist an impact. Stress–strain curves, especially those obtained under impact conditions, are linear near the origin. Therefore the triangular area under these curves for small strains is equal to $\frac{1}{2}$ the modulus of elasticity times the square of the strain. The modulus or initial slope of the stress–strain curve thus becomes a suitable parameter for characterizing the impact-resisting ability of a textile yarn.

Table V lists those textile yarns whose initial tensile moduli exceed an arbitrarily chosen value of 1000 g./tex. Except for acrylic and vinal (I) the yarns in this table are different from those appearing in Table IV. This demonstrates that the impact-surviving and impact-resisting abilities of the same yarn are usually very different in degree. An extreme example is provided by glass fiber which is the worst of all the fibers tested in impact-surviving ability, but best in impact-resisting ability.

TABLE V. Textile Yarns with Initial Tensile Moduli Exceeding 1000 g./tex

Yarn	Initial tensile modulus, g./tex	
	Low strain rate	High strain rate
Vinal (H)	2430	2760
Glass fiber (F)	2430	2470
Rayon (Q)	1140	1530
Rayon (N)	1120	1420
Rayon (M)	1080	1360
Vinal (I)	940	1130
Polyester (E)	1100	1100
Acrylic (K)	980	1020

Impact-resisting ability is an important property to be considered in the selection of a textile fiber for use in a laminate. When a composite material of this type is strained, the matrix usually breaks or cracks when the imbedded fibrous material has been strained only a few percent. Therefore for maximum strength and impact-resisting ability the textile fibers used should have a high initial tensile modulus. Impact-surviving ability, however, is important in such applications as parachute lines, and airplane arresting gear. In these applications, the ability to stretch contributes much to the effectiveness of the materials used.

Comparison with Metals

It is interesting to note that specific breaking energies of textile yarns have values that usually are larger than those found for metals. For instance, number 12 A.W.G. commercial copper wire 0.1 in. in diameter annealed at 900° F. has a specific breaking energy of 5.7 joules/g., and a commercial aluminum wire 0.1 in. in diameter annealed at 720° F. has a specific breaking energy of 3.6 joules/g. These values were obtained by Duwez, Wood, and Clark [3] from slow-speed stress–strain tests on 36-in. specimens. In another publication [2], these authors provide data on low-carbon steel wire 0.120 in. in diameter annealed at 1725° F. Gauge length of the specimen which was tested at slow speed was 10 in. From the data a specific breaking energy of 6.0 joules/g. was calculated. In a final report [1], Duwez and Clark submit breaking-energy data obtained by both low- and high-speed tests on a selection of steel samples. These tests were performed on specimens of 0.300 in. in diameter having a gauge length of 8 in. Specific breaking energies ranging between 4 and 16 joules/g. were obtained.

When compared on the basis of weight, most textile fibers excel the metals aluminum, copper, and steel in ability to absorb or survive an impact but they do not excel them in ability to resist an impact. The comparison, however, is not unfavorable. Young's modulus for aluminum is 2600 g./tex, for

copper 1400 g./tex, and for steel 2600 g./tex. Table V shows that vinal (H) and glass fiber have comparable values.

Effect of Strain Rate on Stress–Strain Curves

Most of the stress–strain curves in Figures 1–19 have three roughly defined regions in which the behavior is different. In the initial region the stress–strain curve is linear. A second region then follows in which the slope of the stress–strain curve is less than the initial value. In some materials, such as acetate, the slope of the curve is zero and the region may be called a plateau. In other materials, such as high-tenacity rayon, the slope is only slightly less than the initial value. In the final region the slope increases slightly, and in some yarns bends over again as the breaking strain is reached. Behavior in the second region is of special interest when stress–strain curves obtained at different straining rates are compared. The curves tend to run parallel to each other, those with the higher stress values corresponding to the higher straining rates. The relationship between the stresses at a given strain and the corresponding straining rates is given, for many textile yarns, by the equation:

$$f_2 - f_1 = k \log \frac{R_2}{R_1} \qquad (2)$$

where f_1 is the stress at a given strain in the second region of a stress–strain curve obtained at straining rate R_1, and f_2 is the stress at the same strain on a stress–strain curve obtained at straining rate R_2.

Equation 2 has been applied to the data presented in Figures 1–19 with the exception of data for cotton C and D, polyester E, and glass fiber F which do not possess a second region. For this reason, Equation 2 was expressed in the form

$$f/f_1 = 1 + \frac{k}{f_1} \log_{10} \frac{R}{R_1} \qquad (3)$$

f_1 was taken as the stress for a given strain on the stress–strain curve obtained at the lowest rate of straining, R_1, f was taken as the stress for the same strain on a stress–strain curve obtained at the rate of straining R. The value of strain chosen lay in the second region for the family of stress–strain curves, but was not necessarily the same for each of the yarns tested. Plots of f/f_1 versus $\log_{10} R/R_1$ should thus be straight lines for each of the yarn samples. The curves in Figure 20 show that this

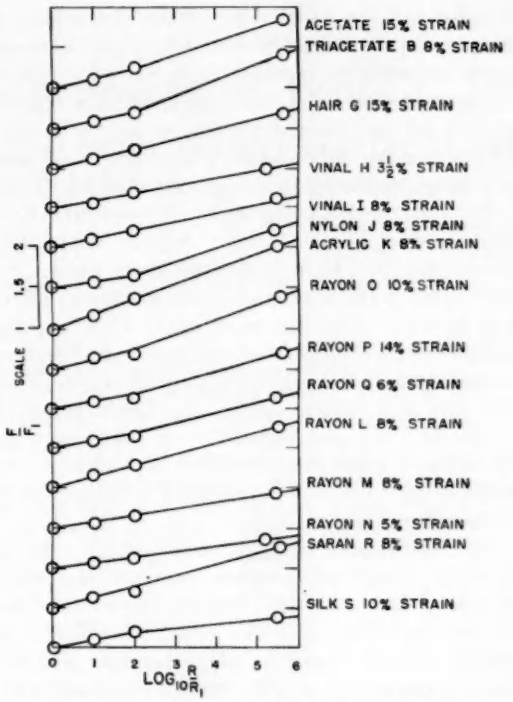

Fig. 20. Plot of stress past the yield point versus the logarithm of the rate of straining for some textile yarns.

is usually the case. The only exceptions are acetate, triacetate, nylon, and silk. Curves for several of the rayon specimens also depart slightly from a straight line.

Relationships similar to that expressed by Equation 2 have been found by other investigators. Entwistle [4] found that for some rayon yarns there was an approximately linear relationship between breaking load and the logarithm of the time to break. Since the breaking elongation for rayon is almost the same regardless of rate of elongation, Entwistle's result is equivalent to that expressed by Equation 2. Meredith [6] finds from his data that when the stress beyond the yield strain is plotted against the logarithm of the rate of extension for viscose rayon, silk, or nylon, a straight line is obtained. In the case of cellulose acetate and viscose staple fiber the plot is slightly concave towards the stress axis but is almost a straight line.

Conclusions

When stress–strain curves for textile materials are obtained at increasingly higher rates of straining, it

is found that the initial slopes of the curves become steeper and the initial linearity of the curves tends to persist to higher values of the stress. The breaking tenacities at high rates of strain are usually greater but the breaking elongations may be greater or less than the values obtained at conventional rates of testing, depending upon the material tested.

For many textile materials the stress–strain curve starts with a linear portion. A yield strain then ensues followed by a region of lesser slope. At higher strains the slope of the curve increases slightly and in some cases decreases again when rupture strain is reached. These features are usually retained in curves taken at rates of straining varying between 1%/min. and 440,000%/min. In such a family of curves for the same material, it is found that the stress for a given elongation just beyond the yield strain is approximately proportional to the logarithm of the rate of extension.

Specific breaking energies exceeding 40 joules/g. have been measured on several yarns by transverse- and longitudinal-impact tests at velocities of the order of 50 m./sec. Yarns meeting this criterion of ability to absorb impact include human hair, silk, and certain varieties of acrylic, vinal, and rayon yarns. The specific breaking energy of high-tenacity nylon decreases from above 50 joules/g. to less than 40 joules/g. under high-speed-impact conditions.

Almost all textile materials excel metals in ability to absorb impact when compared on a weight basis. The latter have impact breaking energies of the order of 10 to 15 joules/g. However, metals excel most textiles in impact-resisting ability. Aluminum and steel have Young's moduli of the order of 2600 g./tex. In all of the yarns tested, this modulus value was attained under impact conditions only by glass fiber and one of the vinal yarns.

Literature Cited

1. Duwez, P. E. and Clark, D. S., "Summary Report on the Influence of Impact Velocity on the Tensile Properties of Some Metals and Alloys," PB20206 (1944). May be obtained from Office of Technical Services, U. S. Department of Commerce, Washington 25, D. C.
2. Duwez, P. E., Wood, D. S., and Clark, D. S., "Factors Influencing the Propagation of Plastic Strain in Long Tension Specimens," OSRD Report No. 1304, PB18882 (1943). May be obtained from Office of Technical Services, U. S. Department of Commerce, Washington 25, D. C.
3. Duwez, P. E., Wood, D. S., and Clark, D. S., "The Propagation of Plastic Strain in Tension," OSRD Report No. 931, PB20274 (1942). May be obtained from Office of Technical Services, U. S. Department of Commerce, Washington 25, D. C.
4. Entwistle, D., *J. Soc. Dyers Colourists* **62**, 261 (1946).
5. McCrackin, F. L., Schiefer, H. F., Smith, J. C., and Stone, W. K., *J. Research Nat. Bur. Standards* **54**, 277 (1955) RP2590; TEXTILE RESEARCH JOURNAL **25**, 529 (1955).
6. Meredith, R., *J. Textile Inst.* **45**, T30 (1954).
7. Smith, J. C., McCrackin, F. L., and Schiefer, H. F., *ASTM Bulletin*, No. 220, 52 (1957).
8. Smith, J. C., McCrackin, F. L., Schiefer, H. F., Stone, W. K., and Towne, K. M., *J. Research Nat. Bur. Standards* **57**, 83 (1956) RP2695; TEXTILE RESEARCH JOURNAL **26**, 821 (1956).
9. Stone, W. K., Schiefer, H. F., and Fox, G., *J. Research Nat. Bur. Standards* **54**, 269 (1955) RP2589; TEXTILE RESEARCH JOURNAL **25**, 520 (1955).
10. Textile World (330 West 42nd Street, New York 36), "Man-Made-Fiber Table—1959 Revision."

Manuscript received November 30, 1960.

The Theory of Shrinkproofing of Wool.

Part II: Chemical Modification of the Fiber Surface and its Effect on Felting Shrinkage, Friction, and Microscopic Appearance[1]

J. H. Bradbury[2]

Division of Textile Industry, Wool Research Laboratories, C.S.I.R.O., Geelong, Australia

Abstract

Lincoln 36's top and Merino fabric were subjected to eight different chemical treatments, each at several levels, which included three well-known shrinkproofing treatments. The shrinkage of the treated material was compared with surface modification observed microscopically and frictional coefficients measured by the capstan method.

Shrinkproofing can be brought about by a variety of chemical and physical surface treatments. The chemical composition of the surface of the treated fiber and its topography (as observed microscopically) vary according to the type of surface treatment. There is good correlation between the amount of surface modification and the change in frictional coefficients. In agreement with the generally accepted theory of shrinkproofing, it is considered that the latter is the basic cause of shrinkproofing. This theory is adequate for most treatments but may have to be modified to account for anomalous cases such as occur on treatment with permanganate in water or on ethanol extraction.

Introduction

In the shrinkproofing of wool by methods which involve modification of the fiber itself (as distinct from methods based on fabric structure [5] or spot welding of fibers and yarns by resins, for reviews see [24, 27]) it is possible to make a rather arbitrary distinction between two different types of fiber modification. The first is modification of the fiber as a whole, including modification of the surface; the second is modification of the fiber surface and cuticle only [8]. In the light of present knowledge on the mechanism of felting it is considered that the first type of modification can effect shrinkproofing by alteration of the elastic properties (ease of extension, bending, and recovery from extension [29]) and also the frictional properties of the fibers. The second type of modification can have only a small effect on the elastic properties and hence produces shrinkproofing by alteration of the frictional properties of the fibers.

Let us now consider the various treatments which produce these two types of fiber modification. Treatments which modify the fiber as a whole include ultraviolet light [8], aqueous sodium hydroxide [8], peracetic acid [4], and hydrogen peroxide [4]. Treatments which modify the surface of the fiber preferentially in such a way that the modification need not penetrate deeper than the cuticle include acid chlorination [8], permanganate in salt followed by bisulfite [8, 22], sulfuryl chloride in carbon tetrachloride [8], permonosulfuric acid [31], alcoholic sodium hydroxide [8], deposition of polyglycine [10–12], ultrasonics [7, 32], and abrasion [30]. However, in some of these treatments there can be modification of the outer layers of the cortex, which is accentuated if the fibers are overtreated.

It is worth while summarizing the evidence available on the depth of modification of fibers by the various treatments. With the acid chlorination treatment, a correlation of the work to stretch the fibers 30% over a series of fibers of different diameters indicated that the fibers were modified to a constant depth of 1.5 μ. The results of the descaling technique show that the reaction is concentrated near the surface but the increase in the cysteic acid content of the cuticle [8, Table II] is not large enough to explain the increase in the cysteic acid content of the fiber as a whole [8, Table I], hence there is some reaction of the cortex. Electron

[1] Part I appeared in *J. Textile Inst.* **51**, T1226 (1960).

[2] Present address: Chemistry Department, Australian National University, Canberra, A.C.T., Australia.

microscopy of strongly modified chlorinated fibers (classes 2 and 3, see below) shows that the outer cortical layers are modified, but as these fibers are representative of only 20% of the total, it is clear that most of the fibers show no modification of cortex [11]. The treatment with permanganate in salt followed by bisulfite gives conflicting results on the analysis of the whole fiber since McPhee [22] finds a 0.3 mole/10^4 g. decrease in cystine, whereas in Table I, an increase of only 0.1 mole/10^4 g. of cysteic acid is recorded. Previous results [8] indicate that the total cystine and cysteic acid is a constant for oxidation treatments. Electron microscopy of brown permanganate treated fibers, before treatment with bisulfite, shows only slight evidence of deposition of manganese dioxide in the layers just below the cuticle [11]. It is therefore very likely that the permanganate reaction is confined almost entirely to the cuticle. With sulfuryl chloride in carbon tetrachloride [8], permonosulfuric acid (see below), and alcoholic sodium hydroxide [8] there is evidence from whole-fiber analysis and descaling which indicates that there is little or no modification of cortex. With polyglycine there is much evidence from descaling and microscopy [10–12] that the polymer is located on (and in) the cuticle. Ultrasonics are known to attack the cuticle quite slowly [7], hence it is unlikely that any degradation of cortex has occurred, and it is probable that abrasion acts in a similar manner [31]. For the four whole-fiber treatments mentioned above there is abundant evidence from amino acid analysis of whole fibers [4, 8] and electron microscopy [11] that the reaction occurs throughout the fiber.

The distinction between the surface and whole-fiber types of treatment may appear to be somewhat arbitrary and poorly defined because of borderline cases such as acid chlorination. Nevertheless there is a large difference between acid chlorination and say peracetic acid; the former shrinkproofs while the latter can do so in aqueous solution only with a large amount of degradation of the fiber [4]. The obvious difference between these reagents lies not in different types of chemical reaction as previously supposed [4], but in the site of the attack. It is necessary to emphasize a point which has been known for many years, *viz.*, that the best shrinkproofing is produced by reagents which limit their attack to the surface of the fibers.

In a previous paper the descaling technique was used to elucidate the chemical changes produced in the surface of the fiber by various shrinkproofing treatments [8]. The subject of this paper is the physical changes in the surface produced by such treatments and determined by optical microscopy and friction measurements. The detailed optical and electron microscopy of the modified fibers is considered in a subsequent paper [11].

Experimental

Materials

Lincoln 36's top and standard wool fabric were used as described elsewhere [10]. All chemicals were of A.R. or laboratory grade.

Chemical Treatments

In each treatment described below, three 10-in. lengths of Lincoln 36's top and three 6-in. squares of fabric were treated separately. Shrinkage tests were carried out in duplicate and one length of top and one square of fabric from each treatment was reserved for the other tests. Untreated control samples were set aside at frequent intervals to provide checks.

Acid chlorination [8]. The samples were wet out in 0.08 *N* HCl with a liquor to wool ratio of 100:1, dilute hypochlorite added slowly, and stirring continued intermittently for one hour at 25°. The levels of treatment were 0.5%, 1%, 2%, 4%, 8%, and 16% available chlorine on the weight of wool. The samples were washed thoroughly in water.

Permanganate saturated with NaCl followed by $NaHSO_3$ [8, 22]. The samples were treated with 2%, 5%, and 10% $KMnO_4$ on the weight of the wool in saturated salt at 25° with liquor to wool ratio of 30:1 until the bath was exhausted (4 hr.). The brown samples were treated with 10% $NaHSO_3$ on weight of wool in 0.1 *N* H_2SO_4 at 25° until the MnO_2 was removed (2 hr.) and were then washed thoroughly in water.

Permanganate in water followed by $NaHSO_3$ [8, 22]. The preceding treatments were repeated in the absence of salt.

Sodium bisulfite. Samples were treated with 10%, 30%, and 60% $NaHSO_3$ on the weight of the wool in 0.1 *N* H_2SO_4 for 2 hr. at 25° with a liquor to wool ratio of 30:1. They were washed with water.

Permonosulfuric acid [31]. The wool was treated with 0.5%, 1%, 2%, 4%, 8%, and 16% H_2SO_5 on the weight of wool for 0.5 hr. at 25° with a liquor to wool ratio of 30:1. Samples were then washed once

TABLE I. Properties of Top and Fabric Treated with Various Reagents

Treatment	Measurements on top								Measurements on fabric		
							Mole/10^4 g. conditioned wool of:			Bursting strength, kg./cm², when:	
	Length shrinkage, %	Shrinkproofing, %*	Surface modification, %	μ_1†	μ_2†	$\mu_1 - \mu_2$	Cystine	Cysteic acid	Area shrinkage, %	Conditioned	Wet
Nil	30	0	0	.42	.25	.17	4.9	0.3	40	—	—
Chlorination											
0.5%	21	30	0.7	.47	.33	.14	—	—	19	7.5	6.0
1.0%	18	40	8	.50	.39	.11	5.2	0.3	16	7.5	5.9
2.0%	15	50	9	.49	.41	.08	5.3	0.5	13	7.7	6.2
4.0%	13	57	24	.51	.46	.05	4.6	0.7	8	—	—
8.0%	14	53	29	.53	.48	.05	4.5	0.7	4	7.1	5.5
16.0%	13	57	37	.51	.47	.04	2.4	1.5	0	6.4	4.4
Nil	30	0	0	—	—	—	4.7	0.3	40	7.2	6.0
$KMnO_4$ in $NaCl/NaHSO_3$											
2%	12	60	7	.40	.28	.12	4.7	0.4	24	7.1	5.7
5%	9	70	13	.37	.24	.13	4.3	0.4	5	—	—
10%	7	77	19	.39	.30	.09	3.9	0.6	0	6.1	5.0
Nil	30	0	0	—	—	—	5.1	0.3	40	—	—
$KMnO_4$ in $H_2O/NaHSO_3$											
2%	21	30	3	.38	.26	.12	4.5	0.4	39	7.2	5.8
5%	23	23	3	.40	.32	.08	4.5	0.4	34	—	—
10%	27	10	3	.36	.28	.08	4.3	0.5	25	6.6	5.0
Nil	30	0	0	.37	.21	.16	4.6	0.3	40	7.3	5.9
$NaHSO_3$											
60%	23	23	4	.40	.22	.18	5.0	0.2	45	7.7	5.9
Nil	30	0	0	—	—	—	5.4	0.1	40	—	—
H_2SO_5											
0.5%	21	30	1	.34	.22	.12	4.9	0.1	23	—	—
1.0%	15	50	3	.36	.23	.13	4.9	0.1	11	—	—
2.0%	14	53	9	.35	.26	.09	5.0	0.2	5	—	—
4.0%	12	60	22	.32	.25	.07	4.8	0.5	2	—	—
8.0%	11	63	32	.30	.25	.05	—	—	6	—	—
16.0%	40	−33	43	.25	.20	.05	4.0	1.2	6	—	—
Nil	30	0	0	—	—	—	5.0	0.1	40	7.2	6.0
H_2O_2											
5 vol. 2 hr.	15	50	2	—	—	—	4.1	0.9	33	7.2	5.8
5 vol. 4 hr.	11	64	—	.44	.29	.15	4.6	0.9	24	7.0	5.8
5 vol. 8 hr.	15	50	9	.46	.36	.10	4.0	1.5	10	7.2	5.6
5 vol. 16 hr.	23	23	—	.40	.35	.05	3.1	2.4	13	7.1	5.5
10 vol. 4 hr.	12	60	—	.38	.32	.06	3.4	1.6	7	7.2	5.6
10 vol. 8 hr.	18	40	17	.33	.26	.07	3.3	2.6	19	6.9	5.8
10 vol. 16 hr.	28	7	—	.27	.24	.03	2.6	3.3	46	—	—
Nil	30	0	0	—	—	—	4.5	0.3	40	7.2	5.9
Peracetic acid											
10%	21	30	0	.33	.21	.12	3.7	1.6	24	7.2	5.8
20%	25	17	0	.34	.25	.09	2.8	3.2	21	7.1	5.5

* % Shrinkproofing = 100 (30 − % length shrinkage)/30.
† Fixed load = 200 mg.

with water, twice with 0.5% $NaHCO_3$ solution, once with water, and reduced with 30% $NaHSO_3$ on the weight of wool for 0.5 hr. at 25°. They were finally washed in water.

Hydrogen peroxide. Samples were treated in 0.2% sodium pyrophosphate solution at 50° using a liquor to wool ratio of 20:1 with 5 volume H_2O_2 for 2, 4, 8, and 16 hr. and with 10 volume H_2O_2 for 4, 8, and 16 hr. All samples were washed thoroughly with water.

Peracetic acid. The samples were wet out in twenty times their weight of water and peracetic acid

added with stirring to a concentration of 10% and 20% on the weight of wool. After 2-hr. treatment at 25° the wool was washed thoroughly with water.

Extraction with ethanol. Lincoln 36's top was extracted with ethanol in a Soxhlet extractor after which it was washed in three changes of distilled water over a period of 24 hr.

Methods

Shrinkage tests on top and fabric and bursting strengths. These were determined as already described [10].

Microscopy. A detailed account of the use of this method with illustrations of the different classes of surface modification observed for each treatment is given elsewhere [11]. The four classes, unchanged, slightly modified, modified, and strongly modified are given the numbers 0, 1, 2, and 3, respectively, and the percentage of fibers in each class multiplied by the class numbers. These three quantities are summed and the total value divided by 3. This gives an empirical measure of the amount of modification of the surface of the fiber expressed as a percentage.

Frictional properties. The anti- and with-scale coefficients of friction, μ_1 and μ_2, were measured by the capstan method [21] using fixed loads in the range of 25 to 1000 mg. Individual fibers were rubbed over keratin rods of various diameters or alternatively over a cylindrical plastic rod on which fibers were wound laterally with their scales all pointing in one direction. The fiber and rod were lubricated with 0.05 *M* borax solution containing 0.02% Teepol.

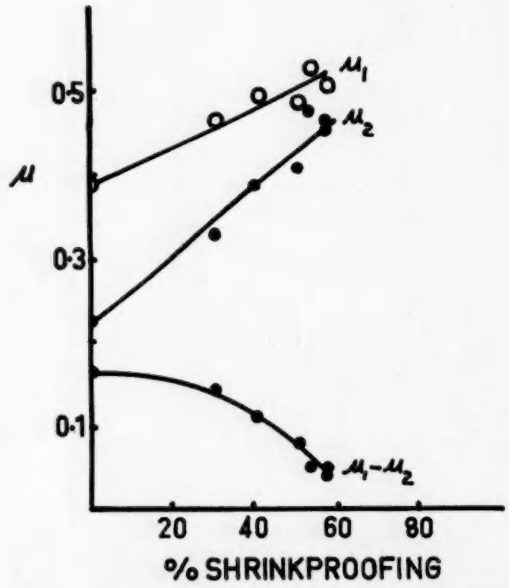

Fig. 1. Graph of frictional coefficients vs. % shrinkproofing for acid chlorinated top.

Amino acid analysis. Single analyses were performed on 5-mg. samples of fibers by the dinitrophenylation method [6].

Results

Table I summarizes the effect on fiber and fabric properties of different chemical treatments at various levels. A complete amino acid analysis of the treated top was carried out by the dinitrophenylation method [6], but only the results for cystine and cysteic acid are recorded since these are the only ones which show a significant change due to treatment (see also [8]). Tyrosine is low in several cases but there is so much uncertainty in its determination [6] that no conclusions can be drawn from the single analyses. In Table I it is noted that permanganate in salt and permonosulfuric acid give no appreciable increase in the cysteic acid content of the whole fiber (except on overtreatment), acid chlorination gives a slight increase, but hydrogen peroxide and peracetic acid give a large increase even with the mildest treatment. This is consistent with the classification of treatments into surface and whole-fiber treatments as given in the introduction. The partial degree of shrinkproofing which has been achieved with hydrogen peroxide is the result of modification of surface and whole-fiber properties. We will simplify the picture by considering in detail only those treatments which do not appreciably alter the over-all properties of the fiber.

The first five treatments in Table I (with the exception of the bisulfite treatment) and the polyglycine treatments reported on earlier [12] were analyzed statistically. The data were fitted by a multiple linear regression equation of the form

$$\% \text{ shrinkage of top} = b_0 + b_1 (\mu_1 - \mu_2) - b_2 \times (\text{surface modification})$$

where b_0, b_1, and b_2 are regression coefficients with the values 14.2, 42.5, and 0.151, respectively. This equation accounts for a highly significant amount

(46%) of the variation in shrinkage. It is also found that $\mu_1 - \mu_2$ and surface modification are so highly correlated that most of the variation of shrinkage accounted for by these two variables together can equally well be accounted for by either one alone.

However, the largest deviations from the above equation occur with the permanganate in water and, to a lesser extent, the permanganate in salt treatments. This would be expected from the friction results in Table I and Figures 1 and 2, where it is seen that the latter treatment effects shrinkproofing with only a small decrease in $\mu_1 - \mu_2$, whereas the former shows a similar decrease in $\mu_1 - \mu_2$ without any appreciable amount of shrinkproofing [2, 22]. It is worth noting that the shrinkage and surface modification results for these two treatments are consistent. We will now consider various attempts which have been made to resolve this apparent anomaly between the results of $\mu_1 - \mu_2$ and shrinkage for the above two treatments.

Effect of Washing on Frictional Coefficients and Surface Modification

Alexander [1–3] observed that some chemical shrinkproofing treatments modified the fibers in such a way that the scales were lost during the washing test used to assess the shrinkage. It has been found that washing of Lincoln 36's top, untreated or treated with 5% permanganate in water or in saturated salt, produces no change in the surface modification or the frictional coefficients. Measurements made on Merino 64's top treated in this way show that the washing produces an increase in the surface modification and a small decrease in $\mu_1 - \mu_2$ which occurs equally for the two treatments, permanganate in water, and permanganate in saturated salt [McPhee, J. R., unpublished results]. This shows that there is some difference between the cuticles of Merino and Lincoln fibers, but does not resolve the difference between the two permanganate treatments.

Surface Modification and Frictional Coefficients of Root and Tip

Flanagan [13] has recently proposed a new mechanism of shrinkage based on the observation that the undamaged root end of a fiber migrates more rapidly during the formation of non-woven felt than the damaged tip end. This mechanism was tested by measuring the frictional coefficients of root and tip sections of untreated fibers and fibers treated with

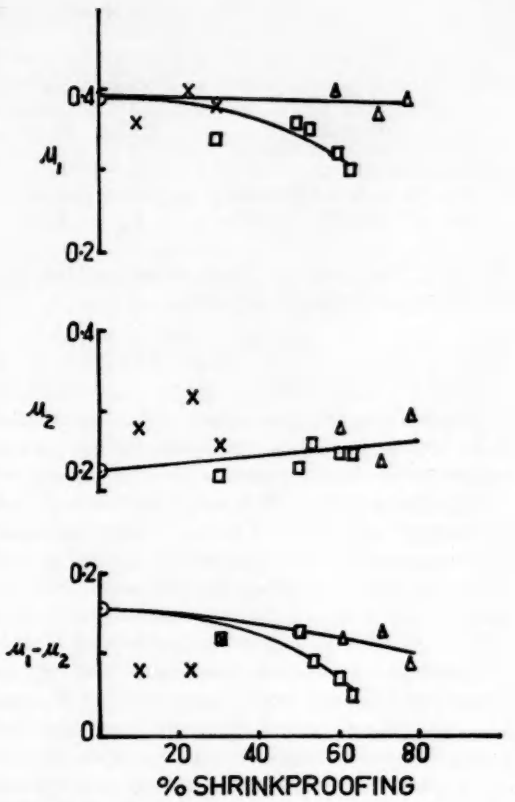

Fig. 2. Graph of frictional coefficients vs. % shrinkproofing for untreated ○ top; permanganate in salt, △; permanganate in water, ×; and permonosulfuric acid, □ treated top.

5% permanganate in water or 5% permanganate in saturated salt. The amount of surface modification of each section of each fiber was measured at ten equidistant points along its length and the mean value calculated. The results in Table II represent the mean values determined over 10 fibers.

It is found that for each treatment there is more surface modification, i.e., removal of scale edges, for tip than root wool, which is coupled with a small decrease in $\mu_1 - \mu_2$. This difference in $\mu_1 - \mu_2$ between root and tip explains the more rapid migration of the former during felting [13], but as the difference is only slightly reduced by the permanganate in salt shrinkproofing treatment, it seem unlikely that it is an important factor in the felting of wool. Since the frictional coefficients of the permanganate in salt and permanganate in water treatments are practically

TABLE II. Surface Modification and Frictional Coefficients of Root and Tip

Treatment	Surface modification		Frictional coefficients					
			Root			Tip		
	Root	Tip	μ_1	μ_2	$\mu_1 - \mu_2$	μ_1	μ_2	$\mu_1 - \mu_2$
Untreated	0	9	.37	.21	.16	.35	.22	.13
5% $KMnO_4$ in $NaCl/NaHSO_3$	5	15	.32	.22	.10	.32	.24	.08
5% $KMnO_4$ in $H_2O/NaHSO_3$	0	4	.32	.22	.10	.33	.25	.08

identical, their very different shrinkage behavior cannot be explained on this basis.

Effect of Variation of Rubbing Surface and Load on Frictional Coefficients

The question has been raised [8] as to whether the frictional coefficients measured by the capstan method, which involve fiber–keratin-rod contacts, are closely related to those frictional properties which are operative in an assembly of fibers. In order to obtain more information on this point it was decided to vary the nature and diameter of the rod over which the fiber is suspended and also the load on the fiber.

Measurements were made using untreated Lincoln 36's fibers at various loads from 25 to 1000 mg. and three different keratin rods of diameters 4.9, 8.2, and 11.3 mm. No consistent differences were observed among frictional coefficients obtained with the different keratin rods. The keratin rod was then replaced with a cylindrical plastic knitting needle of diameter 4.5 mm., on which fibers were wound laterally with their scales all pointing in one direction. Since the fibers wound on the rod had a definite orientation of scales there were four different possible configurations which gave four different frictional coefficients. Of these, the two middle ones had approximately the same value and were not studied in detail, but the lowest and the highest correspond with the value of μ_2 and μ_1, respectively, as obtained using a keratin rod. Each point on the graphs in Figures 3 and 4 is the average of the frictional coefficients of several untreated fibers which were measured over the keratin rod and then over the cylindrical rod wound with untreated fibers. Measurements of this type were also made with fibers shrinkproofed with permanganate in salt rubbing over a keratin rod and then over a rod wound with permanganate shrinkproofed fibers. For both untreated and permanganate shrinkproofed fibers only small alterations of the values of μ_1, μ_2, or in particular $\mu_1 - \mu_2$ were produced by altering the rubbing surface from keratin to wool (compare [25]). It is therefore reasonable to use the keratin rod in preference to the rod wound with wool fibers, particularly as the former gives more consistent results.

As shown in Figures 3 and 4 and elsewhere [16, 23] the frictional coefficients vary with the load or force on the fibers, and it is important to know the magnitude of this force under practical washing conditions. A method has now been devised to give this information [9] and it has been found that the maximum force on fibers in a top during the standard washing procedure used in this laboratory is 1500 mg. In order to obtain the correct loading for the measurement of friction by the capstan method, the number of fiber contacts must be known in both cases. In the absence of such information it is only possible to measure the frictional coefficients over a wide range of loads (25–1000 mg.), in the hope that this will include the loading which obtains in the felting mass of fibers.

Effect of Rubbing Over Keratin Rod on Frictional Coefficients and Surface Modification

Friction measurements involve rubbing a fiber over a keratin rod, during which process changes may occur in its surface which could influence the value of the coefficients. The first approach to this problem was made by selecting a fiber, measuring its

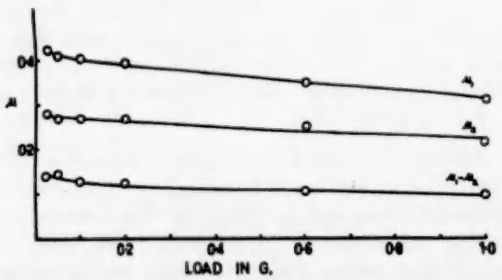

Fig. 3. The load dependence of the frictional coefficients of untreated fibers rubbed over a keratin rod.

surface modification at ten points along one half of its length, and then rubbing the other half of the fiber twenty times over a keratin rod with a fixed load of about 200 mg. About ten fibers showing various degrees of surface modification, produced by each different chemical treatment, were examined before and after rubbing. It was found that fibers treated with permonosulfuric acid, aqueous caustic soda [8], polyglycine [12], or ethanol extraction showed no change after rubbing. However, those modified to the extent of 40% or more by chlorination showed further removal of scale edges by rubbing, which was in agreement with previous work on the washing of chlorinated wool [1–3]. On the other hand, fibers modified to 50% or more by treatment in permanganate in salt showed a marked decrease in surface modification due to rubbing, which is discussed elsewhere [11].

Secondly, ten fibers chosen at random from each of the permanganate in salt and permanganate in water treatments were cut in half and the frictional coefficients of one half measured. The other half of each fiber was rubbed twenty times over a keratin rod with a fixed load of 200 mg. and then its frictional coefficient measured. There was no significant change produced in the values of μ_1, μ_2, or $\mu_1 - \mu_2$ as a result of rubbing over the keratin rod for either of the treatments (compare [19]).

Correlation of Surface Modification and $\mu_1 - \mu_2$

The statistical analysis of the results already described shows that the variation in shrinkage can be accounted for just as easily in terms of variation of surface modification or of $\mu_1 - \mu_2$ or by use of the two variables together. Thus the variables are closely correlated in all surface treatments except permanganate in water (see Table I). In order to check this correlation, a number of fibers were chosen from various treatments and their frictional coefficients measured at loads ranging from 25–1000 mg. over a cylindrical rod wound with fibers from the same treatment. The surface modification of each fiber was then assessed microscopically at ten equidistant points along its length.

Graphs of μ_1, μ_2, and $\mu_1 - \mu_2$ vs. surface modification were constructed at various loads. The load dependence of the frictional coefficients was similar to that already found, hence attention was concentrated on the results at 200 mg. The values of μ_1 and μ_2 for all treatments, except acid chlorination and polyglycine, which are known to produce large values (see Table I and [12]), fitted two graphs with a considerable amount of experimental scatter. The graph of μ_1 vs. surface modification decreases from $\mu_1 = 0.4$ at zero to 0.32 at 10% surface modification and thereafter remains constant. The graph of μ_2 vs. surface modification increases linearly from $\mu_2 = 0.22$ at zero to 0.28 at 100% surface modification. The results of $\mu_1 - \mu_2$ vs. surface modification for individual fibers are plotted in Figure 5. The results show considerable scatter attributable to errors in measurement of both $\mu_1 - \mu_2$ and surface modification. Five out of seven of the permanganate in water values fall below the line, once again indicative of the anomalous frictional behavior of fibers treated in this way. With this exception the steady decrease of $\mu_1 - \mu_2$ with increasing surface modification obtained over three different shrinkproofing treatments is strong confirmatory evidence of the close correlation between the two variables.

Extraction with Ethanol

Although ethanol extraction produces some resistance to felting of fabric [28] and Farnworth, A. J.,

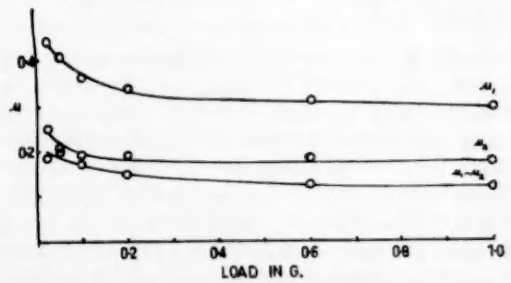

Fig. 4. The load dependence of the frictional coefficients of untreated fibers rubbed over a cylindrical plastic rod wound with untreated fibers.

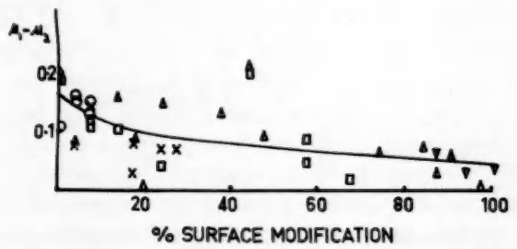

Fig. 5. Graph of $(\mu_1 - \mu_2)$ vs. surface modification for untreated, ○ fibers; acid chlorinated, ▽ fibers; and for fibers treated with permanganate in salt, △; permanganate in water, ×; and permonosulfuric acid, □.

unpublished results) we have found that Lincoln 36's top extracted for 2–24 hr. felted to the same extent as the control. On microscopic examination many of the fibers showed large numbers of small surface marks [11]. The amount of surface modification increased with time of ethanol extraction until after 24 hr. 80% of the fibers were modified. This effect was previously observed by Haller [15]. After 24-hr. extraction the wool showed no change in frictional coefficients or in amino acid composition. During this extraction 0.65% of material was removed and a further 0.1% after a second similar treatment. Human and Speakman [17] found that material was still being removed after extraction for a total of 1800 hr. with ether and alcohol. Elementary analysis of the material extracted by ethanol by Dr. H. Zimmermann (C.S.I.R.O., Microanalytical Laboratory, Melbourne) gave C 69.5, H 10.5, N 1.3, ash 11.4. The very high C, H, and ash content indicates a wool wax constituent (Farnworth, A. J. and Tauber, G., unpublished results) coupled with inorganic material, and the very low N content shows that it contains $\not>$ 10% of proteinous material.

Discussion

This discussion does not apply to whole-fiber treatments such as hydrogen peroxide but is confined to surface treatments as defined in the introduction, including acid chlorination. Shrinkproofing can be brought about by various treatments, summarized in the introduction, which cause chemical or physical degradation of the surface or involve deposition of a layer of polyglycine on the cuticle. The chemical composition of the surface of the treated fibers varies according to the type of treatment. The physical state of the surface as observed by optical and electron microscopy is likewise dependent on the treatment [11]. In view of the diverse effects of the different surface treatments, it is clear that there is no one particular type of chemical change in the surface of the fiber which is essential in order to produce shrinkproofing. Similarly there is no one essential type of change in the topography of the surface as observed by microscopy, except for the possibility of masking the effect of the asperities of the scales (on fiber friction) by a general disordering of the surface [11].

In most theories of felting of wool the physical property which is considered to be of the greatest importance is the friction of the fiber, expressed in terms of μ_1, μ_2, and in particular $\mu_1 - \mu_2$ [16, 27]. Thus, shrinkproofing can be effected by immobilization of the fibers by increase of μ_1 and μ_2 such as occurs by deposition of polyglycine [10, 12] or by acid chlorination (see Figure 1). In both these cases there is also a decrease of $\mu_1 - \mu_2$ which limits felting by allowing fibers which have moved under the felting force to return to their original position afterwards [8]. A decrease of $\mu_1 - \mu_2$, brought about by a slight decrease in μ_1 and increase in μ_2, is the probable cause of shrinkproofing on treatment with permanganate in salt or permonosulfuric acid (see Figure 2).

However, there are several chemical treatments which do not fit into the above scheme. First, treatment with permanganate in water followed by bisulfite reduces $\mu_1 - \mu_2$ without producing shrinkproofing [2, 22] or surface modification. Nevertheless, if the bisulfite after treatment is made more severe, shrinkproofing and surface modification are produced with no further decrease of $\mu_1 - \mu_2$ [8]. Second, ethanol extraction produces no shrinkproofing of top or change in frictional coefficients but does cause surface modification. In this case other workers find that ethanol extraction of fabric produces some shrinkproofing without any change in frictional coefficients ([28] and Farnworth, A. J., unpublished results). Farnworth has found anomalous cases in the shrinkproofing of ethanol extracted wool with sodium bisulfite.

There are three possible explanations of these anomalous cases. First, although the work done in this paper tends to show that the frictional coefficients measured by the capstan method are relevant to the situation in a felting mass of fibers, the large difference between the two systems indicates that it would be worth while to measure the frictional coefficients of the anomalous treatments by another method [16, 18–20]. Second, it is important to obtain a more detailed picture of the cuticle of treated and untreated fibers by electron microscopy, coupled with a knowledge of the site of chemical reaction obtained by techniques such as the microdyescope [26]. Finally, perhaps the theory is inadequate and there is some other physical property of the fiber which is usually less important than friction in determining shrinkage, but which assumes major importance in the anomalous cases.

Acknowledgments

Thanks are due to Mrs. K. Rachel Makinson, Drs. M. Lipson, A. J. Farnworth, and J. R. McPhee and Mr. G. F. Flanagan for useful discussions. I am grateful to Mr. W. B. Hall of the Division of Mathematical Statistics, C.S.I.R.O., for the statistical analysis, to Mr. A. R. W. Lee and staff for the physical testing of fabrics and to Messrs. H. Groll, K. Kelaart, and S. West for technical assistance.

Literature Cited

1. Alexander, P., "Fibrous Proteins," Symposium of Soc. Dyers and Colourists, 199 (1946).
2. Alexander, P., *Am. Dyestuff Reptr.* **39**, P420 (1950).
3. Alexander P., *J. Soc. Dyers Colourists* **66**, 349 (1950).
4. Alexander, P., Carter, D., and Earland, C., *J. Soc. Dyers Colourists* **67**, 23 (1951).
5. Bogaty, H., Lourigan, G. H., and Harris, H. E., TEXTILE RESEARCH JOURNAL **28**, 733 (1958).
6. Bradbury, J. H., TEXTILE RESEARCH JOURNAL **30**, 128 (1960).
7. Bradbury, J. H., *Nature* **188**, 207 (1960).
8. Bradbury, J. H., *J. Textile Inst.* **51**, T1226 (1960).
9. Bradbury, J. H. and Groll, H., TEXTILE RESEARCH JOURNAL **31**, 743 (1961).
10. Bradbury, J. H. and Leeder, J. D., TEXTILE RESEARCH JOURNAL **30**, 118 (1960).
11. Bradbury, J. H. and Rogers, G. E., TEXTILE RESEARCH JOURNAL, in preparation.
12. Bradbury, J. H. and Shaw, D. C., TEXTILE RESEARCH JOURNAL **30**, 976 (1960).
13. Flanagan, G. F., TEXTILE RESEARCH JOURNAL **31**, 576 (1961).
14. Frishman, D., Smith, A. L., and Harris, M., TEXTILE RESEARCH JOURNAL **16**, 160 (1946).
15. Haller, H. C., *Am. Dyestuff Reptr.* **30**, 221 (1941).
16. Howell, H. G., Mieszkis, K. W., and Tabor, D., "Friction in Textiles," London, Butterworths, 1959.
17. Human, J. P. E. and Speakman, J. B., *J. Textile Inst.* **45**, T162 (1954).
18. Lindberg, J., TEXTILE RESEARCH JOURNAL **18**, 470 (1948).
19. Lindberg, J. and Gralén, N., TEXTILE RESEARCH JOURNAL **18**, 287 (1948).
20. Lindberg, J. and Gralén, N., TEXTILE RESEARCH JOURNAL **19**, 183 (1949).
21. Lipson, M. and Howard, P., *J. Soc. Dyers Colourists* **62**, 29 (1946).
22. McPhee, J. R., TEXTILE RESEARCH JOURNAL **30**, 349, 358 (1960).
23. Martin, A. J. P. and Mittelman, R., *J. Textile Inst.* **37**, T269 (1946).
24. Matlin, N. A. and Nuessle, A. C., *Ind. Eng. Chem.* **47**, 1729 (1955).
25. Mercer, E. H., *Nature* **155**, 573 (1945).
26. Millson, H. E., *Am. Dyestuff Reptr.* **44**, 417 (1955).
27. Moncrieff, R. W., "Wool Shrinkage and its Prevention," London, National Trade Press, 1953.
28. Peryman, R. V. and Speakman, J. B., *J. Textile Inst.* **41**, T241 (1950).
29. Speakman, J. B., Stott, E., and Chang, H., *J. Textile Inst.* **24**, T273 (1933).
30. Speakman, J. B. and Whewell, E., *J. Textile Inst.* **36**, T48 (1945).
31. Stevensons (Dyers) Ltd. and E. T. Fell, British Patent 716806 (1954).
32. Wolsey Ltd., and Alexander, P., British Patent 618794 (1949).

Manuscript received December 27, 1960.

Part III: A Method for Determination of the Force on a Fiber During Felting

J. H. Bradbury[1] and H. Groll

Division of Textile Industry, Wool Research Laboratories, C.S.I.R.O., Geelong, Australia

IN comparison with the large amount of work done on the properties of the wool fiber which are responsible for felting, little has been done on the measurement of the felting force. Thus, van der Vegt and Schuringa [2, 3] studied the relationship between the speed (in r.p.m.) of their yarn shrinkage tester, which they related to the felting force, and the rate of shrinkage. However, they were unable to measure the actual magnitude of the forces exerted. This note describes a method of assessing the maximum force exerted on a single fiber during felting of fabric or top.

Lincoln 36's top, cleaned as described elsewhere [1], was dyed with 3% Xylene Fast Red P (Sandoz) on the weight of wool and was washed thoroughly with water and dried. A dyed fiber was

[1] Present address: Chemistry Department, Australian National University, Canberra, A.C.T., Australia.

cut about one quarter of the way along its length and both sections treated at their midpoints with a 0.5-cm.-diameter drop of a saturated solution of Na_2S at 35°–40° for equal time intervals (0.3 to 3 min.). Both sections of fiber were washed with distilled water and the short section mounted in a chainomatic device, by means of which the breaking load was determined by rapidly increasing the load on the fiber until breakage occurred. The fiber was kept wet during this operation by intermittent spraying with water; spraying with 0.05% soap solution made no difference to the breaking load. The long section was then either inserted into a length of undyed Lincoln 36's top which was subjected to the usual felting test [1] or else threaded into the weave structure of an undyed sample of fabric [1] and treated in a washing machine according to one of the methods given in Table I. The shrunken top or fabric was then dried and immersed in *o*-dichlorobenzene in which the undyed fibers became almost transparent. The red fiber was easily identified and, if broken at the weakened point, the two ends were usually at least 0.5 cm. apart. If the fiber was broken, then the force on the fiber during felting must have exceeded the breaking load of the weakened part.

Fibers with breaking loads between 0.3 and 5.5 g. were obtained by treatments with Na_2S for times between 0.3 and 3 min. There was a considerable amount of variation in the breaking load produced by a particular Na_2S treatment from one fiber to the next and also along the length of the one fiber. The variation from one fiber to another was minimized by sorting the treated fibers into groups, depending on the breaking load of the short section of each fiber. In this way the standard error (expressed as a percentage of the mean breaking load) was reduced from 15% over 10 fibers not grouped to an average value of 5%, calculated over a number of groups of 10 fibers. In considering variation along the length of each fiber, preliminary results showed that, contrary to expectation, treatments towards the tip end weakened the fibers to a lesser extent than the same treatment made near the root end. However, a number of fibers were treated without regard to root or tip and both the short and long sections were broken. The breaking load of the long and short sections of ten grouped fibers amounted to 0.85 ± 0.11 g. and 0.94 ± 0.05 g., respectively.

After weakened fibers were obtained in a particular group, i.e., with a particular range of breaking strength, they were subjected to the felting treatment and the number of broken fibers determined as already described. The results of the experiments are given in Table I and Figures 1 and 2. In Table I is also recorded the experimentally determined initial rate of area shrinkage (%/min.) of the fabric in the various washing machines. In all cases there was a linear relationship between shrinkage and time up to at least 10% area shrinkage.

Discussion

A straight line graph passing through the origin is obtained by plotting the results in Table I of initial rate of felting against maximum load. The large mean deviation (0.5 g.) of the points from the line is accounted for by the experimental errors involved in measurement of both quantities and also by the large (deliberate) variations made in type of washing machine and washing conditions. Therefore it appears that these latter factors are not important in determining the rate of felting of a particular fabric in aqueous solution, except in so far as they determine the maximum load on the fiber.

In Table I it is seen that the maximum load is

TABLE I. Summary of Washing Conditions, Initial Rate of Felting, and Maximum Load of Fibers

Type of machine*	Total time of agitation, min.	% Soap	Temp., °C.	Initial rate of area shrinkage, %/min.	Maximum load on the fiber, g.†
Horizontal, rotating cage	20	0.05	35–40	2.5	3.6
Agitator, regular white cycle	13	0.05	45–50	1.7	3.3
Agitator, regular white cycle	13	nil	45–50	1.8	2.3
Agitator, delicate cycle	10	0.05	35–40	1.0	2.1
Top Shrinkage Tester [1]	—	nil	25	—	1.5

* A 2-lb. load of linen squares was used in all cases except for the top shrinkage.

† Obtained from Figures 1 and 2 as the point of intersection of the ascending portion of the graph with the horizontal line at a value of 10 on the ordinate.

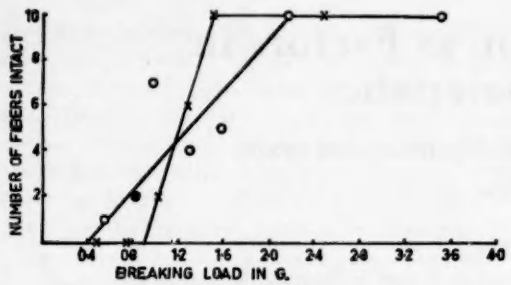

Fig. 1. The number of fibers, out of a total of 10, which remain intact after felting, graphed against breaking load for the top shrinkage tester (×); agitator machine, delicate cycle, 10 min. (o); and agitator machine, delicate cycle, 40 min. (•).

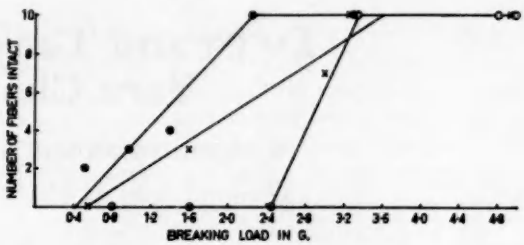

Fig. 2. The number of fibers, out of a total of 10, which remain intact after felting, graphed against breaking load for rotating cage machine (×); agitator machine, regular white cycle in 0.05% soap (o); agitator machine, regular white cycle in absence of soap (•).

increased by the addition of 0.05% soap to the wash liquid. The reason for this is not known. In Figures 1 and 2 it is noted that the slope of the ascending portion of the various curves is lowest for the rotating cage machine and is increased greatly by the addition of soap to the agitator machine. The experiment with the agitator machine on delicate cycle in which the washing is continued for four times as long as normal shows that the number of fibers remaining intact in this case is not altered by increasing the time of washing.

The maximum load of 3.6 g. achieved with the rotating cage machine and measured using weakened Lincoln 36's fibers appears to be too low to break Merino 64's fibers (mean breaking load of 10 fibers by the above method = 5.71 ± .31 g.). This was confirmed by inserting 10 dyed Merino fibers into the yarn and 10 others into the weave structure of the fabric, which was then washed in the rotating cage machine; all the fibers were found to be intact.

We wish to thank Mrs. K. Rachel Makinson, Drs. M. Lipson, J. R. McPhee, and Messrs. G. Flanagan and J. D. Leeder for useful discussions.

Literature Cited

1. Bradbury, J. H. and Leeder, J. D., TEXTILE RESEARCH JOURNAL **30**, 118 (1960).
2. van der Vegt, A. K. and Schuringa, G. J., TEXTILE RESEARCH JOURNAL **24**, 99 (1954).
3. van der Vegt, A. K. and Schuringa, G. J., TEXTILE RESEARCH JOURNAL **26**, 9 (1956).

Manuscript received December 29, 1960.

Twist and Tension as Factors in Yarn Characteristics

K. Sreenivasan and K. S. Shankaranarayana

The South India Textile Research Association, Coimbatore

Abstract

Twist and tension during spinning play an important part in deciding the yarn characteristics. The dual effect of twist and tension on yarn characteristics—their effect after the yarn leaves the front roller nip and before it is wound on the cop—has not received as much attention as it deserves. This effect has been studied here by varying the twist multiplier from 0.65 to 9 on roving and 3.5 to 7 on 32s yarn at different tensions.

Introduction

As the strand of fibers emerges from the nip of the front rollers of a ring frame, twist is introduced into it, mainly in order to impart strength and stability. The yarn, after the introduction of twist, is wound on a bobbin under a varying amount of tension, which depends on a number of factors such as spindle speed, ring traveller, ring diameter, winding diameter, etc., at any given moment. This combination of twist and tension changes some of the physical characteristics of the resultant yarn. While exhaustive work has been done on the strand of fibers during drafting, equal attention has not been paid to what happens to the strand of fibers after it leaves the nip of the front roller and until it is wound on the bobbin. This study is an attempt to investigate the combined effect of twist and tension on yarn characteristics.

The general influence of increasing twist in yarns may be summarized as follows:

1. As twist increases, strength also increases up to a point and then tends to decrease.
2. There is reduction in yarn diameter with a consequent increase in yarn density.
3. There is a contraction in length as a result of the increasing angle between the fibers and the yarn axis.
4. Twist also influences other characteristics such as the amount of light reflected from the yarn surface and the absorptive power of yarns.

Many research workers have studied the influence of twist on yarn characteristics. Morton [4] has found that yarns spun with higher twist multipliers display greater irregularity. According to him, when the twist multiplier is increased from 4 to 7, the increase in irregularity is found to be between 40% and 60% for most of the cottons used. Gulati and Turner [3], working on test specimens 3 in. in length, have worked out a formula expressing the relationship between diameter, twist, and count. They have found that turns per inch in any cross-section are approximately inversely proportional to the number of fibers in that part. A close relationship is also exhibited between fiber fracture and yarn strength, about 60% of the fibers breaking when the yarn strength is at its highest. Barella [1] discusses the influence of twist on yarn diameter, density, and contracture, and has verified experimentally the theoretical relationship worked out.

Evenness as measured by Uster or Fielden-Walker testers measures the degree of variation in weight per unit length. This estimation of evenness does not take into consideration the variation in the cross-sectional area. In a closely packed, twistless strand, unevenness whether measured by weight or cross-sectional area should be the same. But, because of the unequal distribution of twist in almost all yarns and the consequent unequal compression of fibers at thick and thin places, there is likely to be a change in the evenness as measured by cross-sectional area.

Rupture takes place in a yarn as the result of increasing tension along the length. During loading, yarn undergoes elongation in length as well as a contraction in diameter. There is a resultant increase in yarn density, and at rupture, yarn density is equal to fiber density provided there is no slippage. The diameter at the point of rupture is known as the critical diameter. The same effect may be

achieved by preventing the yarn from contracting and increasing the twist. In this case twist at rupture may be called the critical twist. The difference between the mean diameter when the yarn is allowed to contract under constant tension and the diameter at the same twist multiplier but when the yarn is not allowed to contract will give an idea of the contribution of contraction to an increase in diameter.

The effect of tension has not been investigated to any great extent, except in relation to breakages. But yarn characteristics such as diameter and contraction are dependent on twist as well as tension. During spinning, twist is imparted to yarn under a varying tension, and yarn is also subjected to tension during subsequent processing. Hence in this study the dual effect of twist and tension has been investigated.

Methods of Study

A preliminary study was made on a short length of 10 in. of roving, as it was not possible to use very low twist multipliers on the ring frame due to the difficulty of working. The roving was fixed under constant tension between the grips of a Henry Baer Tension Twist Tester. The initial twist multiplier was estimated separately, and by rotating the rotary grip by a definite number of turns, twist was progressively increased. The rate of increase in twist was low at the beginning and high towards the end. Twisting was continued by stages until no measurement could be taken on the specimen due to snarling. The range of twist multipliers studied was from 0.65 to 7. The following characteristics were measured after each stage of twisting: diameter at twenty points at equal intervals of $\frac{1}{2}$ in. using a small microscope; contraction in length; and the weight of the specimen after completing the final stage of twisting.

Measurements were made with low and high tensions of 24 g. and 54 g., respectively. At each tension one sample was measured allowing the specimen to contract and one without allowing it to contract.

The details of the final study on the yarn are as follows. Yarn of 32s with different twist multipliers and tensions was spun on the same set of 15 spindles on a ring frame fitted with a Casablanca A 500 drafting system. Three tensions were applied by using travellers of counts 4/0, 6/0, and 8/0. Five different twist multipliers were used for each of the travellers. All other factors were kept the same. The draft was so adjusted that at a twist multiplier of 3.5 the actual count was 32. The draft was kept constant for the remaining twist multipliers. Though the count became progressively coarser for the higher twist multipliers, the draft was not altered for the following reasons. Drafting is one of the main sources of irregularity in yarns and hence should be kept constant if the effect of twist is to be investigated. It was also considered desirable to keep the number of fibers in the cross-section of yarn uniform throughout the experiment.

For the purpose of twisting the yarn for various characteristics, the cop was divided into four stages of cop build, *viz.*, cop-bottom, half-full, three-fourths full, and nearly full. As far as possible, samples for testing were drawn from each of these stages.

The following characteristics were examined: (1) actual count and lea strength; (2) diameter; (3) evenness; (4) turns per inch and angle of twist; and (5) contraction in length.

Results and Discussion

Diameter

The effects of twist multiplier and tension on diameter are indicated in Figures 1 and 2. In Figure 1 the changes in diameter observed on the roving with tensions of 24 and 54 g. are plotted against twist multiplier. In Figure 2 mean diameters of the yarn for each of the twist multipliers and travellers are plotted.

The mean diameter both in the case of roving and of yarn progressively decreased with the increase in twist multiplier, as is apparent from Figures 1 and 2. The rate of decrease in diameter was found to be higher in the initial stages of twisting than at later stages. This is due to the fact that at very low twist multipliers there is considerable interspace between the fibers, whereas at later stages, due to lack of interspace, reduction in diameter is not possible. The diameter reaches a minimum value after which the specimen begins to snarl as the tension along the axis becomes insufficient to withstand the forces due to twisting.

The general effect of tension on the diameter was that higher tensions produced a lower minimum diameter than did lower tensions for the same strand and, as a consequence, also a higher density. This is clearly indicated in the case of the rovings in Figure 1. Similar conclusions were arrived at in

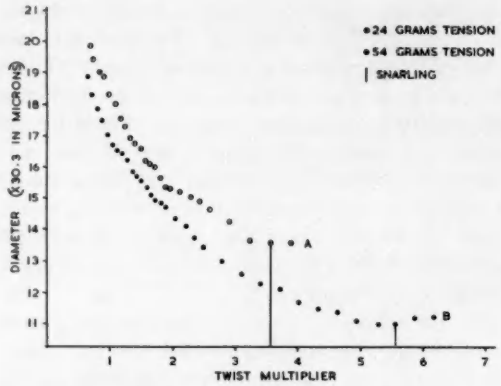

Fig. 1. Effect of twist on diameter of roving at different tensions.

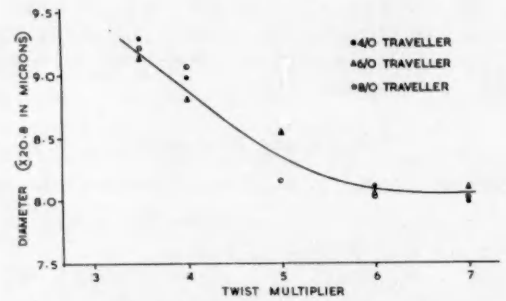

Fig. 2. Diameter of yarn spun at different tensions and twist multipliers.

the case of yarn in the range of twist multipliers studied. However, the mean diameter values did not reveal any significant difference among the three travellers used. This may be attributed to the fact that tensions introduced by the use of the three travellers, 4/0, 6/0, and 8/0, which were about 13, 11, and 9 g., respectively, do not differ enough and their effect has been masked completely by larger variations in the yarn. However, the yarn diameter at the cop-bottom tended to be lower than at the other three stages, where the diameter was more or less same.

Another effect of tension was that, for the same roving, the minimum diameter was reached at a lower twist multiplier with the lower tension than with the higher tension.

When twist is added to a specimen under constant tension two conflicting factors come into play. One is the elimination of air from the specimen, resulting in a reduction in diameter; the other is contraction as a result of which the count becomes coarser, which contributes to an increase in diameter. Figure 3 indicates the contribution of these two factors to the resultant diameter. Curve A was obtained by increasing the twist at a constant tension of 54 g., while Curve B was obtained with the same tension but without allowing the specimen to contract while twist was increased. The difference in diameters at each of the twist multipliers represents the contribution of contraction to an increase in diameter. This is represented as a percentage by the vertical lines in the figure.

Diameter Variation

The coefficient of variation of the diameter for various twist multipliers both for roving and for yarn are indicated separately in Figure 4. An examination of the curve for the roving, where the initial twist multiplier is as low as about 0.65 as against 3.5 in the case of yarn, reveals a tendency for the C.V. to increase initially and then to decrease steadily.

As is well known, twist has a tendency to concentrate at a thin place in preference to a thick place. This results in a higher degree of compression at thin places while the thick places remain more or less the same during the initial stages of twisting, thereby producing a greater degree of variation in diameter. But after a certain stage the thin places become saturated with twist, with the result that the additional twists begin to flow to thick places, resulting in reduction in diameter at the thick places. This naturally goes on reducing the differences in diameter between thick and thin places. In the case of the yarn the initial increase in C.V. of diameter is not noticed since the starting twist multiplier itself is as high as 3.5.

Unevenness and Diameter Variation

Evenness of yarn can be measured either in terms of uniformity of weight per unit length or uniformity of diameter along the length. The former is measured on electronic evenness testers like Uster or Fielden-Walker while the latter is measured on photoelectric evenness testers. For a closely packed, twistless strand of fibers both the methods may be expected to give similar results. But, for a strand of fibers emerging from the front roller nip, introduction of twist introduces additional factors. For it is well known that twist runs into thin places in preference to thick places, which in turn produces a greater

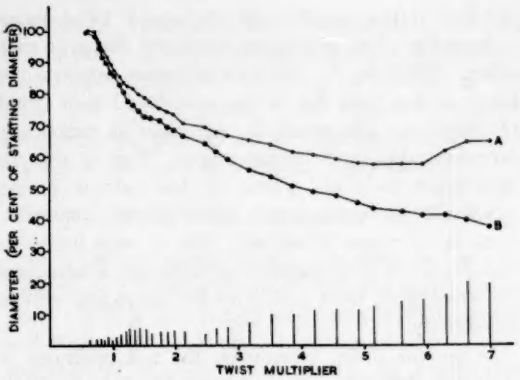

Fig. 3. Effect of twist and contraction on diameter: A, allowing the specimen to contract; B, without allowing the specimen to contract.

degree of reduction in diameter at thin places than at thick places.

The relationships between diameter variation in terms of coefficient of variation, mean deviation as estimated by Uster Evenness Tester, and twist multiplier are indicated in Figures 4 and 5. It will be observed that the C.V. of diameter increases in the initial stages of twisting and then steadily falls until the minimum diameter is reached. In the case of yarns where the minimum twist multiplier employed is 3.5, as against 0.65 in the case of rovings, the C.V. of diameter progressively decreased with the increase in twist multiplier, reaching a minimum value when the diameter was minimum. On the other hand the mean deviation (of weight per unit length) as measured by Uster tended to increase as the twist multiplier increased. This was uniformly so in the case of all the three travellers.

It is interesting to speculate as to the reasons why the percent unevenness should increase while the C.V. of diameter decreases for higher twist multipliers. It is possibly because the factors that operate in the two cases are different. In the case of the diameter, at the initial stages of twisting, twist tends to flow into the thinner places leading to a greater compression of these places, and consequently the C.V. of diameter increases. But as twist is increased and the thin places become saturated with twist, it flows into the thicker places and a greater uniformity in twist as well as in diameter results. This has also been confirmed by the finding of a reduction in C.V. of turns per inch as the twist multiplier increases.

Because of the tension introduced in the spinning

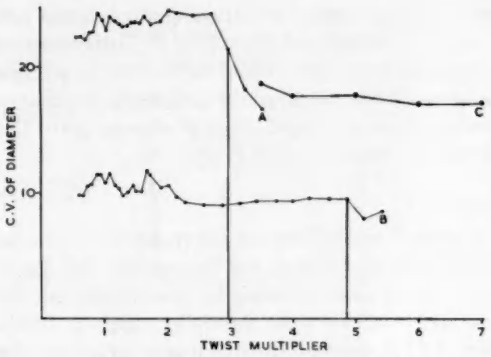

Fig. 4. C.V. of diameter and twist multiplier: A, roving with 24 g. tension; B, roving with 54 g. tension; C, 32s yarn.

process, there is a slight drafting effect on the fibers after they leave the nip of front rollers and before they receive sufficient twist to fix the fibers permanently in position. This drafting effect acts more on the thicker places since the thin places receive more twist in the initial stages. When low twist multipliers are employed, there is greater opportunity for the thick places to be drafted, and the percent unevenness of the yarn is slightly lower than that for the strand of fibers leaving the front rollers. But at higher twist multipliers, due to higher twist, the fibers are very quickly fixed in position and there is no opportunity for the drafting effect to come into play. Hence an increase in the percent uneveness is noticed.

Lea Strength and Strength Variation

The relationship between twist multiplier and lea breaking strength followed the usual pattern, namely rapid increase in count–strength product with in-

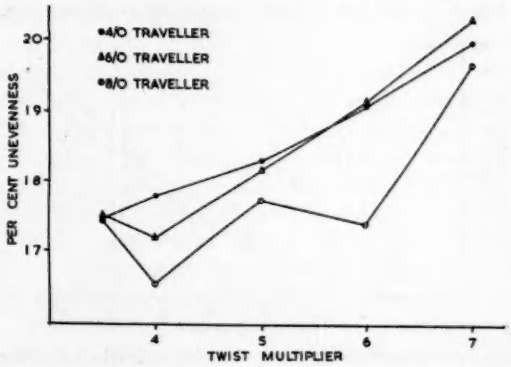

Fig. 5. Percent unevenness and twist multiplier.

crease in twist multiplier, attaining a maximum value at a twist multiplier of about 5, with further increase in twist multiplier producing a reduction in strength. However, it was observed that in general the heaviest traveller, 4/0, produced slightly stronger yarn than the lightest traveller, 8/0 (Figure 6).

Contraction

Figures 7 and 8 illustrate the results of contraction as the twist is increased for the rovings and for the yarn. In the case of roving the contraction has been measured within a twist multiplier range of 0.65 to about 8.5; in the case of yarn it was measured from 3.5 to 7. The top curve in Figure 7 is for a tension of 24 g. and the lower one for the higher tension of 54 g. It will be noticed from Figure 7 that the curves are parabolic in shape.

While contraction increases at a higher rate at higher twist multipliers, over the narrow range of twist that is normally used in spinning, say 3 to 5, the graph is almost a straight line and contraction may be said to increase proportionately with twist.

In the initial stages when the twist in the test specimen is very low and when the fibers are held together rather loosely, any addition of twist seems to have the effect of making the fibers slip over each other. That is, the force of adhesion between the fibers is less than the torque introduced as a result of twisting. The result is that there is practically no contraction in the initial stages. This is also the experience in mills where in low-twisted roving practically no contraction is observed and sometimes even an extension is noticed. But as twist increases and fibers are held together more firmly, contraction increases with twist and goes on increasing almost indefinitely.

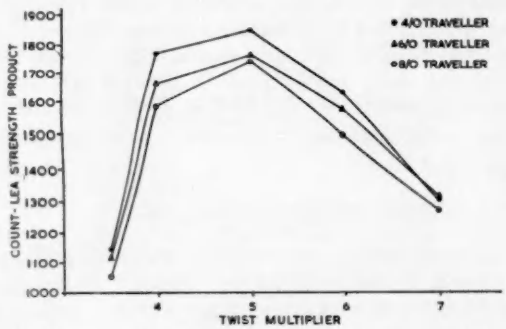

Fig. 6. Count-Lea-strength product and twist multiplier.

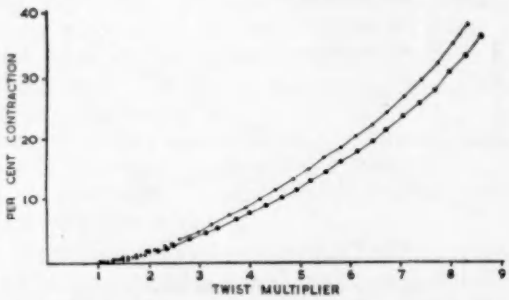

Fig. 7. Contraction in length of roving and twist multiplier. Top curve, 24 g. tension; bottom curve, 54 g. tension.

When the initial tension on the test specimen is increased, there is a greater tendency for the fibers to slip in the beginning (Figure 7, Curve B). The force of adhesion has to contend with the torque introduced by the addition of twist as well as the greater tension along the axis of the yarn. Therefore contraction is observed at a later stage in twist and further addition of twist produces less contraction than in the case of lower initial tension. That the effect of tension in preventing the yarn from contracting is continuous is revealed by the gradual widening in the gap between the two curves. We can therefore conclude that at very low twist multipliers, tension seems to play a major part in contraction; at higher twist multipliers twist contributes more to contraction and the contribution of tension is not appreciable.

The rate of contraction, however, does not seem to be affected in any way by the effect of wave formation. Irrespective of whether the addition of twist has been absorbed or has resulted in waves, total reduction in length seems to follow a uniform pattern, as shown by the uniformity of the curve even after waves are formed. This also tends to indicate that contraction is of the same order whether it is as a result of the increase in helix angle or as a result of the formation of waves.

The values of contraction plotted in Figure 8 in the case of yarn are weighted averages instead of the simple averages of the four different positions of bobbin build. This was done in order to make the estimated over-all contraction for the whole bobbin more representative. The weighted average has been obtained by weighting the contraction at cop-bottom, half-full, three-fourths full, and nearly full stages in the ratio of 1:3:3:1. Analysis of the data revealed that the contraction in length progressively increases with increase in twist multiplier and that

the different travellers had a significant effect on contraction. It was observed that the 4/0 traveller, which was the heaviest traveller, gave less contraction than the 8/0 traveller, the lightest traveller. However, the differences between the 4/0 and 6/0 travellers were not found to be significant.

Theoretical Considerations

It is perhaps appropriate at this stage to consider some of the theoretical aspects of twist and contraction. If L is the length of roving with no twist, and θ the helix angle after a certain amount of twist has been introduced, then $L \cos \theta$ is the length after contraction. Hence the present contraction C is obtained by the formula

$$C = 100 \frac{[L - L \cos \theta]}{L}$$
$$= 100[1 - \cos \theta]$$
$$= 100 \left[1 - \frac{1}{1 + \tan^2 \theta}\right] \quad (1)$$

The relationship between the helix angle, turns per inch, t, and spiral diameter, d, is given by the equation

$$\text{Tan } \theta = \pi dt \quad (2)$$

From Equations 1 and 2 it follows that

$$C = 100 \left[1 - \frac{1}{\sqrt{1 + (\pi dt)^2}}\right] \quad (3)$$

$$C = 100 \left[1 - \frac{1}{\sqrt{1 + (\pi dT)^2 c}}\right] \quad (4)$$

where T is the twist multiplier and c is the hank or count of the material, because $t = T\sqrt{c}$.

The spiral diameter, d, for each of the specimens of roving and yarn was estimated from Equation 4 by substituting the observed value of contraction for each of the twist multipliers. The results for the 10.68 hank roving with 54 g. tension are presented in Table I. The spiral diameter in a twisted strand will be always less than the yarn diameter due to intermigration of fibers, as can be seen from the Table. Also the spiral diameter depends primarily upon the hank or the number of fibers per cross-section and not on the twist multiplier. The increase in twist, although it makes the hank coarser, cannot be expected to affect the spiral diameter as, in the absence of any slippage, there is no change in the number of fibers per cross-section. Also, since the roving diameter decreases with increased twist, the spiral diameter would tend to equal the roving diameter as the twist is increased. This is evident from the increasing trend in the ratio between the spiral and roving diameters.

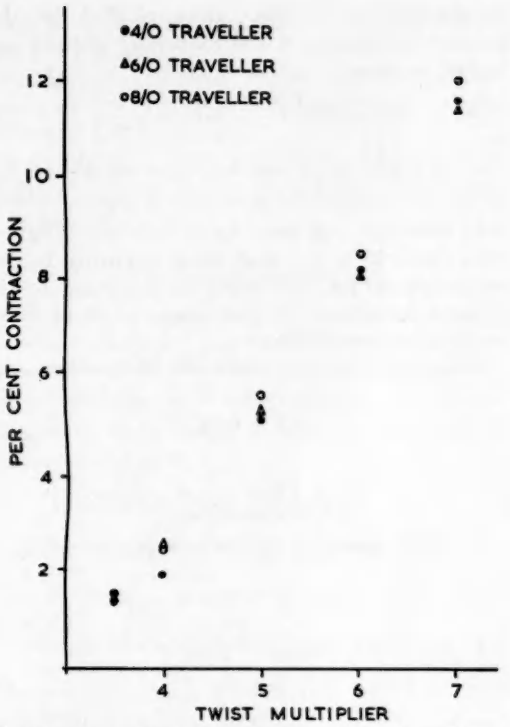

Fig. 8. Contraction in length of yarn and twist multiplier.

The spiral diameter, however, revealed a slight increase with the twist multiplier. The lower values at low twist multipliers could be accounted for by the fact that due to the possibility of fiber slippage at these levels, the observed contraction is an underestimate which in turn produces an underestimate of the spiral diameter also. The same factor could also be explained by the decrease in the number of fibers per cross-section when fiber slippage occurs. At higher twist multipliers, the increase noticed is very slight and on the basis of the number of tests done here, it cannot be taken as definite. Possibly this slight increase in spiral diameter might be due to the decreasing tendency for fiber slippage to occur as the twist increases.

It was noticed that the product of the spiral diameter and the square root of hank or count is more or less a constant at higher levels of twist multiplier.

Substituting the constant value of 26.5 for this product in Equation 4 and converting microns into inches, we have

$$C = 100\left[1 - \frac{1}{\sqrt{1 + 0.01T^2}}\right] \quad (5)$$

A very close agreement was observed between observed and calculated contractions at higher levels of twist multiplier. At lower levels the observed figures were found to be less than those estimated, but, as mentioned earlier, this could be attributed to the slippage between fibers that might occur at lower levels of twist multiplier.

Equation 5 for contraction can be rewritten as

$$\frac{C}{100} - 1 = -(1 + 0.01T^2)^{-\frac{1}{2}}$$

$$= -\left(1 - \frac{T^2}{200} + \frac{3T^4}{80000} \cdots\right)$$

For small values of T, this is approximately

$$\frac{C}{100} - 1 = -1 + \frac{T^2}{200}$$

or

$$C = \frac{T^2}{2} \quad (6)$$

Hence the relationship is in the form of a parabola for small values of T. For all values of T above three and up to six the relationship was found to be linear, the correlation coefficient being 0.998.

Similar equations were worked out for the 6.5 hank roving. The product of spiral diameter and square root of hank was almost a constant, being 29.00 for values of twist multiplier above 2.6.

Besset's [2] equation, in the metric system, for yarn contraction is

$$C = 100\left[1 - \frac{1}{\sqrt{1 + (E10^{-4}T^2)}}\right] \quad (7)$$

Where the coefficient

$$E = \frac{\pi}{100b}$$

and b is the initial density of the material with twist. Besset assumed an initial density of 0.56 for yarn, and substituting this value in Equation 7 we have

$$C = 100\left[1 - \frac{1}{\sqrt{1 + 0.05 \times 10^{-4}T^2}}\right] \quad (8)$$

When similar equations are worked out from equations obtained earlier the values of E in the equations for the different rovings and yarn are

$E = 0.110$ for 10.68 hank roving.

$E = 0.130$ for 6.47 hank roving.

$E = 0.052$ for 32s yarn.

However, since the relationship between twist multiplier, T, and percent contraction, C, was found to be more or less linear within the range of normal twist multipliers, the following regression equations were fitted

$$C = 3.52T - 6.88 \quad \text{(for 10.68 hank roving)} \quad (9)$$

$$C = 2.47T - 7.00 \quad \text{(for 32s yarn)} \quad (10)$$

TABLE I. Relationship between Spiral Diameter and Roving Diameter

Initial T.P.I., 2.15; 10.68 hank; 54 g. tension

Hank, c (1)	T.M., T (2)	Spiral diameter, d, estimated from Equation 4 by substituting observed contraction* (3)	Roving diameter,* D (4)	d/D (5)	$D \times \sqrt{c}$ (6)
10.54	1.892	7.08	14.7	0.482	22.98
10.50	2.068	7.37	14.4	0.512	23.89
10.47	2.234	7.51	14.1	0.533	24.30
10.43	2.367	7.63	13.8	0.553	24.65
10.40	2.523	7.61	13.4	0.568	24.54
10.29	2.881	8.05	13.0	0.619	25.83
10.19	3.184	8.24	12.6	0.654	26.30
10.08	3.545	8.34	12.3	0.678	26.48
9.98	3.848	8.39	12.2	0.688	26.50
9.87	4.181	8.35	11.7	0.714	26.24
9.73	4.535	8.49	11.5	0.739	26.49
9.59	4.890	8.80	11.4	0.772	27.26
9.45	5.253	8.63	11.1	0.777	26.53
9.31	5.622	8.73	11.1	0.786	26.61
9.14	6.000	8.89	11.1	0.801	26.87

* Readings when multiplied by 30.3 give diameter in microns.

Conclusions

The conclusions may be summarized as follows:

1. Diameter progressively decreases with increase in twist multiplier. The reduction in diameter is a decreasing factor with increase in twist. The minimum diameter of a strand of fibers is determined by the tension along the axis of the strand, higher tensions producing lower diameters.

2. No significant difference was observed in the minimum diameter for the three travellers. This

might be due to the fact that differences in tension produced by the three travellers may not be high.

3. When the minimum diameter is reached, the component of the force due to twisting along the length of the yarn is equal to the tension applied.

4. The maximum yarn density is determined by the tension along the axis of the yarn, higher tensions producing higher density.

5. The most even yarns, as measured by the uniformity of diameter, are produced when the diameter is minimum. On the other hand the percent unevenness as measured on the Uster Evenness Tester increases with increase in twist in the case of all three travellers.

6. In the initial stages of twisting, because of slippage of fibers, there is practically no contraction. But as twist increases and the fibers are held together more firmly, contraction increases with twist and goes on increasing almost indefinitely. Though the contraction curve is parabolic over various ranges of twist multipliers, at normal twist multipliers it is almost a straight line.

7. Tension had a significant effect on contraction. A significant difference was noticed in contraction between the extreme travellers 8/0 and 4/0, the lighter traveller producing a slightly higher contraction. The contraction at the cop-bottom stage was found to be slightly lower than at the other three stages of cop build.

8. The spiral diameter is less than the yarn diameter and the ratio tends to approach unity as twist increases.

9. For a given count and tension the product of spiral diameter and square root of count was found to be constant.

Acknowledgments

We thank the staffs of the Mechanical Processing Laboratory, Physical Testing Laboratory, and Computing Section for their help in processing, testing, and calculations. We are grateful to Mr. T. V. Ratnam for his assistance in doing the mathematical analysis of this study.

Literature Cited

1. Barella, Alberto, *J. Textile Inst.* **21**, T205–T224 (1930).
2. Besset, N. C., *L'Industrie Textile*, no. 737 (April 1948).
3. Gulati, A. N. and Turner, A. J., *J. Textile Inst.* **21**, T561–T582 (1930).
4. Morton, W. E., *J. Textile Inst.* **21**, T205–T224 (1930).

Manuscript received December 27, 1960.

Letters to the Editor

A Quick Method for Determining the Elongation, the Breaking and Tearing Strengths of Plain Woven Fabrics

Southern Utilization Research
and Development Division
1100 Robert E. Lee Boulevard
New Orleans, Louisiana
April 21, 1961

To the Editor
TEXTILE RESEARCH JOURNAL

Dear Sir:

An abbreviated fabric testing method which deviates from the conventional procedure (where warp and filling directions are tested separately) for quickly determining fabric breaking strength, elongation, and fabric tearing strength is suggested. The method involves composite testing of fabric samples. In brief, two conventionally prepared fabric samples, one warpwise, the other fillingwise, were superimposed on each other, loaded on the apparatus, and tested simultaneously.

Fabrics investigated included gray goods, and scoured, bleached, and bleached and mercerized samples, with fabric structures ranging from type 128 sheeting to combed broadcloths. The composite strip breaking strength tests were made on the Instron[1] Tester while the tear resistance measurements were made by the Elmendorf[1] method according to ASTM methods [1b] and [1a], respectively. These data are presented with the admission that the fabrics were not randomly selected to represent all types of fabric structure, but were taken as a matter of convenience by random selection from fabrics which were available at the SRRL.

Warpwise and fillingwise values of breaking strength and elongation of the samples tested compositely can be read from the Instron chart as shown in Figure 1. The low elongation fabric broke long before the high elongation fabric during a composite test, thus allowing separation of warpwise and fillingwise values of strength and elongation. If samples having similar warpwise and fillingwise strengths and elongations are tested by the composite method, the Instron chart shows only one set of elongation and strength values. In this case the elongation value is nearly equal to, while the strength value is almost double the values obtained by testing the samples separately. On the other hand, the composite strength value of two fabrics similar in elongation value but differing in strength is less than the sum of the two separate strengths. However, fabrics of similar warpwise and fillingwise elongation are seldom encountered.

Fabric breaking strength and elongation data obtained by the composite testing method compared very favorably with data determined by the conventional method, as shown in Figures 2 and 3. Points closely surrounding the 45° lines indicate good correlations between data obtained by the two methods.

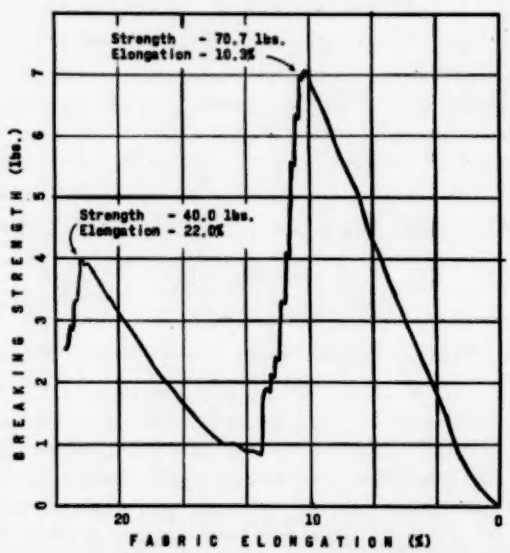

Fig. 1. Sample Instron chart on fabric breaking strength and elongation tested by the composite method.

[1] Use of a company and/or product name by the Department does not imply approval or recommendation of the product to the exclusion of others which may also be suitable.

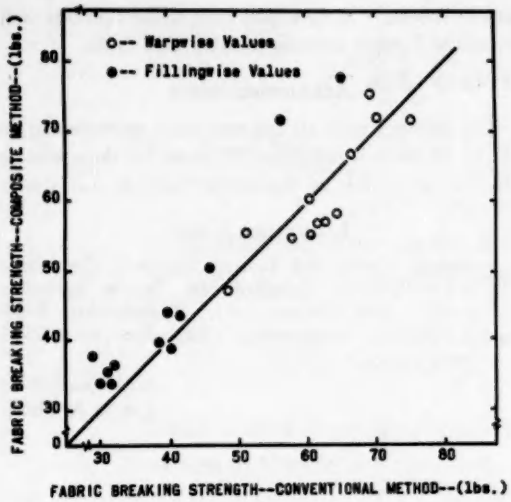

Fig. 2. Comparison between the fabric breaking strength values obtained by conventional and by composite methods.

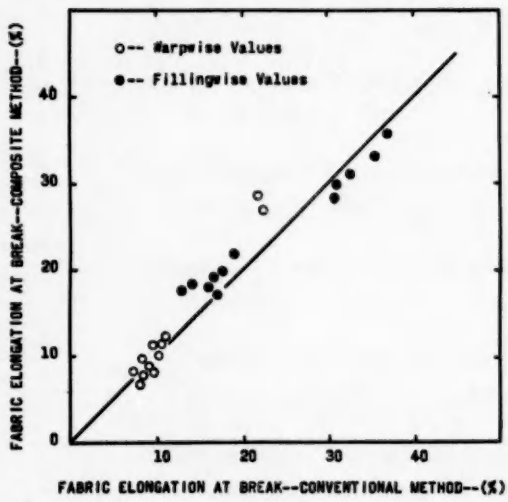
o-- Warpwise Values
●-- Fillingwise Values
FABRIC ELONGATION AT BREAK--COMPOSITE METHOD--(%)
FABRIC ELONGATION AT BREAK--CONVENTIONAL METHOD--(%)

Fig. 3. Comparison between the fabric breaking elongation values obtained by conventional and by composite methods.

Figure 4 indicates that two distinct curves are in evidence when the warpwise and fillingwise tearing strength data are separately plotted against the tearing strength data obtained by the composite method. However, Figure 5 shows that the sum of the warp and filling direction tearing strength values correlate very closely (coefficient of correlation of 0.99) with fabric tearing strength data obtained by the com-

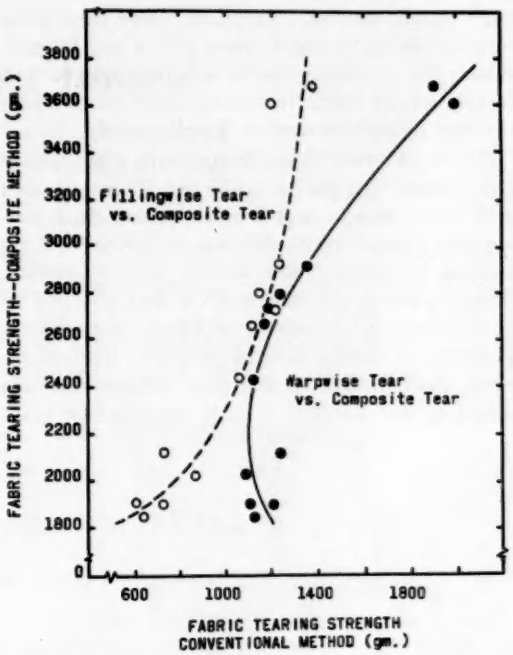

Fig. 4. Comparison between the fabric tearing strength values obtained by conventional and by composite methods.

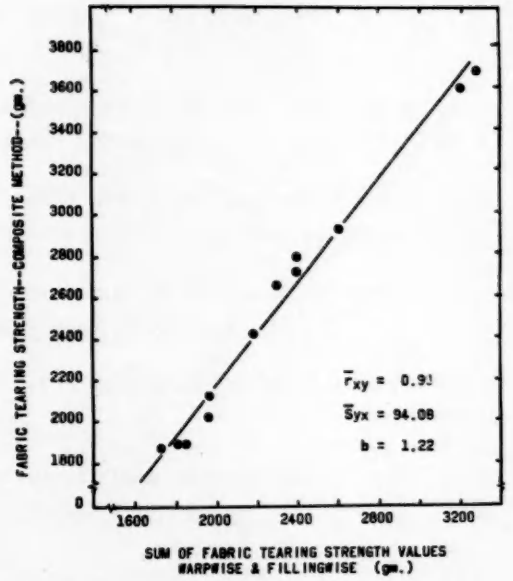

Fig. 5. Relationship between the sum of fabric tearing strength values obtained by conventional methods and the tearing strength values obtained by the composite method.

posite testing method. Therefore, using the sum of warp and filling tearing strength values may be more suitable for expressing the fabric's resistance to tear, since in-service fabric is usually subjected to warpwise and fillingwise stresses simultaneously.

This exploratory investigation with plain woven fabrics shows that the composite test method appears to be as accurate as, and is much quicker than, conventional techniques for determining fabric breaking strength, elongation, and tearing strength values. However, due to the nature of the data obtained by the composite test method, it may be considered more applicable in quality control programs than in research work. Also, limited data indicate that this composite test method is only suitable for plain woven fabrics. It is hoped that these findings will stimulate further investigation in this field.

Acknowledgment

The authors wish to express their appreciation to W. F. McSherry and Julia M. Sloan for determining physical properties of the fabrics used in this study.

Literature Cited

1. American Society for Testing Materials, Committee D–13, "ASTM Standards on Textile Materials (with related information)," Philadelphia, 1959. (a) ASTM Designation D 1424–59; (b) ASTM Designation D 1682–59T.

GAIN L. LOUIS
LOUIS A. FIORI

In Coming Issues

The Use of Unheated Air in the Drying of Wool. *J. G. Downes and G. B. McMahon*

Moduli of Cotton Fibers and Yarns in Relation to X-Ray Angles. *Louis C. Weiss, Rollin S. Orr, Jerome J. Redmann, and James N. Grant*

A Study of Reactions between Cotton Cellulose and Difunctional Epoxides. *Ruth R. Benerito, Beverly G. Webre, and J. B. McKelvey*

Kinetic Studies of the Wool–Water System. Part III: The Mechanism of Sorption at High Water Concentrations. *I. C. Watt and J. E. Algie*

Rate of Felting of Untreated and Shrink Resistant Wool Fabrics. *J. R. McPhee*

Wrinkle Resistant Properties of Dialdehyde Cotton. *Charles H. Mack and Wilson A. Reeves*

A New Staining Technique for the Study of Skin and Core of Nylon Yarns. *W. Rhett Berry*

The Oxidation of Cotton Cellulose in the Presence of Direct Cotton Dyes. *K. V. Datye, G. M. Nabar, and G. G. Shroff*

Quantitative Investigation of the X-Ray Diffraction Picture of Some Typical Rayon Specimens, Part II. *P. H. Hermans and A. Weidinger*

The Spectral Distribution of Sound Produced by Fibers and Fabrics in Friction. Part I: Improved Instrumentation. *Walter J. Thorsen and Paul Veneklasen*

Studies of High Fastness to Light in Coloring Matters in Hydrophilic Substrates. *Charles H. Giles, George Baxter, and Syed M. K. Rahman*

The Statistical Interpretation of Fiber Counts in Yarn Cross Sections. *D. N. E. Cooper*

Radiation-Induced Interaction of Acrylonitrile with Cyanoethylated Cotton. *Robert J. Demint, Jett C. Arthur, Jr., and Wilbur F. McSherry*